2012

Biofunctional Coatings Using Direct-Write Fabrication Technique For Surgical Implant Devices

Jessica L. Perkins
North Carolina Agricultural and Technical State University

BIOFUNCTIONAL COATINGS USING DIRECT-WRITE FABRICATION TECHNIQUE FOR SURGICAL IMPLANT DEVICES

by

Jessica L. Perkins

A dissertation submitted to the graduate faculty
in partial fulfillment of the requirements for the degree of
DOCTOR OF PHILOSOPHY

Department: Industrial and Systems Engineering
Major: Industrial and Systems Engineering
Major Professor: Dr. Salil Desai

North Carolina A&T State University
Greensboro, North Carolina
2012

ABSTRACT

Perkins, Jessica L. BIOFUNCTIONAL COATINGS USING DIRECT-WRITE FABRICATION TECHNIQUE FOR SURGICAL IMPLANT DEVICES. (**Major Professor: Dr. Salil Desai**), North Carolina Agricultural and Technical State University.

Surface modification of biomaterials is of critical value to attain desired functionality of biomedical devices and implants. Many of the conventional manufacturing methods used for the fabrication of thin film coatings lack the ability to precisely dispense biological compounds without compromising its chemical integrity. This research investigates the use of direct-write inkjet technique for the deposition of multi-layer coatings of biodegradable polymers. The Direct Write inkjet method provides selective deposition and patterning capability for depositing multi-material coatings on biomaterials for a vast array of surgical implant devices (e.g. stents for cardiovascular applications and orthopedic implants).

In the first phase of the research, an elastomeric polymer, namely polyester-urethane urea (PEUU) was used to encapsulate an anti-proliferation drug paciltaxel (Taxol). The direct-writing process was employed to coat multiple layers of this polymeric formulation on a model titanium alloy surface. Characterization experiments were conducted to observe the influence of drug dosage and coating thickness on the release kinetics of the multilayer coatings. Drug release kinetics were characterized using an ultraviolet-visible spectrum (UV-Vis) spectrophotometer and surface morphology was assessed using optical microscopy and scanning electron microscopy (SEM). Biocompatibility tests were conducted to assess the smooth muscle cell inhibition and platelet adhesion properties of the coatings. The effects of drug dosage and layer

thickness were evaluated via statistical significance tests. Tunable drug release coatings can be developed for an intended application by manipulating a given set of input factors.

In the second phase of the research, the direct-write printing process was utilized to deposit precise layers of multilayer polymeric coatings on magnesium alloy surface. Biodegradable magnesium alloys provide substitutes for permanent metal implant materials such as titanium or stainless steel. Polymeric coatings provide a barrier layer that can retard the corrosion process of the magnesium alloys for vascular and orthopedic applications. Poly(lactic-*co*-glycolic acid (PLGA), polycaprolactone (PCL), and PEUU were chosen based on their varying degradation properties. Immersion studies were conducted in a simulated body fluid (SBF) to determine the corrosion behaviors of different sample types using inductively coupled plasma spectroscopy (ICP). Biocompatability tests such as the lactate dehydrogenase (LDH) assay were conducted to assess the cytotoxicity levels induced from magnesium ion exposure. A reduction in magnesium ion content was observed from the polymer-coated samples. Findings also showed correlation between the release of the magnesium alloy and the health of normal human bronchial epithelial cells evaluated using the COX-2 gene expression. This research establishes a foundation for identifying candidate polymer coatings to control the corrosion of magnesium alloys.

School of Graduate Studies

North Carolina Agricultural and Technical State University

This is to certify that the Doctoral Dissertation of

Jessica L. Perkins

has met the dissertation requirements of
North Carolina Agricultural and Technical State University

Greensboro, North Carolina
2012

Approved by:

_____	_____
Dr. Salil Desai Major Professor	Dr. Steven Jiang Committee Member
_____	_____
Dr. Daniel Mountjoy Committee Member	Dr. Jag Sankar Committee Member
_____	_____
Dr. Jenora Waterman Committee Member	Dr. Paul Stanfield Department Chairperson

_____
Dr. Sanjiv Sarin
Associate Vice Chancellor of
Research and Graduate Dean

DEDICATION

This research is dedicated in memory of my grandmother, the late Ada Alberta Winbush who lost her battle to Lung Cancer in September of 2011. She was a great support to me in every one of my endeavors and for that I am grateful. From her I learned to stand strong, remain faithful, and see things through to the very end. It is my hope that this research will bring us one step closer to finding a cure! To my parents, Harry and Deborah Perkins, thank you for all of your love and support over the years. And to my daughter, Corynn, thank you for your patience. Thank you and I Love You!

BIOGRAPHICAL SKETCH

Jessica Lynn Perkins was born on June 26, 1984 in Washington D.C. She received her high school diploma from Riverdale Baptist School (2002) in Upper Marlboro, MD. She was accepted into the Department of Biology at North Carolina Agricultural and Technical State University (NC A&T SU). She later decided to change her major to Industrial and Systems Engineering and soon after received her Bachelor of Science degree in Industrial and Systems Engineering in 2007.

In the fall of 2007, Jessica was accepted into the School of Graduate Studies at NC A&T SU to pursue a Master's of Science in Industrial and Systems Engineering with a focus on Production Systems. She defended her thesis titled, "Characterization of Absorbance and Time Release Kinetics of Calcium Alginate Microcapsules using Drop on Demand Inkjet Printing Technology" and received her Master's Degree in 2008.

In 2009, Jessica began her Doctoral Studies, also in Industrial and Systems Engineering. Her study and research interest came full circle, as she was able to integrate her first love, biological studies, with engineering manufacturing processes. She is now a doctoral candidate in Industrial and Systems Engineering with a focus on Manufacturing and Service Enterprise Engineering.

ACKNOWLEDGEMENTS

First giving honor to God for the great things He has done in my life and the great things He will continue to do! I would like to acknowledge my parents, Harry and Deborah Perkins, because without their support, I would not have made it this far. I would also like to acknowledge Corynn for her sense of humor when things just got too serious. To my family, I would like to thank you for your prayers and great words of encouragement.

A heartfelt thank you to the Title III Ph.D. Fellowship Program and the Title III administration for the financial support provided for me to pursue my doctoral studies. A sincere thank you to the Department of Industrial and Systems Engineering for providing me the foundation necessary for professional success. I would like to thank my advisor, Dr. Salil Desai, for his continued support throughout my research endeavors. For his time spent with me in the laboratory, I am extremely grateful. To my research committee (Dr. Jiang, Dr. Mountjoy, Dr. Sankar, and Dr. Waterman), Thank you for your guidance and encouragement.

I am also thankful for those who were not named as committee members but have contributed greatly to my research efforts. I am grateful to Dr. Xu and Mr. Christopher Smith for their generous contributions despite their busy schedules. To the members of the Waterman Lab (Dawn, Carresse, Chakia, and Sarah), thank you for all the time you spent training me on several of the biological protocol that were pertinent to this research. To Dr. Ye and Dr. Hong at the University of Pittsburgh (UPITT) McGowan Institute of Regenerative Medicine for training me in biocompatibility studies as well as testing

several of my samples. Dr. Roy and Satitsh Signh for their input and help with their ICP despite their busy schedules, thank you for all of your help. I would also like to thank Mr. Kwame Adarkwa for assisting me with my experiments.

I would like to thank the National Science Foundation and the Engineering Research Center at NC A&T SU for entrusting me with the specifics of this research. To the members of the Student Leadership Council, thank you for your support and encouragement through this time. And, last but not least, I would like thank the members of Turners Chapel A. M. E. (my second family) for the love and support that they have shown Corynn and I over these past several years. Thank you for helping with Corynn, inviting me to Sunday dinners, and stopping by to offer words of encouragement along the way. I am truly grateful for you all!

TABLE OF CONTENTS

LIST OF FIGURES

LIST OF TABLES

CHAPTER 1

INTRODUCTION

1.1 Overview

The design of newer and more effective drug delivery systems have begun to emerge in the field of biomedical engineering, specifically pertaining to the development of biodegradable and bioabsorbable implant materials. Developments in metal alloying and surface modification processes are at the forefront of many research endeavors where the intent is to develop revolutionary biomaterials. Concurrently, the study of temporal and spatial release kinetics of pharmaceutical reagents from drug-eluting surgical devices such as cardiovascular and tracheal stents and orthopedic implants is of growing interest [1-4]. Surface modifications via different coating techniques, can be applied to various biomaterials to enhance their biocompatabily and thus enhance their effectiveness in treating the various post operative effects associated with surgical implant procedures [5-9].

The use of metallic biomaterials for biomedical applications requires that a number of conditions be met. The material must be biocompatible and corrosion resistant so as not to release undesired metal ions into the body [10]. It must posses an adequate mechanical strength, thus eliminating potential for fracture and must be free of toxic response within the body or host site [11]. Some commonly known materials used for fabrication of metallic stents include stainless steel [11], nickel [14], titanium alloys [10-11], iron, and magnesium alloys [10-14]. Similarly, silicone and certain polyurethanes have been used for fabrication of cardiovascular and thoracic devices due to their

favorable biocompatible properties [15]. A comparison of the various implant materials with their respective advantages and disadvantages is provided herein.

1.2 Biomaterials for Implant Manufacturing

The most common stent materials include metallic, polymer, and silicone [15]. Of the metallic group, materials can be further cateragorized into those that are toxic, non-toxic and bioinert, non-toxic and bioactive, and non-toxic and bioabsorbable [16]. Metallic materials which have already been accepted for use as surgical implant materials such as stainless steel and titanium are considered as non-toxic, bioinert materials as they do not release any immediate toxic ions into the body, however materials in this category may result in the death of surrounding cells or tissues over time [17]. This is depicted in Figure 1.1. The Wallstents generally used today are manufactured using these non-toxic, bioinert materials.

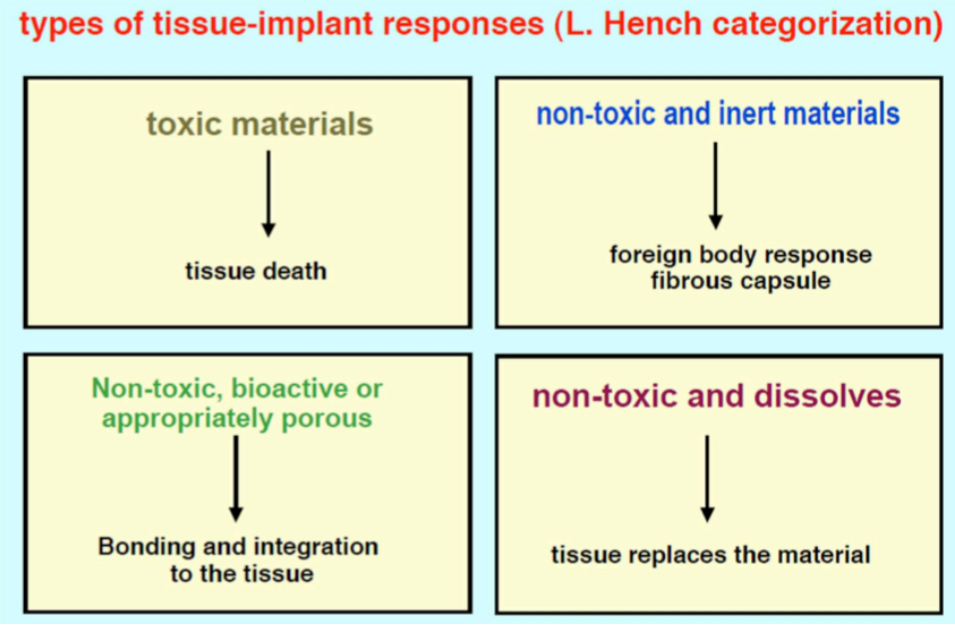

Figure 1.1 L. Henchs' catergorization of tissue implant responses

The metallic stent (or Wallstent) generally consists of a wire-like, criss-cross, stainless steel mesh having a tubular shape and offers the mechanical strength necessary to prevent restenosis, or collapse of the arterial wall, after angioplasty [18]. The diameter of the metallic stents' outerwall is also thinner, allowing for a larger inner diameter and increased blood flow through the arteries. Another important advantage is the lack of migration that occurs once the device has been placed. In contrast, the silicone design has a rather narrow inner diameter due to its thicker outer wall and issues with migration and dislodging have been observed [19].

Disadvantages of the metallic, mesh-like design is that it is generally permanent due to partial or full integration into the airway or arterial wall, making the removal process difficult whereas the silicon stent is easily removable and may be exchanged frequently [19]. Environmental factors that inhibit the effectiveness of metallic tubular supports include in-stent granulation tissue formation, inflammatory disease, smooth muscle cell migration, stent thrombogenicity, and neointimal hyperplasia [20]. The presence of these factors are more prominent when bioinert materials are employed. Thus, they are identified as a foreign body object within the physiological environment and become encapsulated within a fibrous mesh. Subsequently, this can bring about increased external forces causing the tubular mesh to collapse, also referred to as restinosis [21]. With the transition from bioinert to biodegradable and bioabsorbable, more and more research scientist are beginning to focus on magnesium and its alloys as ideal candidates for surgical implant materials.

Magnesium is the fourth most abundant mineral found in the body, thus it is necessary in order for the body to remain in good health [22]. What makes magnesium such the ideal candidate for surgical implant materials is its ability to perform an intended function, degrade and become absorbed by the body without leaving any trace or toxic effects [23]. In a study conducted on atherosclerosis risk in communities, the authors suggests that there exists a connection between patients who suffer from cardiovascular disease and magnesium deficiency [24]. Thus magnesium-based, bioabsorbable stents are of increasing interest for patients suffering from heart disease.

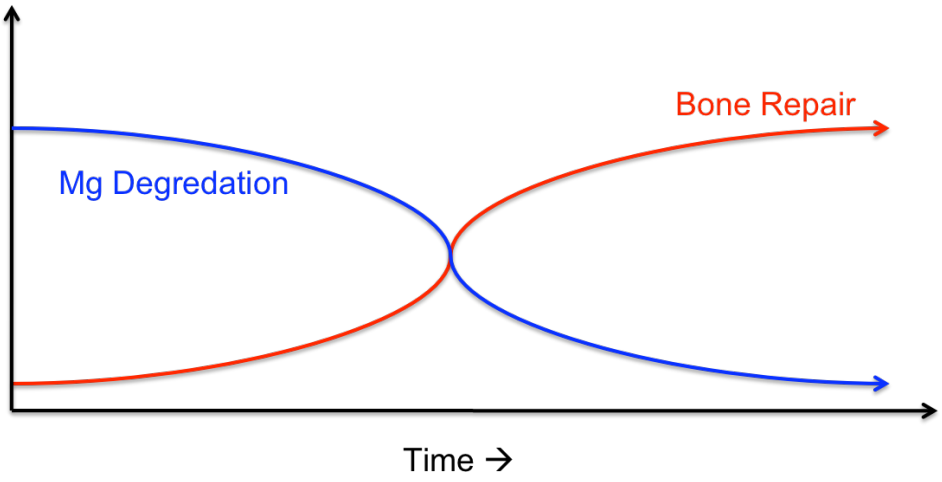

Figure 1.2 Depiction of matching Mg degradation and bone growth processes

Magnesium is also an ideal candidate for orthopedic implant devices for bone growth and fracture repair due to it similar mechanical properties to bone. The material offers such advantages as more physiological and less invasive repairs, possibility of tissue growth, temporary support during tissue recovery, and gradual dissolution by the physiological environment after it has performed its intended purpose. However magnesium alone tends to degrade at an accelerated pace in saline environments thus not

allowing enough time for the device to perform its intended purpose. A depiction of this concept is shown in Figure 1.2. Recent research being conducted at the Engineering Research Center for Revolutionizing Metallic Biomaterials has applied various metal alloying and surface modification techniques to control the corrosion of magnesium.

In addition to the use of magnesium alloys for implant and stent manufacturing, these materials can be coupled with a multi-functioning polymeric coating that can extend magnesium corrosion rates long enough for the stent to serve its purpose as well as administer any necessary therapeutic drugs. These coatings also add several other benefits, which are described further in the upcoming sections.

1.3 Polymers for Stent Coating

Over the past decade researchers have examined a number of ways in which pharmaceuticals can be transported via stent-mediated drug delivery methods. Some of the methods found in literature range from synthetic and organic biodegradable polymers to non-degradable polymers. The perusal of non-degradable polymers for biomedical uses led to less than satisfactory results for stent coating applications [25]. It is believed that the presence of the foreign body causes inflation and infection at the implant site, thus magnifying an already complex situation. Biodegradable polymers were studied for stent coating as they offered a decrease in the number of surgical procedures required for device removal and a significant reduction in the number of restinosis cases [21]. Contrasting studies from other cases, however, claim that the use of polymers in general may be incompatible with the blood thus increasing the risk of thrombosis. This

conclusion caused experts to investigate other alternatives for achieving localized drug delivery using stents.

The uses of degradable polymers as a mechanism for drug delivery was revisited (after considering a number of other coating materials and their associated effects). Materials such as Sirolimus [26,28], Paclitaxel (Taxol) [25-28], and Phosphorylcholine (PC) have been used to directly coat bare metal stents (BMS). In some cases these materials were used as mechanisms for the entrapment of other medicines within themselves. The use of PC has been used as a binding mechanism to carry drugs to treatment sites [29].

The employment of non-polymeric coatings showed great promise in the fact that in most cases 100% efficacy was observed in terms of the intended amount of drug required for healing [25-28]. There was, however, an essential limitation of this method. The rate at which these substances were released ranged from around 60% to 80% in the first two or three days with subsequent elution of the remaining drugs releasing over the next 28 to 35 days [30]. This phenomenon is commonly called as a burst effect or initial burst period. However, a procedure for mediated delivery of pharmaceuticals over extended periods of time was desired.

1.4 The Model Stent

The model stent design would be one that contains select properties of both the metallic and biopolymer tubular support systems. The selected material for stent manufacturing would be bioabsorbale, having the ability to dissolve into the surrounding tissue without toxic effect. The metallic wire mesh covered with a biodegradable

polymer would offer the mechanical strength required to maintain an open airway or blood vessel and allow for a higher blood flow rate (cardiovascular). A thin biopolymer coating would not only add a second dimension to the stenting device as a protective barrier to increase the time span in which the stent remains operative, but could also serve as a drug carrying device.

In addition to the increased functionality of tubular support structures following coating and/or polymeric surface treatments, more case specific advantages are realized. For example, late-stage lung cancer patients facing acute tracheal restenosis due to the rapid in-growth of a malignant tumor would require rapid, site-specific, chemotherapeutic sessions over an extended period of time. Local delivery of a drug to the cancerous site via a polymer-coated stent can reduce the exposure of toxins to the body, thus ridding the impaired site of only the unwanted cells. Also, the polymer matrix grants sustained treatment over time, eliminating the need for repetitive surgical procedures and their associated risk as well as substantial medical costs [31]. Literature suggests that a biodegradable polymer matrix containing drugs such as Palcitaxel and Sirolimus, which inhibit the migration and proliferation of smooth muscle cells, could be used as a mechanism for treatment of neointimal hyperplasia [32].

The study of sustained drug release has important implications in the biomedical arena. Research in the field of tissue engineering has integrated the theory of sustained release to deliver Nerve Growth Factors (NGF) encapsulated in polycaprolactone (PCL) to preserve bioactivity for the construction of biofunctional tissue scaffolds [33]. Sustained release of NGF was achieved for three months [33]. Research scientists at the

Wake Forest Institute of Regenerative Medicine have achieved sustained release of oxygen ions to facilitate cell survivability during the brief period between the implantation of tissue engineered organs and the establishment of neovascularization where eventual tissue and cell necrosis may occur [34].

The above-mentioned applications have demonstrated the success of achieving prolonged periods of release for biomaterials having a single polymer matrix layer in which the resulting release profiles are a function of degradation properties of the biopolymer (carrier) and the rheological properties of the eluting substance (drug). Careful consideration of controllable factors such as polymer type, layer thickness, drug/agent use, and spatial distribution can result in distinctly, defined temporal release patterns.

1.5 Coating Technologies

A number of technologies have been applied for the deposition of polymer thin films onto metallic substrates, each having their own advantages and disadvantages. Techniques such as sputter deposition use a physical vapor deposition (PVD) process, which involves the bombardment of the targeted coating material followed by the evaporation and transportation of the evaporated material to a particular substrate.

Sputtering offers great surface adhesion properties, a variety of grain sizes and orientations, and easy control of coating thicknesses. This process usually takes place inside a vacuum with line of site deposition making it difficult to coat substrates, such as stents, designed with undercuts and special features [35]. An important limitation with this process is the restricted amount of control over the vaporized coating material as

they are transported to the substrate resulting in wasted material. Lastly, some of the targeting coat materials are susceptible to premature degradation due to the ionic material used during the bombarding process [35].

The electro-spinning and -spraying techniques both use electricity, or an applied voltage as the source for carrying out deposition processes. The electro-spinning requires a high voltage to be applied to the coating solution, which has been previously loaded into a spinneret [39]. Once a voltage is applied to the spinneret it is subjected to a whipping motion and a continuous jet is ejected. This continuous jet is collected on an oppositely charged substrate. This process is more appropriate where a mesh-like coating with high porosity is desired.

Dissimilarly, the continuous jet emitted from a stationary metallic or glass capillary during the electro-spraying process is subject to electrostatic forces, which result in a cloud of positively charged particles. The particles are then deposited onto an oppositely charged substrate [36-39]. Both the electro-spinning and spraying processes are able to deposit highly porous films using a variety of different materials. They each have displayed high tensile strength and tunable mechanical and degradation properties. Neither of the two methods requires the use of heat, making them ideal for the use of biomaterials. However, they do result in high amount of wasted materials and lack precision abilities for patterning.

The dip coating and spin coating deposition processes are less complex yet they provide a more uniform coatings. The dip coating process is good for coating more complex structures and has a high deposition and processing rate [40]. This process,

however, does not provide variance as far as spatial control and is also inflexible in terms of switching out coating materials. The spin coating process is also an extremely fast paced process, however it is limited to possessing only one substrate at a time. It also lacks in the areas of material efficiency (only two to five percent of deposited material left on the substrate), repeatability, and thin film deformity. Lastly, this technique cannot accommodate the need for coating two or three-dimensional structures [41].

A newer and more complex technique is one known as Layer-by-Layer self-assembly [42-44]. This is a process in which thin films are deposited by alternating layers of positively and negatively charged coating materials incorporating a wash step in between. This technique might offer a high degree of controlled thickness (atomic thickness), ability to coat a variety of materials such as biomaterials, the coating of difficult geometries. In contrast, this method also has its limitations. This process produces excess film build up, hence the need for a washing process in between layers and further study is required regarding the reaction between the charges coating materials and blood containing ions and polyelectrolyte (proteins). This process is usually performed in combination with another deposition method (e.g. dip coating, spraying) and so one might also notice some similar advantages and limitations to those already discussed [42-44].

As implicated, all of the processes mentioned allow for the manipulation of coating thickness and surface morphology to some degree, therefore providing some control over the fabrication procedure. Each process is capable of depositing varying types of materials such as metallics, polymers, and other organic materials for a range of

different applications. It has also been noted that the achievable film (or layer) depth for this set of deposition processes range from atomic to nano thicknesses. Though the aforementioned techniques all possess some desired features of a deposition process to be utilized for the manufacture of biodegradable coatings, they all commonly lack the ability to deposit precise and localized coatings of three-dimensional complex structures.

Inkjet printing techniques have been studied and applied as a method of drug delivery. The technique produces droplets of ink through a jetting process via a small aperture, such as a nozzle or glass tip, onto a media. Inkjet printing can be achieved using either of two methods [45]. The first, being continuous inkjet printing process. Continuous inkjet printing yields a continuous stream of ink that is broken down into droplets of uniform size and spacing. An electric charge is selectively applied to the droplets passing through an electric field and are retained and recycled into the system, whereas the droplets free of the electric charge are deposited onto the media to form and image [45].

1.6 Drop-on-Demand Inkjet Printing Technologies

More appropriately used is Drop-on-Demand (DOD) Inkjet printing process. This method produces droplets of ink as they are needed as opposed to a continuous stream. The need for electrical charge in a magnetic field as well as the complex and unreliable recirculation systems required in the Continuous Inkjet System are eliminated, making this system more desirable for coating of complex structures (picoJet technology). Jetting is observed through one of the following approaches: thermal, piezoelectric, electrostatic, and acoustic. The two most popular are thermal and piezoelectric.

The piezoelectric method is named after the deformation ability of the piezoceramic material used in the inkjet device. In it there are four different methods in which the piezoceramic material can function. The four methods include squeeze, bend, push, and shear. Squeeze mode ink jet can be designed with a thin tube of piezoceramic surrounding a glass nozzle. In a typical bend mode design, the piezoceramic plates are bonded to a diaphragm forming an array of bilaminar electromechanical transducers. In a push mode design as the piezoelectric rods expand; they push against the ink to eject the droplets. The shear mode design deforms the piezoelectric against ink to eject the droplets. In this case the piezo becomes an active wall in the ink chamber. Interaction between ink and piezoceramic is one of the key parameters of a shear mode print head design. For the purposes of this research, the piezoelectric approach would be more suitable as the thermal approach is expected to alter the properties of the biological agents used [45-48].

1.7 Research Objectives

This dissertation focuses on the application of a novel surface modification technique for developing functional coatings for metallic biomaterials. Inkjet printing offers several advantages such as the capability to produce coatings on extremely complex structures, deposition onto the outer surfaces only, and flexibility to change coating design and materials. This technique also allows for the adjustment of coating thickness with the objective of obtaining desired release patterns.

Direct write inkjet printing techniques were used develop multilayer coatings laced with a pharmaceutical reagent for the purpose of studying controlled release

kinetics. The coatings types were varied in concentration and thickness to determine how manipulating the two would affect the drug release profile. The reagent chosen, Paclitaxel, has been proven to inhibit accelerated cell proliferation in cancerous environments, thus biological testing was conducted to relate the drug release profiles to cell inhibition. Hemocompatability test were also conducted to relate drug release to blood coagulation on the functionalized surfaces.

In a second study, the direct write techniques were used to develop polymer coatings that would aid in corrosion retardation of magnesium alloys for orthopedic and vascular applications. It was believed that by manipulating droplet sizes and pitch distance as well as polymer type and thickness, that desirable corrosion rates based upon a given application could be obtained. Cell viability and surface interaction of the magnesium alloy and various coating types were also explored. The main objectives of this research are plainly stated:

1. Develop controlled release coatings using direct write inkjet technologies.
2. Study the relationship of drug release profiles to cell growth inhibition and hemocompatability of coated and uncoated metallic surfaces.
3. Develop polymeric coatings for corrosion retardation of magnesium alloys using direct write inject technologies.
4. Assess the corrosion behavior magnesium alloys (AZ31) with modified coating surfaces.
5. Assess the cell viability and biocompatibility of Normal Human Bronchial Epithelial cell after controlled magnesium exposure.

CHAPTER 2

LITERATURE REVIEW

2.1 Surface Modification and Functionalization

The surface modification and functionalization of metallic materials is being proven to be an essential step in making materials more biologically compatible with the human physiological environment. Its relevance has become intensely important in the medical field as different materials are explored for their use and performance in the development of transplant and surgical devices. As the need for more biocompatible surfaces arise, research scientist have began to focus their efforts on ways to enhance the physical, chemical, and biological properties of surfaces which they do not originally possess. The uses for multi-functional surfaces can increase the life span of implant devices and reduce the need for surgical procedures.

A number of processes that are employed for use in surface modification procedures are explained. These procedures are necessary to inhibit the profound environmental reactions to surfaces causing wear, corrosion, and fatigue. Biochemical modification through physical vapor deposition [49], self-assembly modification [50], and radio frequency glow discharge [51] are a few of the most popular techniques used.

Ferretti et al. argued that the advancement of self-assembled monolayers (SAM) could be sufficiently used for the development of monomolecular layered bionsensor devices [52]. By fabricating layers of biomolecular agents, which could simulate reactions with natural bodies, these devices could eventually be used to facilitate natural

functions [52]. An in depth review of processes to be used for this application accompanied by the advantages and disadvantages of each were described.

With an effort to improve thromboresistance, or blood compatibility, of a titanium alloy ($TiAl_6V_4$) for ventricular devices, recent research efforts have been focused on possible chemical surface modification techniques [53]. A silane-coupling agent (APS) was used to covalently attach a phospholipid polymer (PMA) through radio frequency glow discharge. The coupling agent was used to tightly bond together the PMA to the titanium alloy, where typically a reaction would not occur. PMA was chosen due to its excellent ability to reduce platelet adhesion and coagulation of the blood at the medical implant site [53]. Modification of the Ti alloy surface added functionalization to the surface, which would have otherwise been biologically incompatible. Characterization by X-ray photoelectron spectroscopy showed success of the surface modification procedures and thereby a reduction in adsorption of ovine sheep blood platelets [53].

2.2 Controlled Degradation of Magnesium for Surgical Implant Materials

Towards the study of Magnesium (Mg) and its alloys for its application in implant materials, it has been noted that the material exhibits excellent biocompatible properties (similar to that of the bone structure) [54]. Its high tensile and yield strength as well as its density makes it an ideal material for biomedical implant devices [54]. However, its position on the galvanic chart is an undeniable indication of its susceptibility to corrosion in certain environments. Several studies have been conducted in efforts to control the corrosion rates of magnesium-based implants long enough for the device to carry out its

intended purpose. Two of the major mechanisms found in literature include metal alloying and surface modification for controlled degradation of magnesium.

2.2.1 Alloying for Controlled Degradation of Magnesium

In a recent study, Gu et.al. studied the *in vitro* corrosion and biocompatibility of binary magnesium alloys. Nine binary magnesium alloys containing 1% weight, X, of a proposed alloying component (X=Al, Ag, In, Mn, Si, Sn, Y, Zn, Zr) was tested for their potential use as biomedical alloying materials [55]. Each of the proposed materials was subjected to preliminary testing to characterize its microstructural and tensile properties. Electrochemical and immersion tests were conducted to understand corrosion potential of each material. Finally, cytotoxicity and hemocompatibility test were conducted to determine the suitability of the materials for more specific biomedical applications (e.g. bone and blood vessel related cellular responses). Gu et. al were able to conclude that Mg-Al showed positive response for nearly all of testing [55].

Aluminum as a potential magnesium-alloying candidate showed improved strength of the material, reduced corrosion, acceptable cell viability and toxicity on fibroblast, osteoblast and blood vessel cells. However, other recent studies have proven aluminum to have neurotoxicant effects which have been associated with such neurological disorders as dementia, senile dementia, and Alzhiemer disease. In the same study zinc, as major magnesium alloying component, also showed similar and favorable characteristics as aluminum [55].

In another study conducted at the Laboratory of Metal Physics and Technology, scientist proposed two new Mg-Y-Zn alloys (ZW21 and WZ21) for use as implant

materials for blood vessel repair (Hanzi et al, 2010). The study focused on *in vitro* and *in vivo* electrochemical and biological responses through electrical impedance spectroscopy and standard immersion testing [56]. New alloys were compared to the first generation ZQ30 (Mg-Zn alloy) and a reference alloy, WE43 (Mg-Y-RE alloy) to characterize grain structure, corrosion potential, and degradation performance [56]. This reference alloy has been used in clinical trial settings as a stent was developed from this material and inserted into the aorta of a newborn patient. Upon characterization of the proposed alloys, the authors conducted animal testing in which sample disks of the WZ21 alloy (chosen because of its more favorable mechanical performance) were implanted into two Gottingen minipigs. The samples and surrounding tissues were extracted after 27 and 91 days and results proved that there was a significant reduction in foreign body reaction activity after more extended implant periods [56].

Many efforts have been made to develop magnesium alloy specifically for bone regeneration and repair. Li et al. propose a binary Mg-Ca alloy for use as biodegradable materials with the bone structure [57]. In this study Mg-Ca alloys of various calcium percentages (Mg-1Ca, Mg-2Ca, Mg-3Ca) were tested to determine structural and mechanical advantages to bone repair and its potential environmental behaviors. Immersion tests proved that the Mg-1Ca samples were protected from increasing corrosion rates due a protective layer formed on its surface from the electrolyte solution.

The findings of the preliminary mechanical and immersion tests led the authors to select Mg-1Ca to conduct further cytocompatibility and animal testing [57]. Mg-1Ca pins were manufactured and implanted into the left femoral shaft of 18 New Zealand

rabbits. The pins were removed after one, two, and three months and characterized by weight and degradation. Results showed that the pin had completely dissolved at three months post operation and that newly formed bone was detected using radiographic examination. However, the issue of premature degradation still remains and further effort must be made to synchronize rate of degradation with the rate of bone formation [57].

2.2.2 Surface Modification for Controlled Degradation of Mg Alloys

The research group at the Tsinghua University in Beijing, China reports that the appropriate application of surface modification techniques can be employed to increase corrosion resistance of Mg and Mg alloys, thus making this material one that could be used for bone replacement as well as a delivery mechanism to benefit human metabolism [58]. In addition, Gao and his research group used the heat-self-assembled monolayer (HSAM) technique to modify the surface of 4N-Mg biomaterials. This group conducted *in vivo* studies in which the treated and untreated magnesium materials were implanted into the thighbone of white rabbits to induce bone growth. They found that the modified surfaces were beneficial in reducing the rate of corrosion and that corroded magnesium content in the blood remained within a normal range [50].

2.3 Drug Delivery

Drug delivery is the idea of administering pharmaceuticals to patients needing medical treatment in specified dosages. There are several methods in which drugs have been delivered such as orally (through the mouth), topical (through the skin), transmucosal (through the nose), inhalation, and injection. These methods encompass the ability to delivery various types of drugs and biological compounds as vaccines, proteins,

and other therapeutic systems. Over the past few decades localized, or targeted delivery has become a favorable drug delivery method in that it limits toxicity to the human body by only treating the infected site [59]. This type of drug delivery system (DDS) also increases bioavailability of drugs [59].

An earlier inception of localized drug delivery involved the use of drug-eluting nanoparticles for the treatment of restenosis. Insertion of the nanoparticles was administered through a catheter apparatus. Researchers investigated the effect of two different agents, dexamethasone and an aminochromone antriproliferative agent, on restenois in a rat carotid and porcine coronary model [60-61]. The results showed promising signs towards the inhibition of restenosis. Furthermore, herparin anti-coagulation drugs were incorporated into the nanoparticles for testing in pig coronary arteries for the reduction of platelet deposits and desirable results were achieved [62]. The findings proved to be even more promising as it was observed that the nanosized particles could be dissolved into the arterial walls without damage to the treated site.

Another study integrated the use of a rat model to deliver the growth factors IGF-I and TGF-B1 from a biodegradable matrix previously coated onto a titanium plate to treat the instability of long bone fractures [63]. Biomechanical testing was incorporated to determine if the growth factors effectively enhanced the healing process. The results showed that complete healing of the fracture had not taken place 42 day after surgical implantation, however biomechanical strength was restored with two days of surgery. The results obtained from the coated group were significant compared to the controlled (uncoated) group [63].

2.4 Temporal Release

Recent studies have introduced complex biphasic/triphasic and tetra-layered systems when a series of treatments are required over an extended period of time. Careful consideration of controllable factors such as polymer type, layer thickness, drug/agent use, and spatial distribution can result in distinctly, defined temporal release patterns. Okuda et al. were able to develop tetra-layered nanofibrous meshes for *in vivo* testing to obtain timed-programmed release patterns [64]. Timed release was achieved by setting the parameters for fiber diameter, mesh layer thickness, polymer concentration, and the use of a barrier mesh with controlled thickness. Each layer was fabricated using electrospinning technique and a polymer solution doped with two different types of dyes to simulate the release of pharmaceutical compounds [64].

Li et al. present a method for achieving well-defined spatial and temporal release profiles for a drug-eluting MEMS device loaded with various compounds to be released sequentially [65]. Fabrication of the MEMS devices requires the use of an etching process and a silicon substrate to etch strategically placed, well containing reagents. The wells were covered with a gold membrane expected to corrode based on electrochemical principles [65]. In the article titled "Modeling and Simulation of drug release from Multi-layered Biodegradable Polymer Microstructure in Three Dimensions," cellular automa 3D modeling software was used to describe the dynamic behavior of multi-layered polymer structures with uniform and nonuniform chambers [66]. The article presents a novel method for modeling drug delivery microstructures. Polyanhydride was employed to create structures with various micro chamber shapes capable of

encapsulating a variety of different agents. The structures were stacked using glue to create a single multi-layered structure. The outer boundary was expected to degrade over time to promote sustained release [66]. A Monte Carlo based two dimensional model developed in the late 90's has been able to predict prolonged release rates of encapsulated drugs; however, the authors determined that a three dimensional model was needed for more valid characterization. The 3-D model was compared to that of the 2-D model using the same suggested parameters and findings were analogous. The authors then optimized the parameters and formulated a hypothesis that would test the models performance on two different types of multi-layered systems [66]. Results showed that cellular automa could be used as an accurate predicting model to characterize release behaviors.

2.5 Current Coating Technologies

The coating technique proposed for surface modification and/or functionalization of metallic surfaces is one that is unique to a specific application. In some cases it may be necessary to perform two or more different methods successively to achieve the desired results. This section presents a few of the widely used methods for coating metallic surfaces along with their advantages and disadvantages. Desirable characteristics for application of coating biological agents are also highlighted.

2.5.1 Electrospinning

The electrospinning process uses an applied voltage as its main source. The equipment setup can either be one that is vertically or horizontally mounted [39]. Electrospinning requires that the coating solution be loaded into a spinneret apparatus

where a high voltage is applied. Following the application of the voltage, the nozzle portion of the spinneret is subject to a whipping motion and a continuous jet is ejected (Figure 2.1). The collector, or substrate, having an opposite charge is placed opposite of the nozzle capillary where the coating material is deposited and the thin film is formed [39].

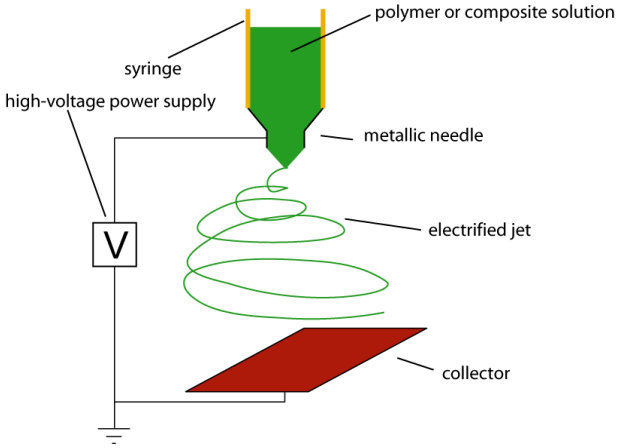

Figure 2.1 Schematic of the electrospinning process [43]

The process parameters having a profound effect on such measures as fiber diameter, pore size, film porosity, and film thickness include: electric potential; flow rate; concentration of the coating material; target motion; and the distance between the spinneret and the target substrate.

The process offers a number of advantages making it an ideal process for depositing bio thin films. For instance, the process provides a high surface-to-volume ratio, good tensile strength and the use of a wide variety of coating materials. It does not involve the use of heat and so it is ideal for the deposition of biological agents. Also, tunable mechanical and degradations properties can be achieved. Limitations of this process are subjective depending on thin film application [39].

2.5.2 Dip-Coating

The dip coating process can accommodate flat or cylindrical substrates. The substrate is submerged into the coating solution. It is during this step that deposition takes place. Withdrawal occurs at a constant speed and this is what determines the thin film thickness (Figure 2.2). For instance, the faster the withdrawal speed, the thicker the thin film layer [40]. Any excess liquid is drained from the surface and the solvent begins to evaporate. This process is repeated for each additional layer that is desired.

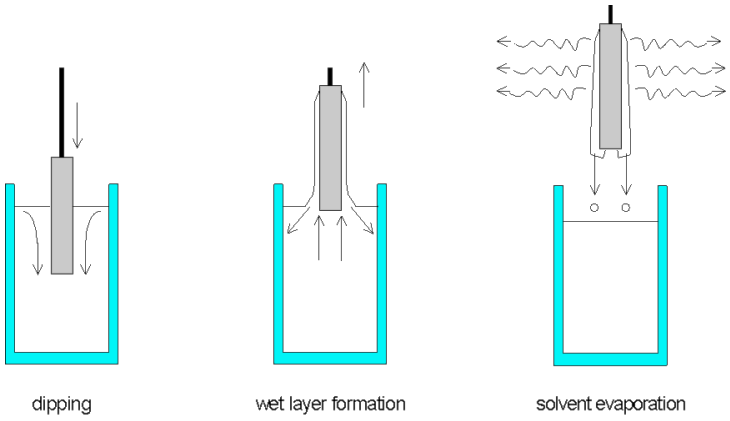

Figure 2.2 Schematic of dip-coating process

The goal throughout the deposition process is to obtain a uniform coating thickness with desirable film thickness and surface characteristics tailored to a specific application. The tunable process parameters include the withdrawal speed, gravitational acceleration, rate of solvent evaporation, number of dipping cycles, dwell time, and fluid properties.

Like many other thin film fabrication techniques, this process also has its advantages and disadvantages. For instance, dip coating is more suitable for coating substrates with complex shapes and undercuts. The production rate is extremely high as

multiple collectors can be processed at a single time. Contrarily, coatings cannot be spatially controlled and the changeover time is extended making the process one that is inflexible for coating layers of various materials.

2.5.3 Layer-by-Layer (Self-Assembly)

A newer and more controllable thin film fabrication technique is layer-by-layer deposition. This process involves the growth of thin films by depositing alternating layers of positively and negatively charged layers with a washing procedure in between. The bonding of the two charged layers is termed as a bilayer. Deposition of each layer is usually performed by a more simplified deposition technique (e.g. dip coat or spray) [43]. Measures of the film thickness, roughness, and porosity are usually a function of pH, ionic strength, and polyelectrolyte concentration (Figure 2.3).

Due to the compositions of ionic bonding layers, one might be able to insinuate that a great advantage of this coating process is the fine control of drug loading and layer thickness. With this process atomic monolayers of the coating materials are achievable. Concurrently, a wide variety of coating materials from biological agents to metallics can be deposited onto complex geometries. This process does, however, pose several limitations in that an extra washing step required is due to excess film build up, also implicating a high volume of wasted material. In addition, it was mentioned that further studies must be conducted to study the reaction between the charged coating materials and blood containing ions and polyelectrolytes in proteins [44].

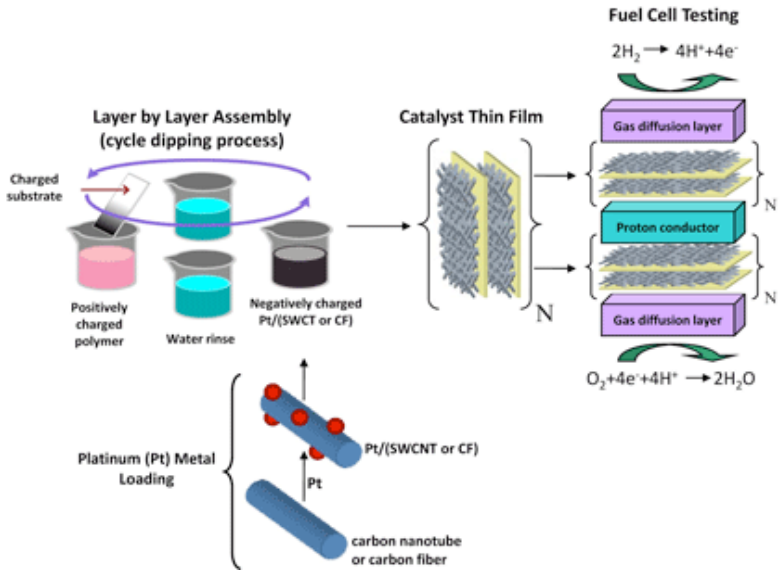

Figure 2.3 Schematic of layer-by-layer assembly process [45]

2.5.4 Sputter Deposition

Sputter deposition is a physical vapor deposition process in which a discharge of sputter gas, usually argon, is directed at a target containing the coating material [35]. The reaction between the gas (or ions) and the target materials brings about a sputtering reaction, which initiates the transport of atoms from the target to the substrate (Figure 2.4). The sputtered atoms are condensed on the substrate resulting in a thin film coating.

A great advantage to the application of depositing biomaterials is that this process does not require the use of heat, which could possibly alter the biological properties of the substrate. In contrast, the bombardment of the ions may introduce impurities to the collector, or substrate, thus resulting in its premature degradation. Use of this technique also provides the enhancement of adhesion to surface and easy control of film thickness. Nevertheless, the transportation of atoms is non-directional so consequently they may be

deposited on any surface within the vacuum chamber [35]. This can result is elevated amounts of waste.

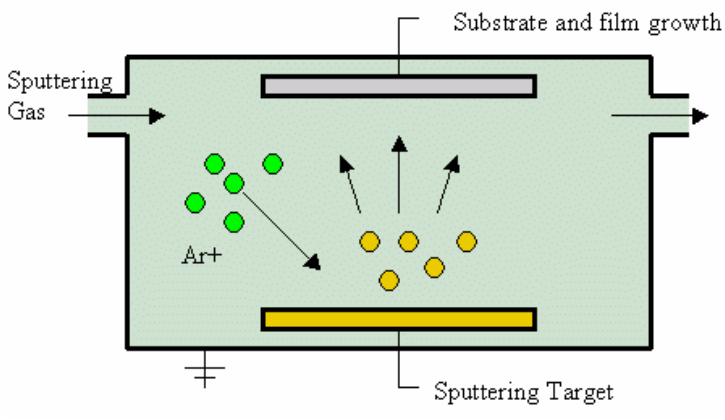

Figure 2.4 Schematic of electron sputtering process [46]

2.5.5 Spin Coating

Spin coating techniques have been used to apply thin films with less than 10 nanometer thicknesses. The procedure involves discharge of the bulk coating material from a nozzle onto the substrate, previously loaded onto a rotational tool. The loaded substrate containing the coating material is then subjected to high centrifugal forces causing the fluid to be directed to its edges [41]. During the rotation process the solvent begins to evaporate resulting in a thin film coating (Figure 2.5).

Spinning is a rapid process and the variables required to adjust the coating thickness is limited [41]. The primary process parameters include spin speed, viscosity of the coating solution, and spin time. The use of this process, however, is limited in that it can only coat flat surfaces one substrate at a time resulting in a low production rate. Literature also suggests that after completion of deposition only two to five percent of the loaded coating solution remains on the substrate. It seems, however, that the greatest

drawback is low repeatability and difficulty to maintain a uniform film despite consistency of the processing parameters. This issue results in a number of unusual deformities that may be undesirable for certain applications.

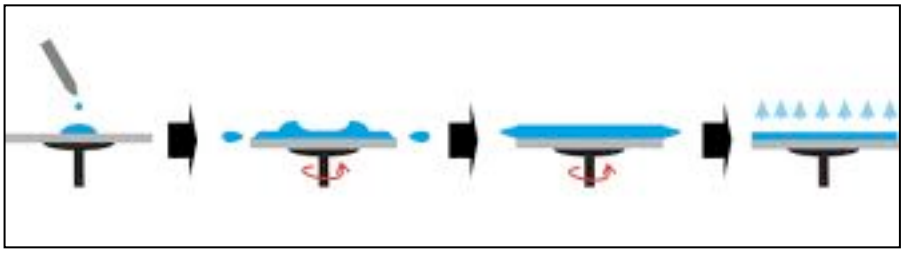

Figure 2.5 Schematic of spin coating process [47]

2.5.6 Electro-Spraying

Electro-spraying deposition is another apparatus that employs the use of electricity to coat thin films. The electrostatic forces applied to a continuous stream of the coating materials aids in the deposition process [36]. During this process, the liquid at the capillary becomes unstable to the point were it can no longer hold the charge and disperses into a cloud of highly charged particles (Figure 2.6).

The process parameters having a profound effect on such output measures as film thickness, morphology, uniformity, and porosity include the following: growth rate, solvent evaporation rate, concentration, spray temperature, and deposition time. This process, however, is extremely sensitive to the physical properties of the fluid and is limited to the use of solutions with low conductivity. Advantages of the electro-spraying techniques are that it does not cause damage to the deposited biomaterials. Also, high definition efficiency can be achieved (about 80%) [36-38].

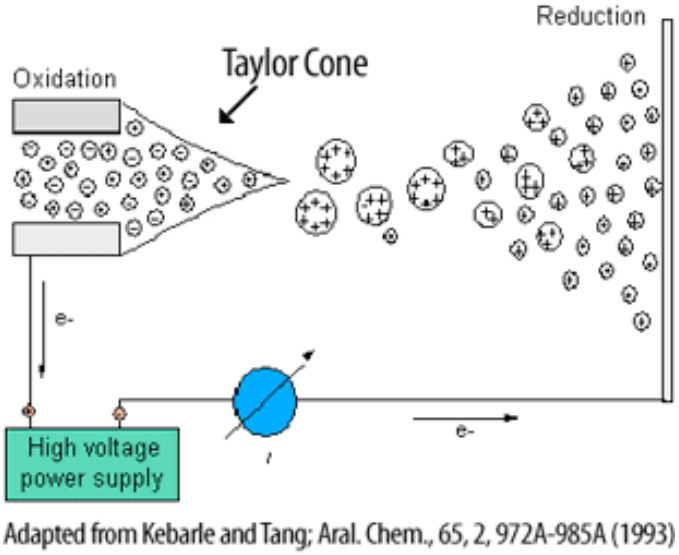

Figure 2.6 Schematic of electro-spraying process [48]

2.5.7 Coating Processes for Drug-Eluting Stents

Careful consideration is required when determining the appropriate technique to be used for the fabrication of biological materials and thin films. Processing that involves the altering of biological agents and/or their characteristics such as those that require the excessive use of heat or elevated pH or acidity levels should be avoided. When coating surfaces of drug eluting stents the drug containing solution should not be subjected to processes in which excessive heat or inappropriate pH levels would alter the performance characteristics of the device *in vivo*.

Researchers at the National Cardiovascular Center Research Institute developed a multi-drug-eluting stent with micropores to reduce neointimal hyperplasia and minimize coagulation of blood platelets at the implant site. The dip coat method was used to deposit a layer of segmented polyurethane (SPU) onto the inner and outer surfaces of a Palmaz-Schatz stent manufactured by Johnson and Johnson. A excimer laser apparatus

was used for micropore fabrication and then again to ensure immobilization of the heparin coating (inner surface) and FK506 immunosuppressant (outer surface) coatings that were applied [67].

The coating method that was chosen aided in the prevention of plaque build-up within the struts of the stent, limiting thromboresistance. The technique resolved the issue of the undesired structure of the luminal surface resulting in the flat surface needed for experimental success. The irradiation process used for the immobilization process did not pose any threat to the functionality of the chosen biological agents. *In vivo* results showed that the multi-drug coating did reduce neointimal hyperplasia and thrombosis [67].

Another study claims the development of a novel biodegradable polymeric matrix-coated cardiovascular stent for controlled drug delivery through the use of an individualized drug-eluting stent system to abrogate restenosis (ISAR). The authors here use a modified air suspension coating technique in which the wire mesh-like stent is suspended vertically between two hooks that are linked to the coating device. The coating solution reaches the 0.2mm diameter nozzle while under gravitational influence and is eventually ejected from the capillary and subjected to a pressure drop atomizing the liquid into fine droplets. Multiple layers (4) of coating solutions were collected on the rotating stent [68].

It was observed that the coated stent in this study maintained a standard uniform coating free from impurities following the successful optimization of parameters such as gas pressure, flow rate of the solution, and distance between the nozzle and stent.

Mechanical properties of the coating were also tested at stent site and subjected to the maximum permissible stress. The results of SEM imaging and the findings of film stability confirmed complete adhesion of the film. Finally, processing of the coating materials through the use of gravitational forces and air pressure did not result in the alteration of either the biological components or substrate [68].

In a research study published by the American Heart Association, an on-site coating apparatus is used to apply pharmaceuticals for the direct use of drug eluting stents. The process maintains sterility throughout the duration of the application period. The drug-eluting stent fabrication design allows for individual doses of a specified drug in a drug reservoir to be connected to a disposable stent cartridge under sterile conditions. The stent, mounted onto a balloon catheter is positioned inside of the disposable cartridge and is ultimately motioned horizontally through a ring containing three nozzles. Upon application of the coating solution via spray coating mechanism, the stent is dried by sterilized air pressure and is removed for immediate use [69].

A process such as this was necessary to ensure that materials are free from contamination. Given that the deposited solutions are bare drugs, appropriate precautions were taken to ensure that the functionality of the drugs is not disturbed. The coated drug-eluting stents were immediately used for inhibition of neointima, or accelerated growth of unwanted cells.

The recent application of this method was carried out for the fabrication rapamycin-eluting stents [70]. The systematic release of probucal was also reviewed. This non-polymeric coating technique was sought as a method to deliver drugs in a way

that does not introduce unnecessary cardiac events into the healing process. To assess the effectiveness and safety of these newly developed stent coating techniques, rapamycin and polymer coated stents as well as a control (bare metal stents) were placed in a porcine model where the effects of fibrin deposition was closely monitored [70]. Results showed that fibrin deposition was significantly higher in biodegradable polymer-based stents.

2.6 Uses of Ink-jet Printing Technologies

The use of inkjet printing technologies for the deposition of biological materials is becoming more relevant for applications in biomanufacturing. The non-contact printing technique has been used for the fabrication of solid and multilayered microspheres, deposition of biopolymeric materials for uses in tissue engineering, and bioMEMS and microfluidic applications [71]. Inkjet printing, also referred to as a direct-write process, offers several advantages in the deposition of biological agents such and DNA, proteins, and growth factors for tissue engineering applications. A primary advantage is that during the deposition process, the coating materials are not subjected to elevated temperatures that could potentially alter both the biological and fluidic properties [71]. Other advantages of this technique are its ability to produce highly uniform microdroplets as well as a precise deposition tool to fabricate very small and complex structures. A full list of advantages can be found in Table 2.1.

In an article released from MicroFab Technologies, Cooley et al. presents inkjet printing as a suitable technique for manufacturing biological micro-electromechanical systems (bioMEMS) [72]. The current technique for the fabrication of these devices consists of photolithographic process that requires exposure and/or etching of

biomaterials to create a pattern or coating. The etching process lacks control, which affects the thickness of the applied coatings. The direct-write technique is a safe procedure that does not introduce harmful chemicals. It is a three-dimensional printing process that allows for easy manipulation and achievement of uniform coating thicknesses [72].

Table 2.1 Advantages of Direct-write inkjet technique

Advantages of Direct-Write Inkjet Printing
1. Non-contact, reduced cross-contamination of substrates 2. No thermal influence 3. Precise and accurate printing 4. Prints a variety of materials and biomaterials on a variety of substrates 5. Fast Process 6. Low start-up cost 7. Data-driven and safe process 8. No chemical waste

The inkjet printing process may be achieved using one of three different methods: thermal, continuous, or piezoelectric drop-on-demand. For reasons mentioned above, the use of the first two methods have been discouraged for printing biological agents onto small, complicated structures.

In a recent study, also conducted in conjunction with MicroFab Technologies, Inc., a standard JetLab system was used to fabricate PLGA microspheres, which had been loaded with paclitaxel drug and thin films of fenofibrate for stent coating applications. The materials selected were required to meet four specific criteria: 1) the ability of the material to degrade after performing its drug delivery function 2) the ability to sustain cell viability 3) the ability to sustain proper cell functioning and 4) the ability to be jetted at high concentrations for extended time periods [73].

Drug release and bioactivity of the drug containing microspheres and thin films were observed using UV spectroscopy and MTT assay respectively. The results obtained showed that the drug containing microspheres were able to sustain release of the paclitaxel drug for at lease 50 days with 80% of the loaded drug being released. The results of the MTT assay proved that the inkjet printing techniques did not alter the functional properties of the drug [73]. Attesting to the claims of high speed and accurate deposition, release profiles from the coated stents demonstrated that this technique could be used to improve drug-loading efficiency as compared to other coating techniques.

A more recent study was conducted to revisit the use of commercial inkjet printers and ink cartridges, which have been modified for bioprinting applications [74]. Khan et al. sought to prove that when using a modified inkjet printer, the short period of time in which bio-inks containing proteins are subject to elevated temperatures are negligible and, in fact, enzymatic activity was present after printing[74].

The need for a more suitable deposition technique for stent coating applications is desired that can achieve high drug loading efficiency through accurate and localized printing methods and maintain extended drug release periods. A review of current deposition methods for biofunctional surface modification applications has been presented, each with their parameters, benefits, and limitations. It has been shown that, while each technique has its list of advantages, they are relevant only for certain applications. The use of other more conventional deposition methods has been discouraged whether it be for issue with substrate contamination, lack of control during

the deposition process, or the possibility of decreasing bioactivity upon being subjected to heat or some harsh chemical.

Many techniques have been used to coat drug-eluting cardiovascular stents for drug delivery and a combination of techniques have been used to grow multilayer thin films. However, none have employed the use of piezoelectric direct-write systems to develop polymeric coatings for corrosion retardation of magnesium alloys and drug release of antiproliferative cancer drugs.

CHAPTER 3

METHODOLOGY

3.1 Overview

Direct-write printing is a novel method that is currently being considered for the development of targeted and precise polymer coatings for a vast number of biomedical applications. More specifically, these coatings can serve as protective barriers when applied to the surface of an implant device and/or be used as a mechanism for the delivery of anti-proliferative drugs via a coated stent model system. The device or stent model system consists of the substrate, or biomedical device, in which the coating is applied, and the coating itself. The nature of the coating can take a variety of forms with the ultimate goal of achieving a specific release profile.

In the sections to come, a system of experiments is described that will provide an understanding of the factors which have a profound impact on drug release profiles from biodegradable thin films fabricated using direct-write printing technologies. A second set of experiments will describe the effectiveness of polymeric coatings, applied using this same novel technique, for the retardation of magnesium corrosion. Details of the experimental design and process description will be provided followed by a mention of the possible challenges.

3.2 General Approach

Titanium and its alloys are among the list of metallic biomaterials used to manufacture surgical implant devices (i.e. stents, orthopedic implants). Other noted metals include stainless steel and cobalt-based alloys. Metallics as biomaterials are ideal

due to their ability to resist the fatigue, wear, and fracture sustained from the daily forces present in the body. The inert presence of these materials also makes them ideal for use within the body, as they do not present any obvious adverse effects when implanted into the host site. Many of the cardiovascular stents on the market are made using stainless steel; however, this dissertation will employ the use of polymer-coated titanium alloy substrates as a model system to simulate the behavior of drug-eluting stents because of their strength and biocompatibility in biological environments.

Despite the excellent strength and corrosion resistance properties of titanium for the manufacture of biomedical devices, there exist some limitations. The most important is that the surface oxidized layer, which forms after the natural reaction between the titanium atoms and the oxygen atoms present in body fluids, can also be disrupted by the metallic ions. Extensive research has been conducted that suggest different ways in which surface modification of titanium can enhance its biocompatibility. Also, since the introduction of synthetic and biodegradable polymers for biomedical uses in the early 1900's, they have been successfully applied in a number of ways to advance the properties of metallic biomaterials.

Hwal Suh, suggests three classifications of polymeric biomaterials in an article titled, "Recent Advances in Biomaterials" [75]. The use of biodegradable polymers to coat metallic materials not only add flexibility to the metal but also provides the additional benefit of mimicking the functionality of the surrounding tissues present at the host site. As a result the implanted material is able to remain at the implant site for extended periods and not pose any immunological threat. Biodegradable polymers have

the ability to absorb within the body, and in some cases, regenerate lost tissue and or cells.

An added dimension to the use of biodegradable polymers for coating medical devices is their ability to sustain and transport medicinal drugs for prolonged drug release. This is possible due to the natural characteristics associated with a specific polymer type. The degradation properties of a given polymer type is one factor that has a significant effect on the time in which it is capable of sustaining drug release. A second factor is the physiological environment in which the degradation process takes place. Some commonly used biodegradable polymers for drug delivery include poly-(lactic-co-glycolic acid) (PLGA) [76-78], polycaprolactone (PCL) [77,78], and poly(ether urethane) urea (PEUU) [78].

The listed polymeric biomaterials all possess exceptional biocompatible and biodegradable properties. As such, they have been approved for use in the human body specifically for drug delivery applications. However, research is currently being conducted to improve its biostability. The degradation rates of these polymers have the ability to be manipulated such that a desirable rate of release may be achieved [78]. For instance, PLGA, which consist of the natural monomers lactic and glycolic acid, can be manufactured in such a way that the ratio of lactic acid to glycolic acid is 75:25 resulting in a faster degradation rate. Several other advantages to the use of these polymers support the decision for its use.

Drug release rates not only depend on the polymer type, but also the pharmaceutical agent and a specified dosage. The types of drugs chosen to deliver drugs

from cardiovascular stents are numerous, yet they are dependent on the application. For instance, if the main purpose is to prevent coagulation of blood platelets or increase blood compatibility of the device then the choice of drug may be Heparin. Chemotherapeutic drugs have also been used to treat late stage lung cancer patients [79]. A common drug that is used to inhibit the increased growth or proliferation of unwanted cells around the stent device is Paclitaxel, also referred to as Taxol [80].

Paclitaxel is an antimicrotubule agent that is used to treat an array of cancers (e.g. breast cancer, lung cancer, ovarian cancer). This drug is usually used after other treatments have been explored and have resulted in failure. Uses of this drug in excess can lead to depletion of the white blood cells needed to fight infection thus resulting in fatality. Ideally, this drug would be delivered in small amounts over extended periods of time, making it the perfect candidate for testing release from biodegradable polymers [80].

The use of bioinert metallics can eventually lead to foreign body reaction following implantation due to the body's inability to recognize the material as one that compliments normal physiological processes. Thus, magnesium and its alloys have been identified as a lightweight metallic biomaterial that can withstand the daily forces imposed by natural body function. It is also the fourth most abundant element found in the human body making it essential for many of the physiological processes. Magnesium is an ideal candidate for surgical implant materials because of its ability degrade after performing its intended purpose without posing any toxic effect to the body.

Although, magnesium has been identified as an ideal candidate for surgical implants such as cardiovascular stents, the issue of its fast corrosion rate still remains. Thus, in a second study we propose that the application of biodegradable polymeric thin films can be used as a method for retardation of the corrosion process.

The deposition process for loading the drug containing polymer matrix onto the titanium substrate is one that should also be carefully chosen, particularly for coating complex structures such as stents. A description of the commonly used deposition processes for surface coating and modification is found in preceding chapters.

Direct-write inkjet printing offers several advantages to the process of coating metallic devices such as stents for biomedical applications. One main advantage is the ability to print local and precise patterns onto three-dimensional structures. With stent coating the ability to print precise patterns is ideal because of its complex, helical, mesh-like design. This technique also prevents webbing of the coating materials, which has been known to alter the stents functionality. Direct-write printing techniques also permit biological agents such as drugs and proteins to be deposited without altering their physical and chemical compositions.

The present research uses the direct-write inkjet printing technique to 1) deposit biodegradable polymer thin films, laced with the antiproliferative paclitaxel drug, to coat bioinert titanium substrates and 2) apply polymeric thin films to a magnesium alloy as a protective barrier for corrosion retardation.

3.3 Governing Facilities and Equipment

This research is conducted in conjunction with the National Science Foundation Engineering Research Center (ERC) located in the Interdisciplinary Research Center at North Carolina Agricultural and Technical State University. The present study is only a small segment of the ongoing research within the ERC which consists of three Engineered Systems: (I) Craniofacial and Orthopedic Applications, (II) Cardiovascular and Thoracic Devices and, (III) Responsive Biosensors and Neural Applications. Research at the center relies on four enabling technologies: biodegradable metals, biofunctional surface modification, sensing and controlled degradation and, controlled release. This dissertation will focus on the ES-II component driven by biofunctional surface modification and controlled release technologies.

3.4 Fundamental Challenges

Several challenges have been noted, however they are not expected to have a significant impact on the validity of this research. The first challenge is that, although we are using planar titanium substrates as the model stent (which are actually three dimensional), the direct-write system used in this research is not actually capable of printing on these types of structures. A second challenge is that the consistency between batches of biological agents and polymers could see small variations in their physical properties, which could have an effect on the outcome of the experimental results. These variations can be taken into account in the analysis portion of the research to ensure that this research effort remains valid.

Pertaining to the direct-write inkjet printing technique that will be used to coat the titanium substrate, there are several challenges that may be encountered. For instance, this technique is limited in the fluids that can be jetted. Fluids having non-Newtonian properties, which are highly viscous, may not be appropriate for deposition by this technique. Thus, drug loaded carriers or thin films may not be loaded with a realistic dosage of drugs needed for treatment. Also, this process is sensitive to the properties of the fluids being jetted making it difficult to obtain the optimal jetting parameters for a given fluid concentration. As a result, the jetting optimization process can be time consuming making it sometimes infeasible to obtain a large number of samples as might be suggested from conducting a statistical power analysis. Moreover, the optimal jetting parameters obtained for a given fluid varied from one user or jetting session to the next. Though not able to be completely eliminated, these challenges were minimized by designing a protocol for reaching optimal jetting parameters as well as equipment training sessions.

3.5 Methods and Materials

This section will provide a description of the processes and factors, which are expected to have a significant effect on the output parameters. The output parameters are also stated with a description of each to follow.

3.5.1 Direct-write Equipment and Jetting Optimization Process

The deposition technique chosen for this research is a modified inkjet printing technique designed by MicroFab Technologies Drop-On-Demand Test Stand inkjet system (MicroFab Technologies, inc., Plano TX). This system consists of a pneumatic

controller, a MicroFab JetDrive III external waveform generator with heat source, JetServer software with waveform amplifier, horizontal- and vertical-plane optics system and a piezoelectric nozzle tip with a 50-micron orifice diameter [48]. The schematic of the MicroFab test stand is pictured in Figure 3.1.

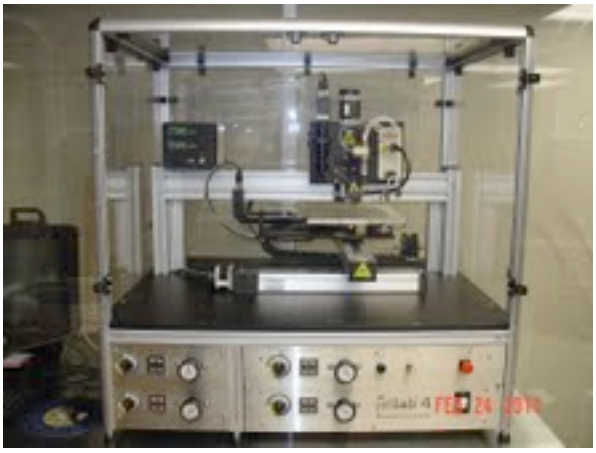

(a)

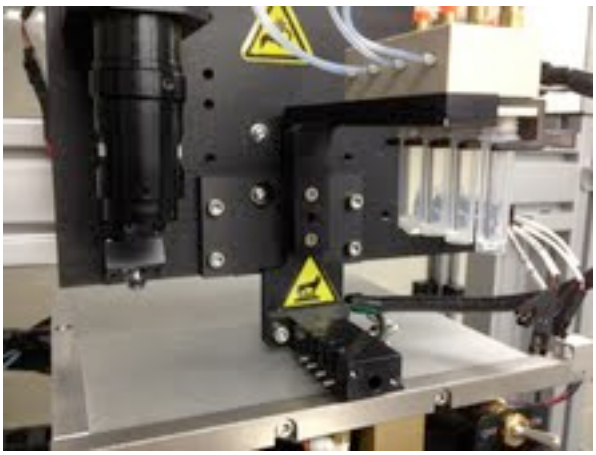

(b)

Figure 3.1 (a) Depiction of MicroFab JetLab 4 inkjet printing machine (b) nozzle printing apparatus and motion panel

Direct-write inkjet printing can be accomplished using one of two different inkjet technologies, Continuous (CIJ) and Drop-on-Demand (DOD) inkjet printing. More

suitable for this research is the DOD (or direct-write) technology. This method requires electromechanical pulses (or an applied voltage) over a piezoelectric material that causes the material to deform. The deformation of this material causes an increased pressure within the nozzle after which a single droplet is ejected [48].

After the droplet is ejected, there is an obvious reduction of fluid volume within the solution-containing reservoir, thus the solution must be replaced. As the piezoelectric crystal returns back to its resting state, a negative pressure forces the replacement of the ejected fluid [48]. A list of the input parameters required to characterize the above described process is in Table 3.1.

Table 3.1 List of piezoelectric Direct-write parameters

Piezoelectric Direct-Write Process Parameters
1. Frequency 2. Jetting Voltage 3. Waveform (driving signal) 4. Print head Design 5. Jetting Fluid Properties

It is desired to optimize the jetting process to achieve a steady stream of uniformly shaped droplets for the deposition of thin film coatings onto prepared titanium substrates. The parameters, which influence this optimization process, include: pulse waveform, print head design, and jetting fluid properties (Figure 3.2). A description of the print head design has been discussed previously. It is designed to include a nozzle orifice as low as 10 micrometers in diameter where it is expected that the variations of the droplet size (diameter) distribution from the orifice diameter may be neglected.

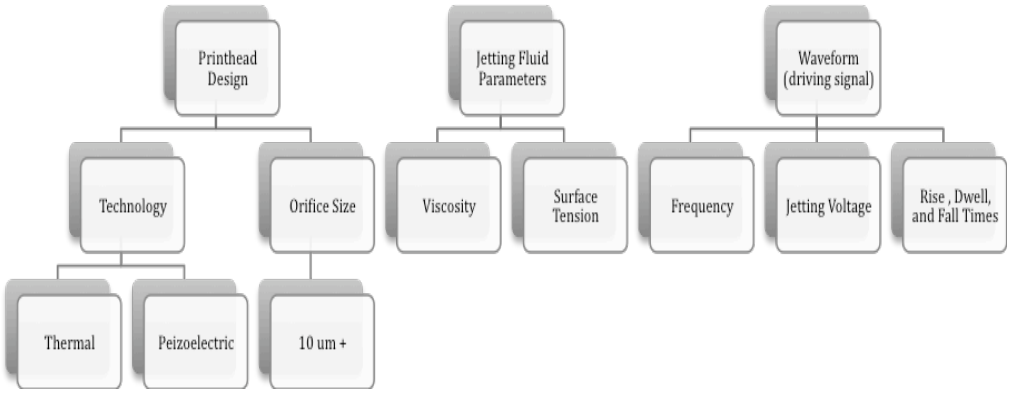

Figure 3.2 Direct-write process parameter relationship

The pulse waveform requires its own set of parameters that can be optimized for the manipulation of drop size and speed, jetting sustainability, drop placement and drop uniformity. The waveform parameters include the frequency, positive/negative jetting voltage, rise time, dwell time, fall time, and final rise time denoted by f, $+V/-V$, T_R, T_D, T_F, and T_{FR}, respectively. Where the jetting voltage is the optimal voltage $(+V)$ applied causing deformation of the piezoelectric material. $-V$ is usually set at 0, setting the voltage back to 0 and returning the material back to its initial resting state [81].

The rise and fall times with respect to the characterization of the pulse waveform are the time for the driving signal to reach the optimal amplitude (voltage) and the time for which it takes to decrease the voltage back to its original state. The dwell time that the optimal voltage is applied to the piezo material and the frequency refers to the number of drops jetted over a given time span. Figures 3.3 (a) and (b) below depicts the resulting waveform for piezoelectric direct-write processes and the MicroFab JetServer interface used to vary these parameters respectively.

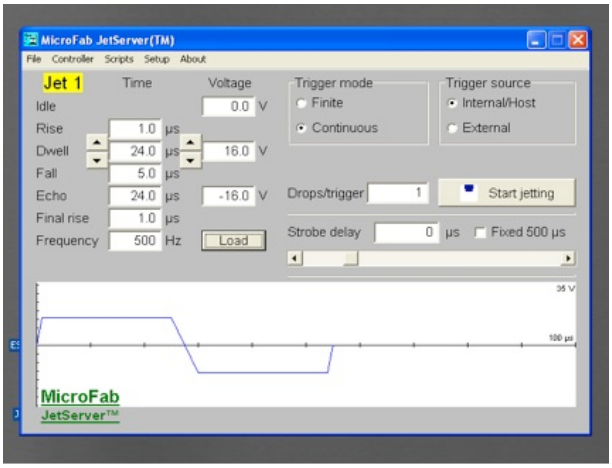

(a)

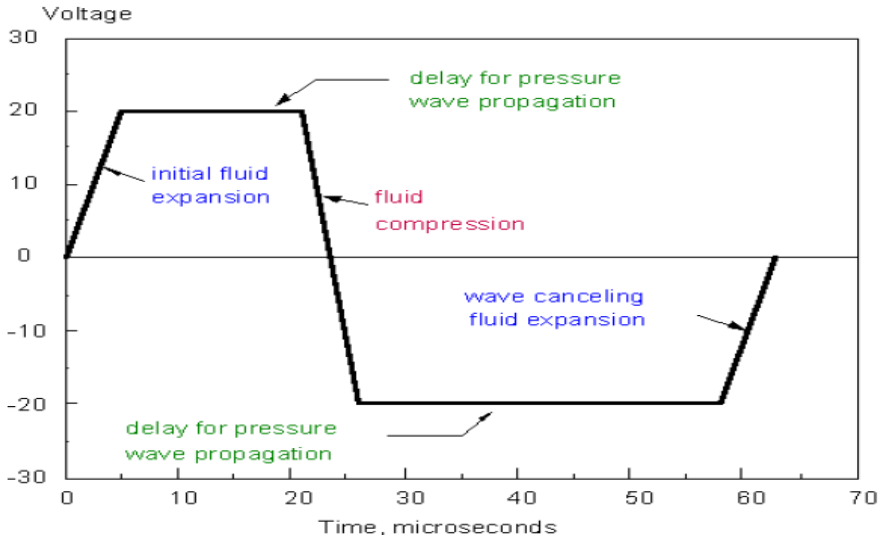

(b)

Figure 3.3 (a) Depiction of JetLab interface (b) pulse waveform formation

Much research has been conducted on the manipulation of the waveform shape and parameters to determine their effects on the jetting process. Such a parameter that contributes greatly to the success of the jetting process is jetting stability. The jetting stability is greatly affected by the retraction of the meniscus (fluid surface at the nozzle tip), which is directly related to the reservoir pressure resulting from T_F. Polymer

buildup at the nozzle tip negatively affects the success of the jetting process. In literature this is referred to as puddling and is directly related to the frequency of droplet accumulation.

A final parameter having a significant effect on the jetting process is the jetting fluid chosen and its associated fluid properties [82]. The fluid properties significantly affects the jettability of a substance, which is the fluid's ability to maintain a jet stream of droplets for an extended period of time (e.g. two to three hours). Jettable fluids can be broken down into two categories: Newtonian and Non-Newtonian fluids [82]. This research deals with polymeric solutions, which display Non-Newtonian properties, that is, fluids with high viscosity, density, and surface tension values.

The manipulation of fluid properties can be obtained by varying fluid concentration (in this case, polymer concentration) given a solid polymer percentage (weight, %) and solvent (volume, mL) to obtain a weight/volume solution. More specifically, the concentration of a given polymer such as poly(lactic-*co*-glycolic acid) (PLGA) used in our experiments, can be altered by adjusting its ratio of lactic and glycolic acid to obtain a higher concentration of solution thus resulting in a higher viscosity. The effects of the fluid properties directly relate to tail break-off of the jetting solution. Also, a more viscous solution will have a longer tail (break-off period), which will slow the drop speed.

Residual vibrations may occur even after a single drop has been ejected and could influence the nature in which the resulting drops are ejected. Robustness against disturbance deals with the optimal parameter settings and system abilities in dealing with

such disturbances as dust and air bubbles that could stop the jetting process. Lastly, aging of the piezo material could have a profound effect on the optimal achievable jetting process parameters. There are many other operational issues that could limit the optimality of the direct-write printing process, however, these issues were controlled to the best extent possible.

3.5.2 Characterization of Coating Morphology and Thickness

Surface morphologies were characterized using optical and scanning electron microscopy. The use of this technique allowed for monitoring any changes regarding the coating surface, not only before and after optimal release has occurred, but also to track any possible changes in thickness during sample collection periods. This is due to the non-destructive nature of the imaging process. For further characterization, SEM imaging may be used before and after sample testing periods but only for general characteristics across groups of samples at the same stage in the testing process. This is attributed to the destructive nature of SEM sample processing. The film thicknesses of the drug loaded polymeric coatings were evaluated by using both scanning electron microscopy and optical profilometer, respectively where the polymer film was cut to reveal the cross-section areas and thickness profiles. The SEM technique was also used for qualitative characterization of surface interaction between blood platelets and drug loaded polymer coatings. Images resulting from this technique were also used to quantify adhesion of the platelets to the surface.

3.5.3 Characterization of Drug Release

Release kinetics for the characterization of release profiles were measured using Ultra-Violet Spectrophotometry techniques. This technique is generally used to detect traces of a given substance within a sample by transmitting a source of light through its contents to measure its absorbance. The absorbance is measured over a given wavelength where a maximum absorbance is said to exist. For example, literature states that the wavelength for which the maximum absorbance reading for Paclitaxel may be obtained is somewhere in the realm of 227 nm. This wavelength value for achieving the optimal absorbance readings for the samples were validated using a Shimadzu UV-2450 Spectrophotometer to ensure repeatability. Performing serial dilutions on concentrated paclitaxel solutions and gaining absorbance readings from the UV spectrophotometer, we were able to develop a standard curve. The process described allowed us to calibrate and compare the release values on the standard curve to determine total concentration of the drug, which was released.

3.5.4 Selection of Materials

The placement of foreign bodies, specifically bare metal stents (BMS), within the human body can pose serious threats at the implant site. Moreover, the rapid growth of undesirable smooth muscle cells triggered by the presence of the foreign body is found to be a main cause of late-stage restenosis. The collapsing of the cardiovascular stent, due to excessive forces is caused by neointimal hyperplasia. Generally cardiovascular stents and other surgical implant devices are manufactured using metallic materials, such as

stainless steel, nickel, and titanium, which are not recognized within the physiological environment.

This research focuses particularly on the manufacturing and design aspects of drug delivery systems (DDS's). Thus, an actual cardiovascular stent will not be used. A bare titanium substrate will be used as a substitute. For the characterization of the controlled release coatings, 10x10 mm coupons were used primarily to scale up the drug concentration so that absorbance detection was possible. For biological testing, the titanium substrates used were round having an approximate diameter of 6 mm. The round shape of the substrates is necessary to conduct an MTT assay for the determination of cell proliferation later on in this study.

For the characterization of polymer coatings for corrosion inhibition, a magnesium alloy with the composition (Mg:90%, Zn:8.9%, Ca:0.5%, rest impurities) was smelted as ingots within an inert environment (argon) in our laboratory. The Mg alloy was used as-cast without further processing such as cold work or heat treatment. A flat piece (10mmx10mmx2mm) of this Mg alloy was casted into a disc-shaped epoxy resin so that only the top surface of the Mg alloy was exposed. This is because we are interested in studying the corrosion behavior of Mg alloy with different polymeric coatings on only the top surface without affecting the corrosion of the other sides. The sample top surface was then polished to eliminate the magnesium oxide layer.

The general expectations of a biopolymer suitable for coating cardiovascular stents is that 1) it must be biocompatible; 2) it must demonstrate selective permeability;

3) it must have the ability to biodegrade; and 4) it must demonstrate high mechanical strength. A depiction of the aforementioned (Figure 3.4) and a brief description follows.

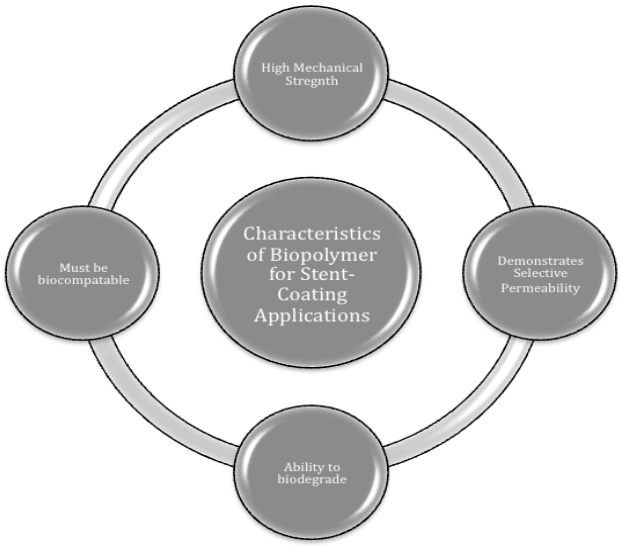

Figure 3.4 Characteristics of biopolymer for stent coating applications

Biocompatability of a polymer can be measured in a number of ways. One common measurement is to count the number of plasma protein, or blood platelets, that accumulate at the surface of the polymer over a period of time. If amassing is excessive than it can be concluded that that the polymer is biologically incompatible. A second qualitative measure is excessive tissue growth at the implant site. This leads to a discussion of mechanical strength.

In keeping perspective of the excessive tissue build up around the bare metal stent, the remaining requirements of a biodegradable polymer is further discussed. The application of a thin film biopolymer coating displaying high mechanical strength could aid in maintaining the structural vigor of the of the stenting device for lengthier periods of time. Alongside good mechanical strength is selective permeability. The polymer

membrane should maintain some level of control over what is allowed to cross it and the rate at which any substance (or drug) is allowed to do so. In a practical sense, the drug, paclitaxel, is expected to permeate through the polymer membrane at a controlled rate to slow the growth of the smooth muscle cells. The decreased rate of cell growth due to the controlled release of paclitaxel along with increased mechanical strength is said to decrease the probability that restinosis will occur.

The preparation stages are expected to be one of the most vital segments of the series of components involved. This is due in part to the extremely high volatility of the materials that will be used. Aside from that, the dosages of paclitaxel to be embedded into the polymer are so small that special care must be taken in making sure that all materials are measured accurately in order to decrease variations of the results obtained.

Recall that paclitaxel has been chosen to simulate release profiles for alternative drug-polymer systems. Paclitaxel (taxol) is a cancer treatment compound, which is derived from the bark of taxus brevifolia found in the Pacific. Taxol is commonly used to treat breast, ovarian, and late stage lung cancers as well as occurrences of restenosis within the arterial wall.

Though recently there has been much controversy to the use of this drug, its use as an inhibitor of the rapid division of undesirable cells has proven effective for the treatment of rapidly growing tumors and neointimal hyperplasia. The compounds effectiveness can be attributed to its ability to inhibit the breakdown process of microtubules, a major component of the cell division process. The molecular breakdown of paclitaxel is depicted in Figure 3.5 below.

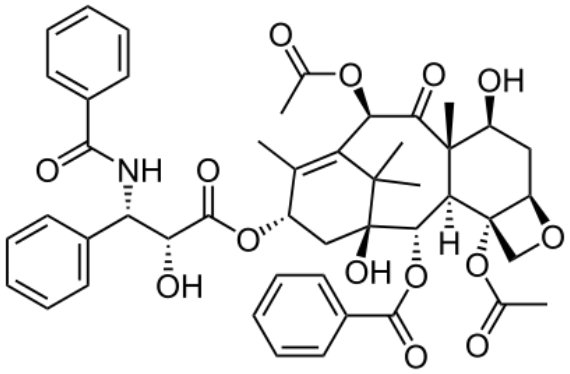

Figure 3.5 Breakdown of a single molecule of paclitaxel

The uses of paclitaxel for the drug-loaded polymer thin film coating is desirable for stent coating applications mainly because it has demonstrated properties such as anit-proliferative and anti-inflammatory on cell interaction. Drug-eluting stents, using paclitaxel, are necessary to inhibit unwanted cell growth that will prevent the re-narrowing of the arterial wall due to this growth.

Preceding the discussion of Taxol's dissolution mechanism, the mention of the difficulties in characterizing these properties is deemed necessary. It is important to understand the process by which this drug is obtained and how drug development can contribute to variations of its dissolution properties. For instance, a recently reviewed article attributes the challenges of describing the dissolution of paclitaxel to variations between batches of the drug resulting from the different environmental factors of which the drug was subjected. Examples of factors that influence these variations include; weather, soil composition, water and sun. It is inferred that these factors could indirectly impact the repeatability of dosages required to treat tumor growth and, in our case, neointimal hyperplasia.

Aside from possible variations between batches of the drug, paclitaxel has demonstrated low solubility within the physiological environment. This phenomenon been demonstrated *in vitro*, via studies of dissolution after incubation in phosphate buffer saline (PBS) solution at 37 degrees Celsius to simulate physiological environments as well as *in vivo* in numerous rat models. Taxol is generally mixed with harsh solvent to relax its dissolution. It has been noted in recent *in vitro* studies characterizing the insolubility of paclitaxel that increased concentrations of the drug between 1% and 5% w/v, homogeneously dispersed in aqueous polymer solution, begin to crystallize following polymerization after a period of days. This is a phenomenon that was realized in the preliminary studies of this research. Figures 3.6 (a) and (b) below depict the spherical shape of crystallized paclitaxel by scanning electron microscopy (SEM) technique (courtesy of the Engineering Research Center at North Carolina A&T State University). Images were taken at 800 x and 4,000 x magnification respectively. The reduction of drug particle size is a good aim in future studies of taxol release towards the improvement of solubility.

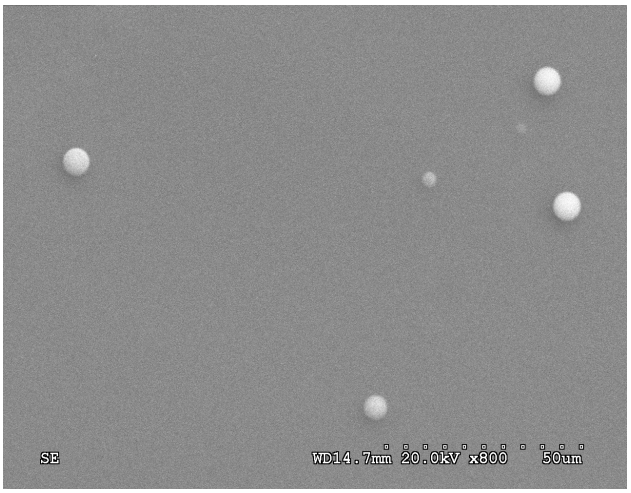

(a)

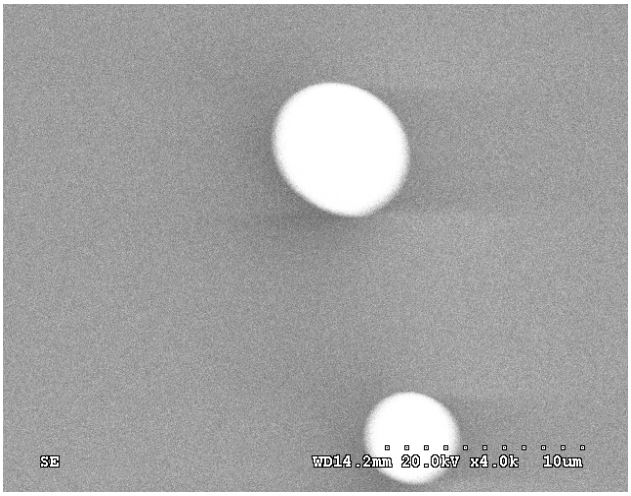

(b)

Figure 3.6 (a) Precipitated taxol beads of PEUU surface 800X (b) 4,000X

For each of the proposed systems variations of polymer and drug concentration, as well as thickness may be applied to achieve the critical viscoelastic and mechanical properties desired for optimal drug release. It is important to note that the optimality of a given drug release profile is dependent on the application. A list of parameters affecting the viscoelasticity of a given polymer solution is provided in the Table 3.2 below

followed by a diagram (Figure 3.7) depicting the influence of viscoelasticity in drug release.

Table 3.2 List of viscoeleastic parameters

Parameters of Viscoelastic Polymer Solutions
1. Temperature 2. Pressure 3. Time 4. Polymer Chemical Composition 5. Molecular Weight 6. Crystallinity 7. Solvent Dilution 8. Polymer/Mixture Composition

Figure 3.7 Influence of viscoelastic properties on drug release

The viscoelastic properties strongly influence the polymer systems ability to maintain structural and mechanical drug efficiency. However, there are other factors that contribute the integrity of these designed systems. Some of the most influential factors include particle size distribution, physical state and concentration profile of the drug with the polymer thin film, and dissolution and diffusion properties of the drug. An effort to maintain structural and functional integrity has been considered in the design of the proposed polymer thin film systems.

A review of literature regarding the dissolution and diffusion properties of taxol in PCL and PLGA, two other biocompatible polymeric materials, is presented. S. Dordunoo et al. characterized the release of taxol from PCL microspheres (Dordunoo et. al, 1995).

It was determined that crystallinity of the polymer is said to be lower with increased taxol loading which resulted in reduced times for degrading. Furthermore, accumulated crystallized taxol particles resulted from increased drug loading (5% to 10% w/v), again, a phenomenon that was validated in our studies. This is said to provide a pathway, initiating at the polymer surface, which could be responsible for the fast paced dissolution of the drug. This is an indicator that the drug loading exceeds the capacitated efficiency of the polymer solution (saturation) or a lack of homogeneity of the drug-polymer solution. The findings for taxol release from PLGA nanoparticles demonstrated similar results, with the exception that faster release rates were obtained.

The present study uses a biodegradable polymer, polyetherurethane urea (PEUU) coating, for characterizing the release of a chosen drug, namely paclitaxel for simulating drug release. PEUU is chosen as a candidate polymer for testing due to its excellent biocompatibility and high mechanical strength.

The use of drug-loaded polymers as thin film coatings for the purposes of conducting therapeutic sessions is eminent for cardiovascular stenting applications. The combination of the biopolymer and curative drug work together as a drug delivery system (DDS) to administer treatment for ailments such as neointimal hyperplasia, the fast-pace growth of unwanted cells, restenosis, as well as late-stage lung cancer patients. It is desired to achieve a DDS, via cardiovascular stent device, that can maintain compatibility within the physiological environment yet retain its ability to achieve drug release over extended time periods.

Along with PEUU, PLGA and PCL were chosen to coat alloyed magnesium substrates to study the controlled corrosion mechanism. PLGA is chosen here because of its excellent biodegradability and biocompatibility properties. It has already been approved for applications in developing therapeutic and implant devices due to the notion that it poses little to no toxic by-products to the body. In fact, PLGA undergoes hydrolysis within the body to produce the natural monomers, lactic and glycolic acid, which are by-products of various metabolic pathways found in the body. An added benefit of its use is that degradation rates can be manipulated by changing the monomers ratio (lactic: glycolic acid). For example, PLGA 70:30 consists of 70% and 30% of lactic and glycolic acid respectively. It is known that higher amounts of glycolic acid decrease the time for degradation.

The second polymer, PCL, is polyester, which degrades by hydrolysis of its ester linkages. The degradation rates here are said to be much slower than that of the other two; however, this polymer also demonstrates excellent biodegradable and biocompatibility. PCL has also been approved for uses in the human body by the FDA for applications such as drug delivery devices and adhesion barriers. An added benefit is that PCL is less viscous as a solution compared to the others making it an ideal candidate for printing using our novel direct-write printing technique. Lastly, as mentioned earlier, PEUU is chosen as a candidate polymer for testing due to its excellent biocompatibility and high mechanical strength.

PCL as well as PLGA were not only chosen because of their excellent biocompatible and biodegradability, but also because they provide other advantages to

the development of polymer thin film layers. For example, the FDA has approved PCL for barrier uses in biological components and PLGA degradation rates can be altered through systematic manipulation of its molar ratio.

3.6 Controlled Release Coatings (Phase 1)

Controlled release coatings are fabricated to suit a variety of different applications. More specifically, the controlled release of various biological agents from biodegradable polymer coatings to treat a vast number of physiological ailments is of particular interest. The use of the Direct-Write inkjet technique as a mechanism for developing controlled release coatings offers a variety of advantages for coating surfaces containing biological and pharmaceutical reagents [48]. For instance, this technique uses a data-driven pressure source for deposition of material onto a given substrate, where other fabrication techniques use electricity, which may compromise the integrity of the biological substances [48]. Other techniques such as spin coating and dip coating are not able to accommodate the complex structures that are usually required by surgical implant devices. None of the deposition techniques discussed earlier offer the ability to deposit target specific coatings, maintain the integrity of the deposition material, and eliminate cross-contamination of materials.

The need for a coating technique that encompasses all of the benefits mentioned above is necessary to develop controlled release coating where spatial requirements can be specified to develop coatings with specified porosity and degradation features. In this research, the intent was achieve a variety of drug release profiles that could be tailored to support the needs of a given drug delivery application. Here, the drug concentration and

layers of coating material were varied to assess coating specifications resulting in a steady state release throughout its intended time of function. This result would be desirable for ailments requiring extended therapeutic sessions such as neointimal hyperplasia, using an anti proliferative such as Paclitaxel, following placement of a cardiovascular stent device [6]. Coatings having a more profound initial burst phase were also attempted. These coatings would be more suitable for applications such as antimicrobial and/or antifibrotic therapy were the majority of the reagent is required in the initial stages of treatment to treat infection at the implant site and promote healthy wound healing [83-84].

3.6.1 Materials Synthesis

Traditionally, cardiovascular stents are fabricated from stainless steel (SS) or titanium (Ti) materials. In this research, a metallic substrate (Titanium) was used to mimic the surface properties of the Ti stent. A 10mm x10mm Ti sheet was deposited with drug loaded polymeric formulation to evaluate the drug release kinetics and coating morphology as described herein.

Biodegradable polyester urethane urea (PEUU) was synthesized at a proprietary source (University of Pittsburgh) and obtained for the experiments. The PEUU was dissolved in hexiflouroisopropanol (HFIP) solvent (Sigma Aldrich) and shaken vigorously until homogenous polymer solutions of 1%, 1.5%, and 2% w/v were obtained. These polymer concentrations were chosen based on the rheological properties of fluids to ensure that they were “jettable” from the direct-write inkjet system. Paclitaxel (Taxol) drug (LC Laboratories) was added at 5% and 10% w/w of the respective PEUU

concentrations within the biopolymer solutions. The drug paclitaxel is an inhibitor of the rapid division of malignant cells and has been proven effective for the treatment of rapidly growing tumors (cancer cells) and neointimal hyperplasia. Prolonged release of the drug from multilayered thin film coatings on cardiovascular stents is proven to be beneficial against this malady.

3.6.2 Sample Fabrication

Biopolymer solutions with varying concentrations of PEUU and Taxol were deposited on titanium (Ti) substrates using a customized direct-write system (MicroFab Technologies Inc., Plano, TX). The unit consisted of a pneumatic controller, a JetDrive III external waveform generator, JetServer software with waveform amplifier, horizontal and vertical plane optic system, and a piezoelectric microvalve nozzle with a 50 micron orifice. Figure 3.3 (b) shows the pulse waveform applied to the nozzle to generate monodisperse droplets. Optimal jetting parameters for consistent deposition were chosen by adjusting the voltage, frequency and pulse waveform. A CCD camera with microscopic zoom lens was used to characterize droplet formation. Further, a motion controller was programmed to create a raster pattern that coats the titanium substrate uniformly. Each layer was allowed to dry before the next layer was deposited. Samples with 10 and 20 layers respectively, were deposited to obtain surface morphology data and release kinetics profiles.

3.6.3 Characterization of Release

Drug release profiles were characterized using an ultraviolet-visible spectrum (UV-Vis) spectrophotometer (Shimadzu UV-2450). Samples were placed in 3mL of

Dulbecco's Phosphate Buffer Saline (DPBS) to initiate drug release. 10% v/v of ethanol was mixed in the DPBS (Fisher Scientific) to obtain accelerated release kinetics of the drug. The solution was shaken for several minutes to ensure a homogenous mixture. The peak absorbance of paclitaxel was confirmed at 230nm. Coated Ti sample readings were obtained at this wavelength after being shaken in an incubator shaker bath at 37°C for 2 hours. DPBS solutions from the Ti samples were extracted into a micro-cuvette to observe the absorbance readings for different polymer and Taxol concentrations. Readings were taken every two to three hours for the first twenty-four hours and daily thereafter. Release kinetics results were recorded for a period of 35 days.

3.7 Controlled Release Coatings (Phase 2)

3.7.1 Experimental Design and Analysis

Release profiles were to be obtained for a total of four different drug-loaded polymer systems using Polyester urathane urea (PEUU) and the bioreactive agent Paclitaxel (Taxol). Two primary factors were controlled to determine their effects on the release profiles obtained. The first factor was drug concentration. Concentration was tested at two levels, 5% and 10% weight per volume. Lastly, the layer thickness, which corresponds to the number of passes, was tested at two levels, ten (10) and twenty (20) passes, respectively Table 3.3.

Table 3.3 Phase 2 descriptions of experiment types for controlled release coatings

Experimental Setup					
Experiment #	Polymer Type	Drug Type	Polymer Concentration %	Drug Concentration %	# of Pass
1	PEUU	Taxol	0.5	5	10
2	PEUU	Taxol	0.5	5	20
3	PEUU	Taxol	0.5	10	10
4	PEUU	Taxol	0.5	10	20

A total of three samples were coated for each experiment. A single experiment consisted of a specified drug concentration having a certain layer thickness. For example, 0.5% PEUU loaded with 5% taxol at 10 passes describes one experiment where 0.5% PEUU loaded with 10% taxol at 20 passes describes another.

The dependant variables in the study of release profiles are identified as the percentage burst release and the total amount of the drug released at the end of the sample collection period. The initial rate of release corresponds to the slope of the release profile in the initial stages. This initial rate is relevant to the speed at which the initial burst takes place from the time the release period is initiated until the time it reaches a steady rate of release. The percentage burst release corresponds to the ratio of drug that is released and drug loaded during the initial burst period. The total release remains as stated above.

The basic research question is as follows**,** *"Can direct-write inkjet printing technique be used as a mechanism for depositing uniformly distributed layers of drug-loaded polymer thin films and furthermore, can tunable drug release profiles be obtained over extended time periods by varying the two main input factors (drug concentration and coating thickness)?"* A set of more specific research questions was extracted that

was expected to help answer the basic research question. These questions are stated below followed by their respective null and alternative hypothesis statements.

1. *Does drug dosage and coating layer thickness have a significant effect on the drug release profile? (Phase 2a)*
2. *Does drug dosage and coating layer thickness have a significant effect on cell inhibition? (Phase 2b)*
3. *Does drug dosage have a significant effect on blood compatibility? (Phase 2c)*

For Phase 2a, a 2x2 factorial design was used to determine the main and interaction effects of the two experimental factors (i.e. drug dosage and coating thickness) on the response variables. There were a total of four experiment combinations and each was replicated twice to assess error. Thus, giving a total of 8 experiment trials. The following null and alternative hypotheses were formed:

H_{01} = the sample means for drug dosage are equal

H_{02}= the sample means for number of layers are equal

H_{03} = there is no interaction effect

H_{11} = at least one of the sample means for drug dosage is different

H_{12}= at least one of the sample means for number of layers is different

H_{13} = an interaction effect is present

In Phase 2b, a one-way ANOVA was conducted to determine if there was a difference in means between each experiment type and its respective control. There were a total of 8 treatment conditions (4 controls and 4 treated surfaces) and each was replicated 4 times giving a total of 32 runs. The metabolic means of samples containing

10 and 20 layers with a 5% w/w drug loading were compared to the metabolic means of samples having 10 and 20 layers of PEUU with no drug respectively. Also, the metabolic means of samples containing 10 and 20 layers with a 10% w/w drug loading were compared to the metabolic means of samples having 10 and 20 layers of PEUU with no drug respectively. Lastly, the metabolic means of each of the experiment groups was compared with the mean metabolic index of cells cultured on Tissue Culture Polystyrene (TCPS). The following null and alternative hypotheses were formed:

H_0 = the sample means for all experiment condition are equal

H_1= at least one of the sample means is different

For Phase 2c, a one-way ANOVA was used to determine if drug concentration has a significant effect on the blood platelet count. For this experiment each of the samples were coated with 20 layers of PEUU and only the drug concentration were varied. There were three levels, which were 5% w/w, 10% w/w and no drug (low control). The experiment was replicated three times for considering error resulting in a total of nine replications. The following null hypothesis was formed to state that there is no difference between the mean platelet count of each sample group. The associated alternative hypothesis states that there exists a difference between means of the sample groups:

H_0 = the sample means for drug dosage are equal

H_1= at least one of the sample means for drug dosage is different

3.7.2 Experimental Procedure

3.7.2.1 Materials Synthesis

Polyester urethane urea (PEUU) and the metallic substrate (titanium) were generously donated by Wagner Laboratory at the McGowan Institute for Regenerative Medicine. Paclitaxel, >99.5% (taxol) was obtained from L C Laboratories and hexaflouor-2-propanol, >99.8% (HFIP) was obtained from Sigma-Aldrich. Under a hood, 20 milliliters of HFIP solvent were measured by micropipette and placed into a glass vessel. For experiment sets one and three, 0.5% w/v (0.1 grams) of solid PEUU polymer was weighed using a Metler Toledo AX DeltaRange digital scale and fully dissolved in the previously measured HFIP to obtain a homogenous HFIP/PEUU solution. A 5% w/w (0.005 grams) dosage of paclitaxel was then weighed using a digital scale and dissolved into the HFIP/PEUU solution.

For experiment sets two and four, 0.5% w/v (0.1 grams) of solid PEUU polymer was weighed using the Metler Toledo AX DeltaRange digital scale and fully dissolved in a separate glass vessel containing a previously measured 20 milliliters of HFIP to obtain a homogenous HFIP/PEUU solution. A 10% w/w (0.01 grams) dosage of Paclitaxel was then weighed using a digital scale and dissolved into the HFIP/PEUU solution. The solutions were shaken vigorously in a mini shaker to ensure that a homogeneous HFIP/PEUU/Paclitaxel solution was obtained. The solutions were filtered using 0.22-micron micropore Teflon filters into two milliliter jetting reservoirs and refrigerated until ready for use.

A third solution was prepared consisting of 0.5% w/v HFIP/PEUU mixture. This solution did not contain the drug, paclitaxel and was stored for use as a control for the cell inhibition and blood compatibility testing samples.

As a release media, DPBS containing 10% ethanol was chosen to simulate accelerated release. One package containing 9.6 grams of Dulbecco's Phosphate Buffer Saline (DPBS) powder (Fischer Scientific) was dissolved in 900 milliliters of deionized water to make a 900-milliliter DPBS solution. 100 milliliters of pure ethanol was then measured and mixed with the DPBS solution to obtain a 10% DPBS plus ethanol solution. The solution was shaken for one minute to ensure a homogenous mixture.

3.7.2.2 Sample Preparation and Coating

Titanium sheets cut into 10x10 mm coupons. The samples were submerged into a glass vessel containing pure acetone and sonicated in a bath sonicator for ten minutes. After ten minutes the coupons were removed from the acetone and submerged into ethanol. The samples were again sonicated for another ten minutes for cleaning. The sample coupons were removed and air-dried. Each sample was assigned a sample number and weighed for its initial starting weight.

The customized direct-write system (MicroFab Technologies Inc., Plano, TX) described above was used to determine the appropriate jetting parameters for each of the biopolymer solutions. The unit consisted of a pneumatic controller, a JetDrive III external waveform generator, JetLab software with waveform amplifier, horizontal and vertical plane optic system, and a piezoelectric microvalve nozzle with a 50-micron orifice. Using the JetLab interface, the appropriate pulse waveform for consistent droplet formation was characterized by manipulating the rise, dwell, and fall times, as well as the voltage and pressure. The JetLab interface includes a motion control component as well as a pattern monitor, which allows us to control length, width and thickness of the coating pattern by

adjusting the step size between droplets. A CCD camera with microscopic zoom lens was used to characterize droplet formation.

Thin films were deposited onto the 10x10 titanium substrates using the direct-write inkjet printing technique. The drop-on-demand (DOD) procedure is a non-contact technique that employs the application of electrical pulses to a piezoelectric material in order to create uniform droplets of a desired solution. A schematic of the deposition pattern (not drawn to scale) can be seen in Figure 3.8 below.

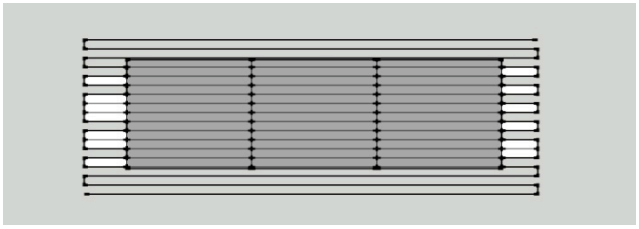

(a)

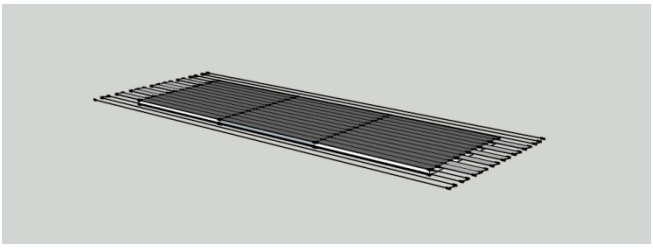

(b)

Figure 3.8 Deposition pattern using array of array command (a) top (b) iso view

An array of arrays command, using the newly acquired Jetlab 4 interface, was used to deposit the printed droplets onto the substrates. Figure 3.9 depicts the interface with input parameters that result in associated pattern, which accompanies it. The step (distance between drops) and pitch (drop diameter) sizes can be optimized to obtain more evenly distributed coating layers. This is depicted in Figure 3.10. The input parameters,

which are required, are the origin of the array which is essentially the starting point of the pattern based on an absolute coordinate system, the step size within arrays (x,y), number of steps per array (x,y), offset between arrays (xy), number of arrays (x,y) and angle. A 0.05 mm step size was employed when coating our samples. The number of layers was input in the "number of arrays" and the offset between origins was set to zero.

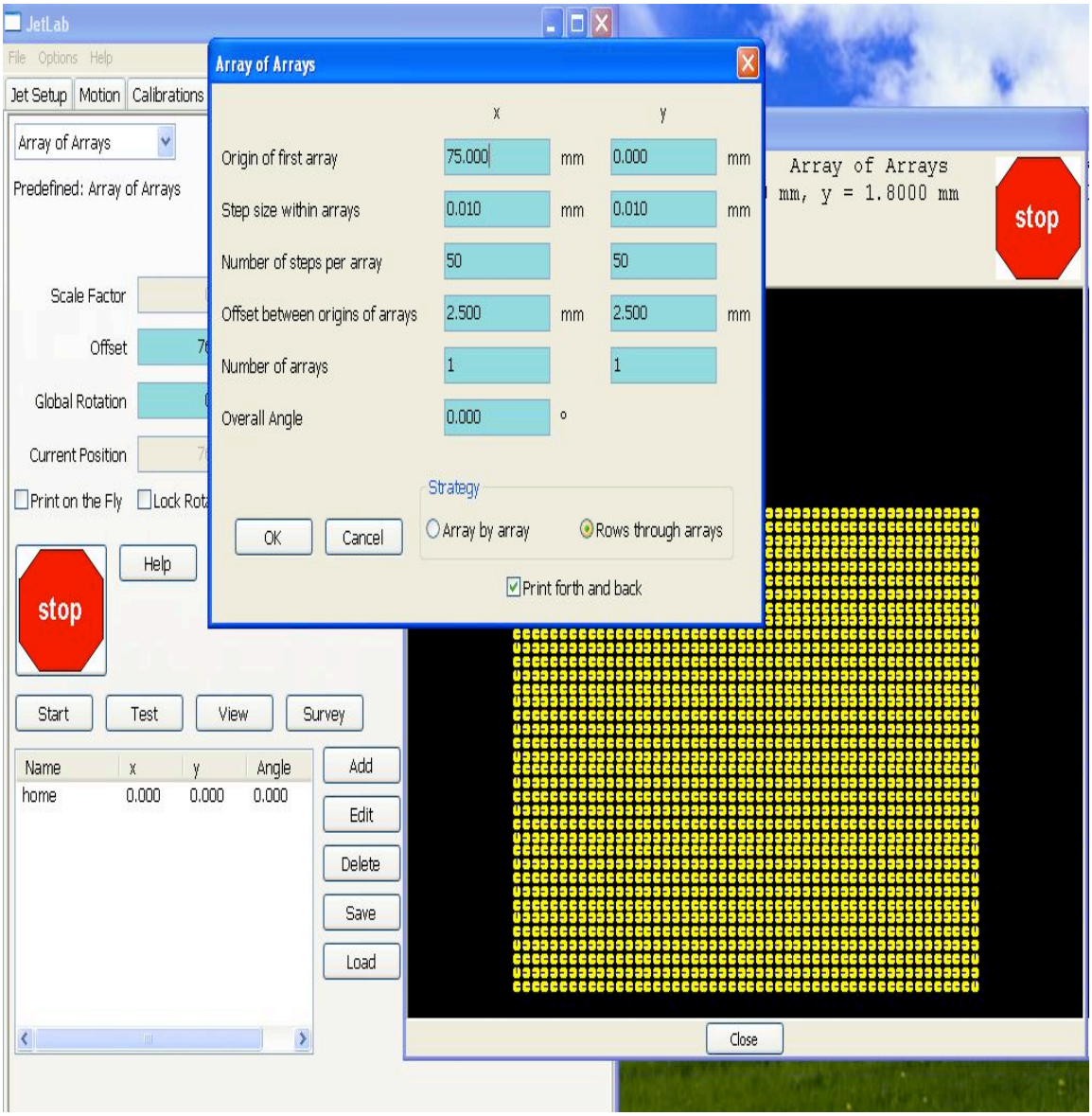

Figure 3.9 Depiction of JetLab print pattern interface

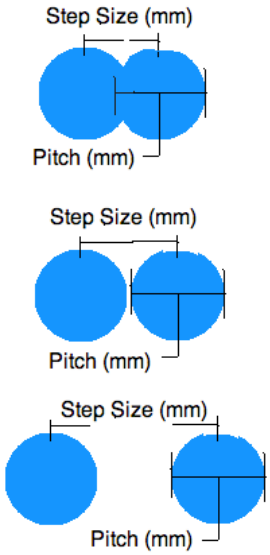

Figure 3.10 Schematic of step and pitch distance

3.7.2.3 Characterization of Release

To initiate accelerated release of the taxol drug, each sample consisting of the titanium alloy coated with the PEUU and Paclitaxel thin film was placed into a glass vessel containing two milliliters of Delbuco's Phosphate Buffer Saline (DPBS) + 10% Ethanol solution. The vessel and its contents were then placed into a Thermo Scientific Shaking Bath (Figure 3.11), set at 37 degrees Celsius and rotating at 50 rpm (mimicking conditions of the human body). After the first 2 hours, the first reading was obtained to determine release of the anti-proliferative cancer drug. Following the first sample reading at two hours, readings were obtained four more times during the course of the first 24-hour period at 4, 6, 22, and 24 hours. Sample readings were again obtained at 26, 48, 72, 98, 170, 242, and 338 hours. Further readings were taken every 2-3 days based on release trends.

Figure 3.11 Depiction of thermo scientific shaker bath

Figure 3.12 Depiction of Shimadzu UV-2450 spectrophotometer

Release kinetics for the characterization of release profiles were measured using Ultra-Violet spectrophotometry techniques. This technique is generally used to detect traces of a given substance within a sample by transmitting a source of light through its contents to measure its absorbance. The absorbance is measured over a given wavelength. Literature states that the wavelength for which the maximum absorbance reading for paclitaxel may be obtained is around 227 nm (Willey et. al, 1993). The wavelength values found in literature for achieving the optimal absorbance readings for the samples were validated to ensure repeatability. Performing serial dilutions of the concentrated substances and gaining sample readings from the UV spectrophotometer

resulted in the development a standard curve. The release values obtained were then compared to the release values on the standard curve.

As described in earlier sections the Shimadzu UV-2450 Spectrophotometer (Figure 3.12) was used for our sample data collection. During these periods, sample aliquots from each of the vessels containing the titanium samples were extracted and pipetted into a microcuvette. The microcuvette was then placed into spectrophotometer and the absorbance peaks were detected and recorded.

3.7.2.4 Blood Collection and Compatibility Test

The care and use of laboratory animals was performed according to NIH guidelines (Wagner Lab, University of Pittsburgh). Fresh ovine blood was collected from healthy ovines by jugular venipuncture into a syringe containing heparin (Hep 6U/ml). Each of the samples, PEUU containing no taxol, PEUU containing 5% taxol, and PEUU containing 10% taxol, were placed into blood collection tubes and containing the heparinized ovine blood and incubated at 37º C on a hematology mixer with continuous rocking. This is depicted in Figure 3.13.

Following the blood contact procedure, the samples were rinsed with PBS. To fix the samples surface containing the adhered platelets, the samples were immersed in a 2.5% glutaraldehyde solution for two hours at 4ºC. The samples were then serially dehydrated by increasing ethanol concentrations and coated using sputter deposition with gold/palladium. Each sample was then observed using scanning electron microscopy.

Figure 3.13 Blood platelet deposition in hematology mixer

The number of platelets deposited on the samples surfaces was quantified by a lactate dehydrogenase (LDH) assay with an LDH Cytotoxicity Detection Kit. The number of cells/mm^2 was determined for each sample in the sample group and the average and standard deviation obtained. The statistical significance between the sample groups was determined using ANOVA followed by post-hoc Newman-Keuls testing of specific differences based on the hypothesis formally stated.

3.7.2.5 Cell Growth Inhibition

All coated titanium disks (6 mm diameter) were placed in a 96-well cell culture plate and then sterilized under UV irradiation for three hours in a biological hood. Tissue cultured polystyrene (TCPS) and uncoated titanium disks were set as controls. $2*10^3$ rat smooth muscle cells (RSMCs) per well were seeded on the sample surface, and cell culture medium (DMEM supplemented with 10% FBS and 1% antibiotics) was exchanged every two days. MTT assay was performed to detect cellular viability at one, four and seven days. Briefly, 20 uL MTT solution (3 mg/mL) was added into the culture

medium in a well. After 4 hours in an incubator at 37ºC, the medium was completely removed and 200 uL of DMSO was added to dissolve the produced blue crystal. The absorbance was detected using a 150 uL dye solution at 540 nm on a UV spectrometer. Four samples were used at each time point for each group.

3.8 Polymer Coatings for Controlling the Corrosion of Mg Alloys (Phase 1)

Biofunctional coatings are necessary to suit a variety of different medical applications. The use of the direct-write inkjet technique as a mechanism for enhancing the structural integrity of a given biomaterial via biofunctional coatings, namely magnesium and its alloys, is of growing interest. Uses for magnesium as a biomaterial offers several advantages and can spread across a number of applications. For instance, magnesium is essential to over 300 physiological functions within the body [85] and has also been identified as a potential biomaterial to facilitate bone growth and repair due to proven similarities of mechanical strength with the cortical bone [86].

Direct-write deposition can be used to fabricate coatings where spatial requirements can be specified to develop coatings with specified porosity and degradation features for inhibiting the corrosion of magnesium alloys. In this study, the intent was to investigate a variety of polymer coatings having various rates of degradation. Here, the polymer type and layers of coating material were varied to assess coating specifications for applications in corrosion protection and controlled release of magnesium alloys. Corrosion protection is essential to ensure that a polymer coating is applied, which can extend the life of the surgical device until its intended function is completed [86]. The controlled release of magnesium in the trachea can be beneficial in

relaxing airway cells when exposed to an environment causing inflammation [87]. Magnesium deficiencies have also been linked to cardiovascular disease. Thus, controlled release of magnesium via controlled release coatings can offer some benefit when applied to tracheal and cardiovascular stent devices [88].

3.8.1 Sample Preparation

A magnesium alloy with the composition (Mg:90%, Zn:8.9%, Ca:0.5%, rest impurities) was smelted as ingots within an inert environment (argon) at our laboratory. The Mg alloy was used as-cast without further processing such as cold work or heat treatment. A flat piece (10mmx10mmx2mm) of this Mg alloy was casted into a disc-shaped epoxy resin so that only the top surface of the Mg alloy was exposed. This process is because we are interested in studying the corrosion behavior of Mg alloy with different polymeric coatings on only the top surface without affecting the corrosion of the other sides. The sample top surface was then polished to eliminate the magnesium oxide layer. Two biodegradable polymer types, poly(lactic-*co*-glycolic acid) (PLGA) and polycaprolactone (PCL), were chosen based on their desired chemical and mechanical properties as corrosion barriers. They offer advantages that include tunable degradation rates based on the adjustable chemical composition of lactic and glycolic acids in PLGA to lengthen or shorten degradation periods, lack of toxic response at the implant sites, and their ability to be metabolized by the body. PCL is a tough biodegradable polyester with applications in tissue engineering and drug delivery. Both polymers were dissolved at 1% w/v in appropriate solvents to possess suitable viscoelastic properties for the coating process.

3.8.2 Sample Coating Procedure

A custom direct-write inkjet setup (Jetlab4 - MicroFab Technologies, Plano, TX) was used to coat the samples. A 50 μm nozzle was used to deposit twenty (20) layers of polymer coating at different pitch distances (inter-drop distance). A single layer consisted of a raster pattern of continuously deposited droplets as shown in Figure 4.14 a and b. Both polymers (PLGA and PCL) were coated with different pitch distances (50μm and 100μm) as shown in Table 3.4. One sample was left uncoated (bare Mg alloy) and used as the control. It was hypothesized that the coatings with larger pitch distances (*100*μm) would result in porous structure and higher corrosion rates when exposed to the media.

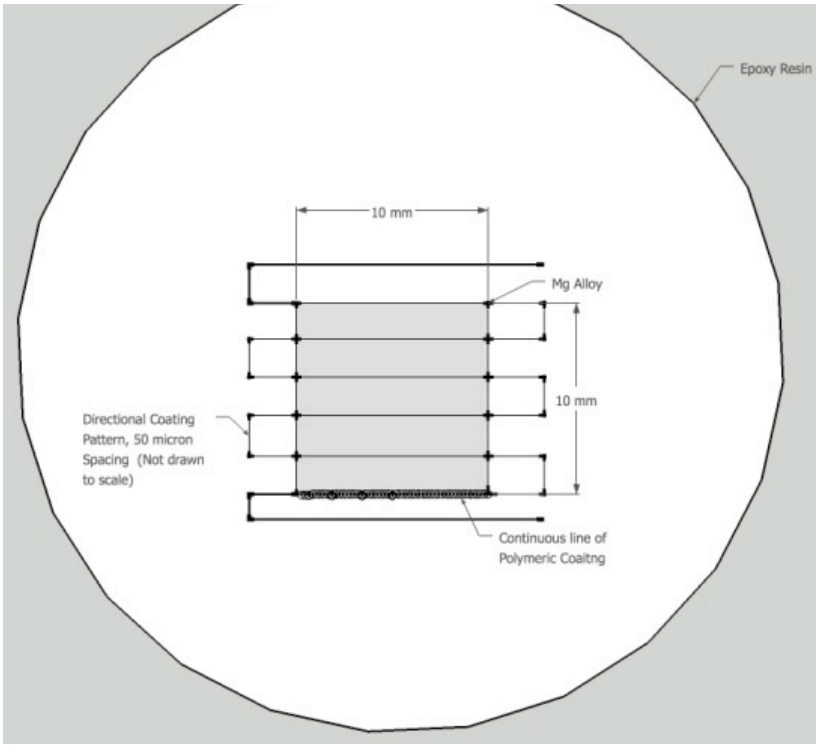

(a)

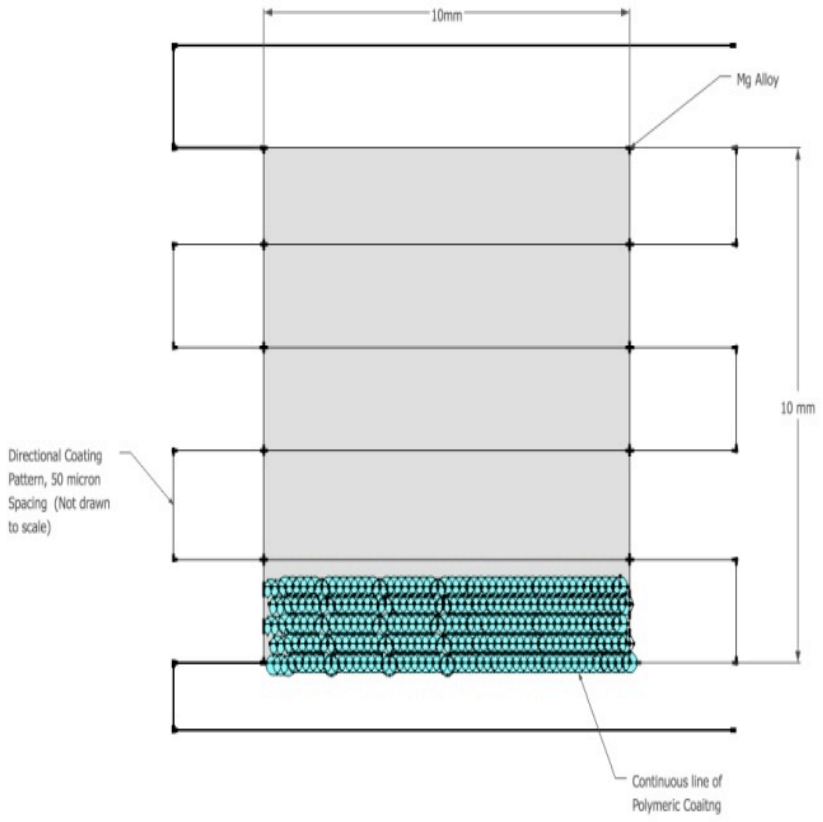

(b)

Figure 3.14 (a) Schematic of magnesium cast in epoxy resin material (b) schematic of deposition pattern

Table 3.4 Phase 1 description of experiment types

Sample No.	Polymer Type	Pitch Distance (m)
1	Bare (uncoated)	N/A
2	PLGA	50
3	PLGA	100
4	PCL	50
5	PCL	100

3.8.3 Sample Immersion Test (Weight Loss)

A 0.9% (NaCl) simulated body fluid (SBF) solution was prepared to mimic the human physiological environment. For each of the five samples, 30 ml of the sodium chloride solution was added to a small vessel. The vessels containing the samples and the solution were covered with parafilm and kept inside a CO_2 incubator at 37°Celsius to simulate human body temperature. The samples were removed from incubation at 6 hours and analyzed using optical microscopy and weight loss measurement. The samples were removed from the sodium chloride solution and placed in a desiccator for several hours to undergo dehydration. After the samples were completely dry, they were weighed and imaged. The samples were then replaced in a new vessel containing 30 ml of fresh SBF solution and incubated. This process was repeated for 12, 16, and 21hour time points.

3.9 Polymer Coatings for Controlling the Corrosion of Mg Alloys (Phase 2)

3.9.1 Experimental Design and Analysis

The question is posed, *"Can direct-write inkjet printing be used as a mechanism for depositing uniformly distributed protective thin films?"* Furthermore, *"Can these thin films aid in retardation of the corrodible magnesium alloy in physiological solutions?"* More specifically, we seek to answer the following questions:

1. *Does polymer type and coating thickness have a significant effect on the rate of metal ion release? (Phase 2a)*
2. *Does polymer-coating type have a significant effect on the percentage of LDH activity from Human Bronchial Epithelial Cells? (Phase 2b)*

In Phase 2a, three polymer types (polyetherurethane urea, polycaprolactone, and poly(lactic-*co*-glycolic acid) have been identified, each having their own unique molecular structure and degradation properties. The samples were coated at varying thicknesses (10 and 20 passes). Thus the independent variables are stated as being the polymer type (PEUU, PCL, PLGA, Uncoated) and thickness, and the dependent variable is the metal ion release over time. A 2x3 factorial design was used to assess any differences among the means of the factor groups as well as the interaction effects between factors. There were seven experiment conditions and was replicated twice to asses error. Thus, there was a total of 14 experiment runs. The following null and alternative hypotheses were formed:

H_{01} = the sample means for polymer type are equal

H_{02}= the sample means for number of layers are equal

H_{03} = there is no interaction effect

H_{11} = at least one of the sample means for polymer type is different

H_{12}= at least one of the sample means for number of layers is different

H_{13} = an interaction effect is present

A one-way ANOVA was conducted to determine any significant differences amongst treated coating combinations. The means of the uncoated samples were excluded from this analysis. There were six experiment conditions and was replicated twice to asses error. Thus, there was a total of 12 experiment runs. The following null and alternative hypotheses were formed:

H_0 = the sample means for the coating combinations are equal

H_1= at least one of the sample means for coating combination is different

For phase 2b, a one-way ANOVA was conducted to determine if there are significant differences between the sample treatment types. In this phase of experiments each of the treated samples were coated with 20 layers of the various polymer types. Thus, this experiment contains one factor (i.e. polymer type) and 5 different levels (PCL, PLGA, PEUU, Uncoated, Cells only) including the low control with no magnesium exposure. Each of experiment was replicated three times to assess error. Thus, there were a total of 15 runs. The following null and alternative hypotheses were formed:

H_0 = the sample means for polymer type are equal

H_1= at least one of the sample means for polymer type is different

The LDH samples also underwent inductively coupled plasma analysis to determine if there was any correlation between cytotoxicity percentage and magnesium ion content. The following null and alternative hypotheses were formed:

H_0 = the sample means for polymer type are equal

H_1= the sample means for number of layers are equal

3.9.2 Experimental Procedure

3.9.2.1 Material Synthesis

Polyetherurethane urea (PEUU) was generously donated by the Wagner Lab at University of Pittsburgh Institute of Regenerative Medicine and mixed with HFIP to make a 0.5% w/v solution. Polycaprolactone (PCL), and poly(lactic-*co*-glycolic acid) (PLGA) were both donated by the Wake Forrest Institute of Regenerative Medicine. The PCL arrived as a 10% w/v PCL and dichloromethane (DCM) solution and was further

diluted with DCM to obtain a 1% w/v solution. A 1% w/v PLGA solution dissolved in acetone was prepared.

3.9.2.2 Sample Preparation and Coating

5x5 mm coupons of the bulk magnesium alloy were cut and polished. The coupons were then set into an epoxy resin so that only the top surface of the magnesium sample was exposed. The surface of the sample was polished again to remove the magnesium oxide layer. The samples were labeled and imaged using optical microscopy technique. Samples were stored in a desiccator until it was time for the coating process.

The custom direct-write inkjet setup (Jetlab4 - MicroFab Technologies, Plano, TX) was used to coat the samples. A 50μm nozzle was used to deposit twenty (20) layers of the polymer materials named above. A single layer consisted of a progressing back and forth pattern of continuously deposited droplets as shown in Figure 3.14 (b). The samples were then used to conduct two different experiments, in vitro cell compatibility and immersion test.

3.9.2.3 Immersion Testing

5x5 mm magnesium coupons were cast in epoxy resin as above. Three polymer types were chosen as coating materials, PEUU, PCL, and PLGA. For each of the polymer types two samples were coated with ten layers and two were coated with 20 layers. Two samples were left uncoated as a control. The samples were fully immersed in 2 ml of DMEM + 10% fetal bovine serum + 1% penicillin strip (Figure 3.15). Aliquots were collected for each of the samples at 6 and 12 hours and then again at 1, 2, 4, 5, 6, 7, and 8 days. At the end of each time point, the old media was collected and

stored. The vesicle containing the immersed sample was then cleaned and replaced with fresh media. When the immersion testing process was completed, a 0.5 ml aliquot of each sample for the various time points was added to 9.5 ml of Tris buffer solution to achieve a 20 times dilution sample.

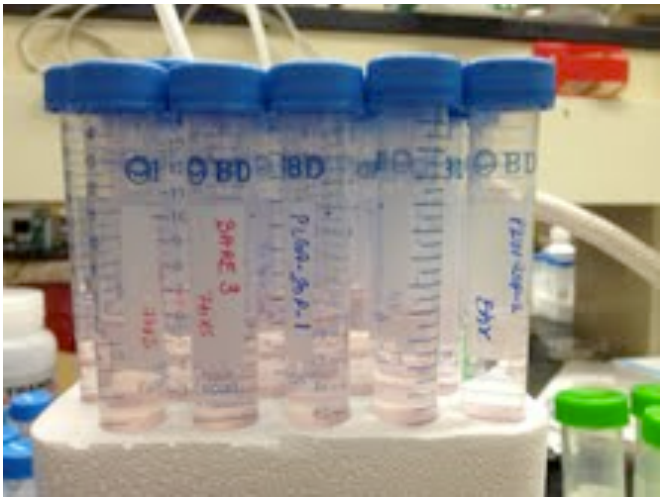

Figure 3.15 Depiction of magnesium samples immersed in SBF solution

Figure 3.16 Depiction of inductively coupled plasma equipment

3.9.2.4 Cell Culture

Normal Human Bronchial Epithelial (NHBE) cells were cultured in complete media, which consisted of a 50:50 mixture of BEBM/DMEM supplemented with antibiotics and growth factors. The cells were rapidly thawed from liquid nitrogen in a 37^{o}C water bath and seeded in 6-well culture dishes fitted with rat tail collagen-coated polycarbonate membrane Transwell® inserts (0.4 μm pore). Complete media (500 mL) was prepared by combining 250 mL of BEBM and 250 mL of DMEM into a flask with SingleQuot® components. The cells were fed apically and basolaterally every other day until they reached 100% confluency (at approximately 7 days). Figure 3.17 (a)-(c) shows cultured in cells in air-liquid interface at 100% confluency. At that point, an air liquid interphase (ALI) was established by removing medium from the apical chamber and cells were fed basolaterally everyday for 14 days to allow full differentiation of the airway epithelial phenotype. The cells were cultured at 37°Celcius in humidified air and 5% CO_2.

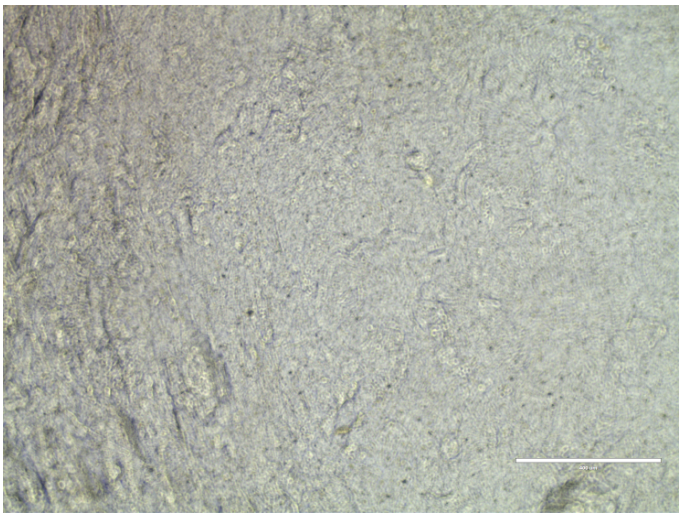

(a)

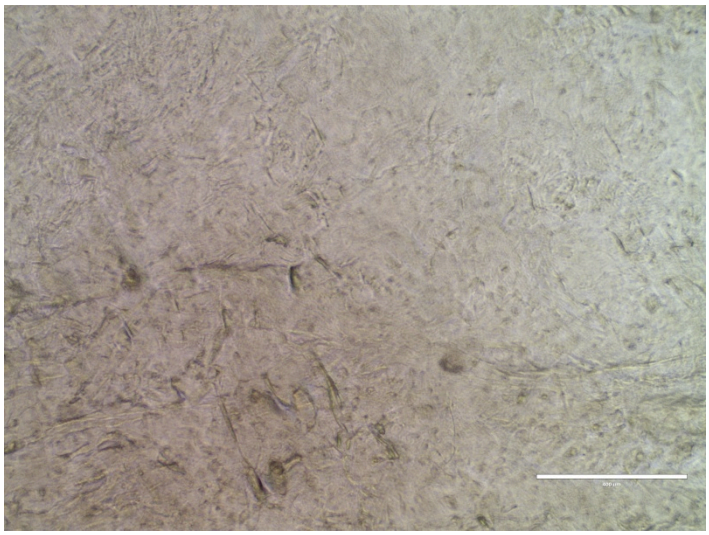

(b)

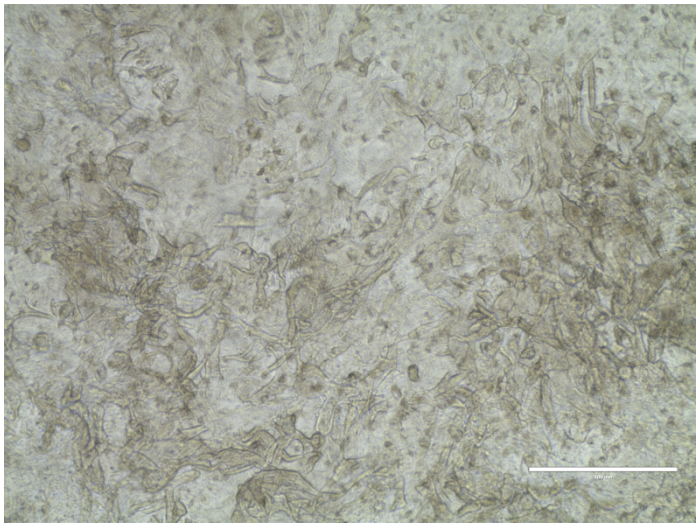

(c)

Figure 3.17 Depiction of healthy normal human bronchial epithelial cells in air liquid interface

3.9.2.5 Cell – Surface Interface Testing

The Mg samples (n=3 per coating) were coated with 20 layers of polymer and sterilized under a laminar flow hood with a UV sterilization bulb for 15 minutes on each side. Each of the samples were then assigned a well number and placed face down such

that the coated magnesium surface was in direct contact with the epithelial cell layer. Three wells were labeled as the low control, thus they were cells, which were untreated. Initial media samples were collected from each well at time zero and stored at -20°C for lactate dehydrogenase (LDH) assay and elemental analysis via inductively coupled plasma mass spectrometry (ICP-MS). Fresh medium was placed in the lower chamber of each well and the plates were placed in incubation at 37°C and 5% CO_2.

Balolateral medium samples were collected again at one hour, four hours, six hours, 24 hours, and 29 hours. During the sample collection period, 1.5 mL of the sample media was collected from each of the wells and placed into a small tube. The tubes were labeled and frozen at -20°C. Any remaining media was aspirated from the cell well and two mL of fresh media was reapplied to the lower chamber. During this period, selected wells were imaged by phase contrast microscopy using an Evos xl inverted microscope (AMG). After the final sample collection, the wells containing the untreated cells were lysed such that all LDH activity would be released. These samples were then labeled as the high control and used for LDH analysis.

3.9.2.6 LDH Assay

Following exposure to coated Mg samples, reactions were terminated by removing materials from the apical surface, collection of basolateral culture medium and plates were wrapped in foil and stored at -80^{o} C until needed for gene expression analysis. The Roche cytotoxicity detection kit was used to determine LDH release by the cells at the indicated time points. This cytotoxicity detection kit measures cytotoxicity and cell death through the detection of LDH activity which has been released from damaged cells.

The low control consisted of the untreated cells (n=3) and the high control consisted of the lysed cells, which provided information about the maximum amount of released LDH activity in the cells. The assay was performed according to manufacture's recommendation and samples (in triplicate) were transferred into a 96-well plate according to the template found in Table 3.5 below.

Table 3.5 96 -well sample template for LDH assay

	96-well plate (Sample Data Key)											
	1	2	3	4	5	6	7	8	9	10	11	12
A	PCL-1-1	PCL-1-2	PCL-1-3	PCL-2-1	PCL-2-2	PCL-2-3	PCL-3-1	PCL-3-2	PCL-3-3	PCL-4-1	PCL-4-2	PCL-4-3
B	PCL-5-1	PCL-5-2	PCL-5-3	PCL-6-1	PCL-6-2	PCL-6-3	PLGA-7-1	PLGA-7-2	PLGA-7-3	PLGA-8-1	PLGA-8-2	PLGA-8-3
C	PLGA-9-1	PLGA-9-2	PLGA-9-3	PLGA-10-1	PLGA-10-2	PLGA-10-3	PLGA-11-1	PLGA-11-2	PLGA-11-3	PLGA-12-1	PLGA-12-2	PLGA-12-3
D	PEUU-13-1	PEUU-13-2	PEUU-13-3	PEUU-14-1	PEUU-14-2	PEUU-14-3	PEUU-15-1	PEUU-15-2	PEUU-15-3	PEUU-16-1	PEUU-16-2	PEUU-16-3
E	PEUU-17-1	PEUU-17-2	PEUU-17-3	PEUU-18-1	PEUU-18-2	PEUU-18-3	BARE-19-1	BARE-19-2	BARE-19-3	BARE-20-1	BARE-20-2	BARE-20-3
F	BARE-21-1	BARE-21-2	BARE-21-3	LOW-22-1	LOW-22-2	LOW-22-3	LOW-23-1	LOW-23-2	LOW-23-3	LOW-24-1	LOW-24-2	LOW-24-3
G												
H	HIGH-25-1	HIGH-25-2	HIGH-25-3	HIGH-26-1	HIGH-26-2	HIGH-26-3	HIGH-27-1	HIGH-27-2	HIGH-27-3			

Absorbance measurements were taken for each time point at 492 nm on a VersaMAX microplate reader (Molecular Devices). To determine the percentage cytotoxicity, the average of the triplicates were obtained and the following equation was applied where exp. is the experimental value (i.e. absorbance value) obtained and high and low are in regards to the controls, respectively (Equation 1).

$$Cytotoxicity(\%) = 100 \times ((\exp. - low)/(high - low))$$

Equation 1 Determination of cytotoxicity obtained from LDH absorbance values

3.9.2.7 PCR Analysis

3.9.2.7.1 RNA Extraction

The cell wells were thawed after being preserved at -80° C following the cell culture experiments. The RNeasy RNA Extraction Kit (Qiagen, Valencia, CA) was

utilized for RNA extractions according to manufacturer's instructions. Briefly, to extract RNA from the NHBE cells 350 µl of RTL buffer was added to each of the 24 wells to lyse the cells. Using a rubber policeman apparatus, the cells were detached from the membrane of the wells. Each lysate sample was transferred into a microfuge tube and vortexed to remove any clumps. Each of the samples were then homogenized by passing the lysate through 20-gauge (0.9 mm diameter) fitted RNase-free syringe 4-5 times. Next, 350 µl of 70% EtOH was added and mixed with the lysate by pipetting. The lysate was then transferred into an RNeasy spin column fitted with a 2 ml collection tube and spun for 30 seconds at 10,000 rpm, at room temperature. The resulting flow through from the collection tube was discarded.

The spin column was then transferred into a second collection tube and 350 µl of RW1 buffer was added. The sample was spun again for 30 seconds at 10,000 rpm. Next, 80 µl of DNase solution was added to the center of the silica-gel membrane in the spin column and left to incubate at room temperature for 15 minutes. Another 350 µl of RW1 buffer was added to the column and spun at 10,000 rpm for 30 seconds to wash.

The samples were then washed twice by adding 500 µl of buffer RPE onto the column and spinning for 30 seconds at 10,000 rpm. The samples were then spun at maximum speed for one minute to dry the columns. RNA was then eluted by transferring the spin columns into a 1.5 ml microfuge tube and adding 50 µl of RNase-free water directly to the sample columns. Finally, the samples were spun at 10,000 rpm for one minute.

3.9.2.7.2 Determination of RNA concentration and purity

Each of the RNA samples were diluted by adding one part RNA and 49 parts RNase-free water to obtain a 1/50 dilution. For each sample, 2 µl of diluted RNA was placed on to the center of a nanoplate reader. The RNA concentration was determined by measuring the absorption over a UV light at 260 and 280 nm. The purity of RNA was calculated by determining the ratio A (260/280). The RNA concentration (ng/µl) was calculated Equation 2.

$$RNA_{conc.}(ng/\mu l) = (A_{260})(40\mu g/\mu l)(dilutionX)$$

Equation 2 Determination of RNA concentration

3.9.2.7.3 Complementary DNA (cDNA) Synthesis

Synthesis of cDNA was conducted according to the iScript cDNA Synthesis Kit (BIO-RAD, Hercules, CA) protocol. A reaction mixture was prepared for a total volume of 15 µl per sample reaction. Each reaction mixture consisted of 4 components, 4 µl of 5x iScript Reaction Mix, 1 µl of iScript Reverse Transcriptase enzyme, X µl of Nuclease-free water, and X µl of the RNA sample (Table 3.6). The amount of Nuclease-free water and RNA sample required for each reaction were calculated based on the RNA concentration per sample. The RNA concentrations and the calculated values for X µl of Nuclease-free water and X µl of the RNA are shown in Table 3.7 below. Each reaction mix was spun for 3 seconds and incubated using an iCycler Thermal Cycler (BIO-RAD) for 5 minutes at 25° C, followed by 30 minutes at 42° C, 5 minutes at 85° C, and finally cooled at 4° C for at least 5 minutes. Figure 3.18 shows the thermal cycler apparatus.

Figure 3.18 Depiction of iCycler thermo cycler from BIO-RAD

Table 3.6 Specified amounts for cDNA reaction mixture

Reagent	Amount	
5x iScript Reaction Mix	4 µl	4µl
Total RNA Template**	1 µl	Refer to Table 3.7
iScript Reverse Transcriptase	1 µl	4µl
Nuclease-free water	q.s. 20 µl	Refer to Table 3.7

Table 3.7 Calculated RNA and nuclease free water required based on RNA concentration

Sample	Concentration	Desired, µg	RNA needed	H_20 Needed
1	148.2	400	2.70	12.30
2	81.5	400	4.91	10.09
3	71.5	400	5.59	9.41
4	48.5	400	8.25	6.75
5	61.6	400	6.49	8.51
6	92.3	400	4.33	10.67
7	77.7	400	5.15	9.85
8	71.1	400	5.63	9.37
9	112.9	400	3.54	11.46
10	132.9	400	3.01	11.99
11	124	400	3.23	11.77
12	70.3	400	5.69	9.31

13	140.3	400	2.85	12.15
14	107.6	400	3.72	11.28
15	59.8	400	6.69	8.31
16	78	400	5.13	9.87
17	64.6	400	6.19	8.81
18	57.1	400	7.01	7.99
19	49.3	400	8.11	6.89
20	58.4	400	6.85	8.15
21	61.7	400	6.48	8.52
22	38.5	400	10.39	4.61
23	34.1	400	11.73	3.27
24	n/a	n/a	n/a	n/a

3.9.2.7.4 Measurement of Cyclooxygenase-2 (COX-2) Gene Expression

PCR was used to measure the COX-2 gene expression in NHBE cells exposed to polymer coated magnesium samples. RNA was extracted and synthesized into cDNA as described above. COX-2 primer suspended in GoTaq (23 µl) was mixed with 2 µl of the synthesized cDNA sample. Beta-actin primer suspended in GoTaq (23 µl) was mixed with the synthesized cDNA sample and used as a reference (Table 3.8). The PCR protocol was set for an initial 95°C for 4 minutes, followed by 35 cycles at 95°C for 30 seconds, 60°C for 30 seconds and 72°C for 3 minutes. The synthesized cDNA was separated on 0.8% agarose gel at 80 V for one hour. The gel was then stained for 20 minutes in 0.01% ethidium bromide. The gel was imaged using Biorad Chemi-doc (Figure 3.19) and Image Lab interface to visualize band density. The densitometry results were analyzed in order to calculate the relative expression of COX-2 against the beta actin genes.

Table 3.8 Synthesis of Cox-2 and beta actin primers

Reagent	Volume	Rxns (ß-actin) = 23	Rxns (COX-2) = 23
Sterile, dH_2O	q.s. = 5 µl	218.5 µl	218.5 µl
DNA Template	variable = 2 µl	11.5 µl	11.5 µl
GOTaq Green	12.5 µl	11.5 µl	11.5 µl
Total Mix	25 µl	287.5 µl	287.5 µl

** GOTaq Green mixture includes 10X PCR Buffer with MgCl2, dNTP Stock (10mM each), and Taq DNA Polymerse (5U/µl)*

Figure 3.19 Depiction of BIO-RAD chemi-doc

3.9.2.7.5 Statistical Analysis for Cyclooxygenase-2 (COX-2) Gene Expression

The average volume intensity of the beta actin genes was used to obtain normalized values for the COX-2 expression gene. The normalized values (n=6) were used to conduct statistical analysis. A one-way analysis of variance was conducted to determine statistical differences between the mean cyclooxygenase-2 (COX-2) gene expressions of cells for each experiment type. After determining the statistical differences between the experimental means, Tukey's post hoc analysis was performed to determine the specific differences between mean pairs.

CHAPTER 4

RESULTS AND DISCUSSION

4.1 Jetting Optimization

Direct Write Inkjet printing can be employed as a mechanism for depositing non-newtonian biopolymer fluids to modify the surfaces of surgical implant devices. The optimal jetting parameters for 0.5% w/v PEUU were obtained by determining the appropriate frequency, positive/negative jetting voltage, rise time, dwell time, fall time, and final rise time denoted by *f, +V/-V,* T_R*,* T_D*,* T_F*,* T_{FR}*,* respectively, and the reservoir pressure as described above. These obtained values are approximate values. This is because of the level of difficulty in obtaining the exact value for the reservoir pressure, thus the remaining input values needed to be adjusted. The final jetting parameters obtained at a reservoir pressure of approximately -16 psi were *f = 500Hz, +V/-V = 58 V/-58 V,* T_R *= 51 μs,* T_D = 50 *μs,* T_F *= 51 μs,* and T_{FR} *= 51 μs.*

4.2 Controlled Release Coatings (Phase 1)

Drug release kinetics and surface morphology and thickness were analyzed to evaluate the possible factors that might affect the release behaviors of the multilayer coatings. The factors of interest included: (1) polymer concentration, (2) drug loading and (3) the number of overprint passes.

4.2.1 Characterization of Release

The measured release kinetics profiles represent an accelerated curve with respect to time. Thus, samples under *in vivo* conditions would release over a longer period of time than those observed here. Figure 4.1 shows the release profiles for samples with

varying polymer, drug (taxol) and number of overprint passes as tabulated in Table 4.1. The nomenclature (1-5-10P-S2) corresponds to 1% PEUU, 5% taxol, 10 Passes, Sample 2. Samples with smaller film thickness and lower drug loadings resulted in longer and steady rates of drug release. While, samples with higher drug loadings resulted in a high percentage of release during the initial burst release period. This situation was attributed to the burst release of crystallized taxol particles (beads) within the polymer matrix. Figure 4.2 (a) and (b) shows the (a) top view and (b) side view of the taxol beads with average diameters of 5 to 8 microns. These beads are a result of reaching the saturation limit of the taxol within the biopolymer solution and they indicate the upper limit for possible drug amount to be loaded.

Table 4.1 Factor levels for multilayered controlled release coatings

No.	Factor	Low level	High level
1	Polymer concentration (%w/v)	1	1.5
2	(Drug) paclitaxel concentration (%w/w)	5	10
3	Number of overprint passes	10	20

The higher polymer concentrations and film thicknesses (20 passes) resulted in an early dislodgement of the polymer thin film. This situation was due to the lack of adhesion between the polymer and the titanium substrate. Release readings were discontinued after partial dislodgement of these coatings after day 5 to eliminate erroneous data. However, the dislodged coatings released approximately double the taxol based on the higher surface area of exposure to the DPBS as compared to the adhered coatings. (Nomenclature: 1-5-10P-S2 stands to 1% PEUU, 5% taxol, 10 Passes, Sample 2)

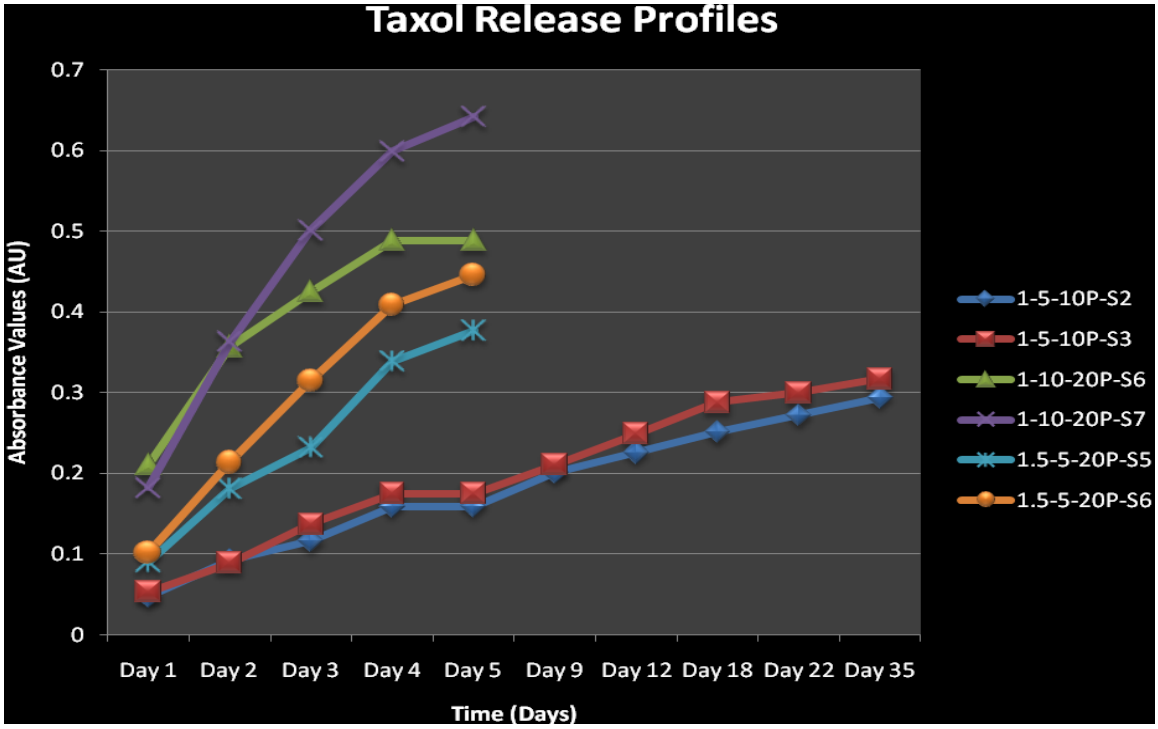

Figure 4.1 Phase 1 taxol release profiles for determining candidate experiment types

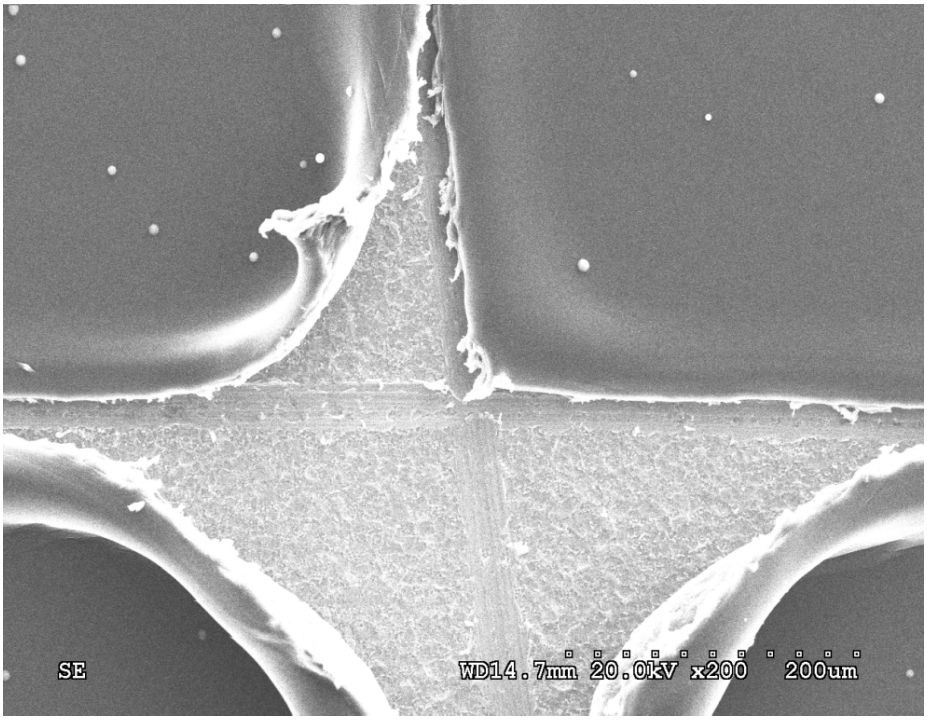

(a)

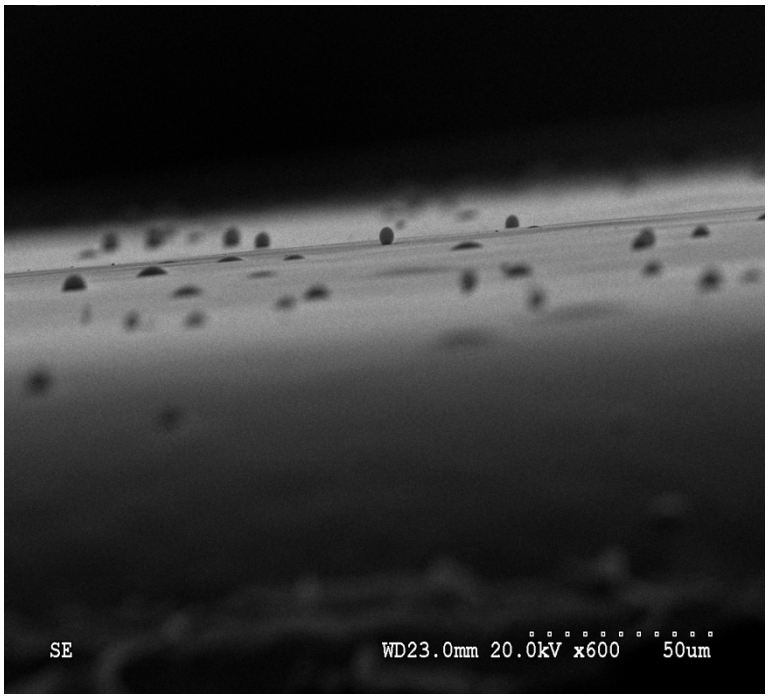

(b)

Figure 4.2 (a) Top view (b) Side view of crystallized taxol particles precipitated from polymer matrix

4.2.2 Surface morphology and film thickness evaluation

The surface morphology and film thickness of the drug loaded polymeric coatings were evaluated using scanning electron microscopy and the optical profilometer, respectively. The polymer film was cut to reveal the cross-section areas and thickness profiles. Figure 4.3 shows the (a) top view and (b) cross-section view of the polymer film with 10 passes of coatings. As can be seen from the top and cross-section views, there are whiskers of polymer that adhered to the Ti substrate for the lower number of passes (10). The average thickness for a 20-pass film obtained from the optical profilometer testing varied between 18 to 22 microns. However, the thickness obtained from the SEM

measurements was around 20 microns in thickness. The approximate coating thickness for each print pass was around 1 micron in thickness.

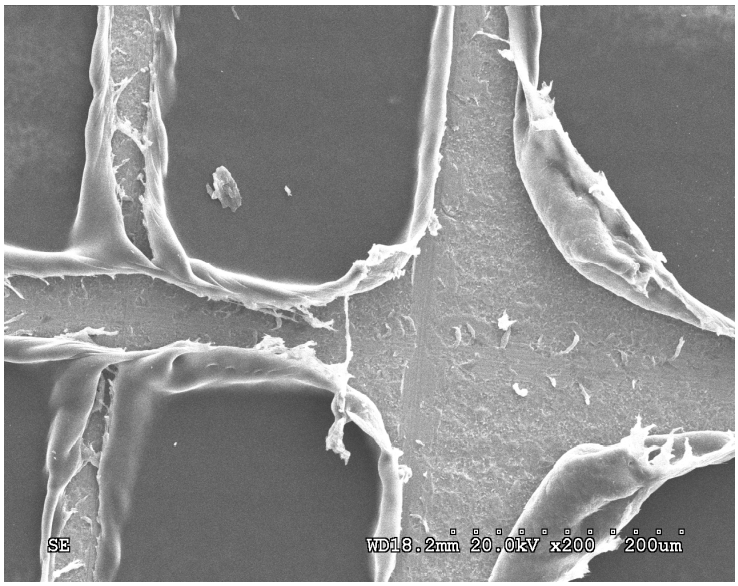

(a)

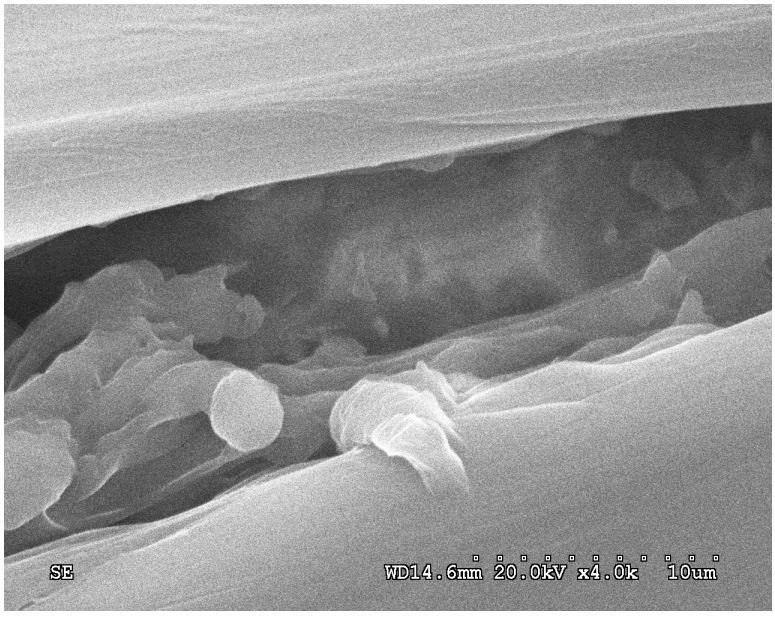

(b)

Figure 4.3 (a) Top view (b) cross-section of drug loaded polymer film on Ti substrate

4.3 Controlled Release Coatings (Phase 2)

4.3.1 Characterization of Release

The two factors studied were taxol concentration and the number of layers. The levels of taxol concentration were 5% and 10% w/v and the two levels of layer thickness were 10 and 20 layers. Thus, there was a total of four experiment types (5% taxol and 10 layers, 10% taxol and 10 layers, 5% taxol and 20 layers, 10% taxol and 20 layers). The absorbance values obtained from the spectrophotometer were compared to the values of the standard curve and the final concentration (μg/ml) of taxol present in the samples was derived. The average concentration of taxol present in the samples having 10 layers and containing 5% and 10% w/w of the polymer content was 26.07 μg/ml and 49.09 μg/ml, respectively. For the samples coated with 20 layers and containing 5% and 10% w/w of taxol, the final concentrations were 31. 29 μg/ml and 83.19 μg/ml, respectively. This condition is depicted in Figure 4.4.

The experimental data were assessed to ensure that the assumptions of normality and randomness were satisfied. It was determined that the data were normally distributed and did not exhibit any obvious trends or patterns; thus the data was, in fact, random in nature. A depiction of the normality and randomness of the data sets can be found in figures 4.5a and 4.5b, respectively. The statistical relevance of the independent variables on the total taxol concentration after 21 days was thus suitable for the application of analysis of Variance (i.e. ANOVA) statistical testing.

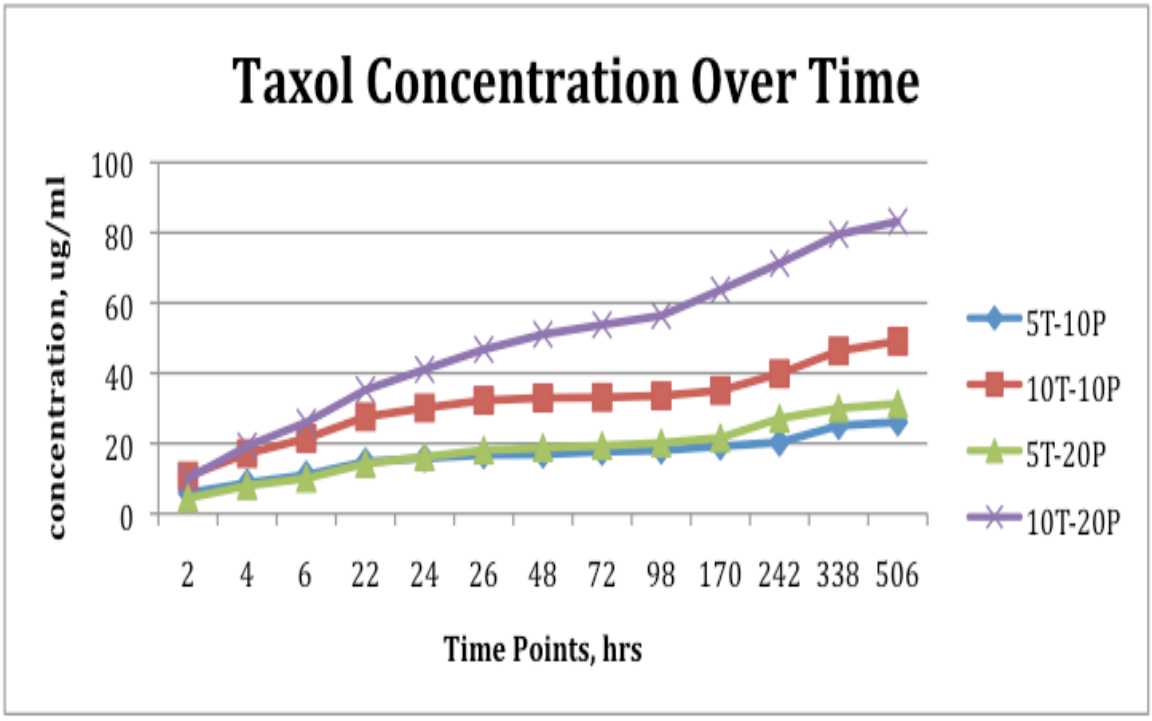

Figure 4.4 Taxol concentration release profile for 21-day period

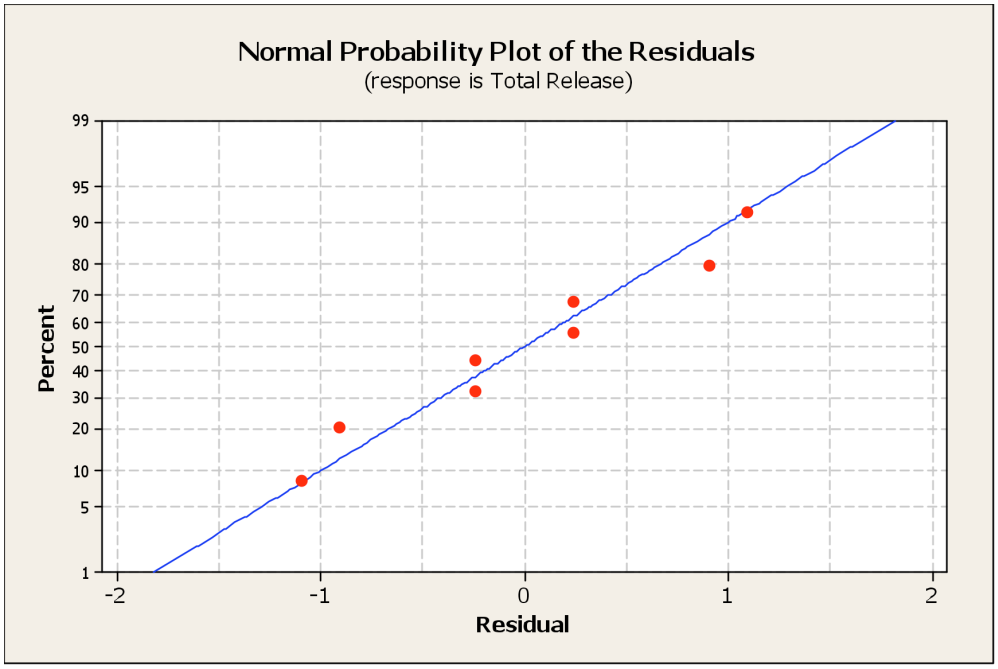

(a)

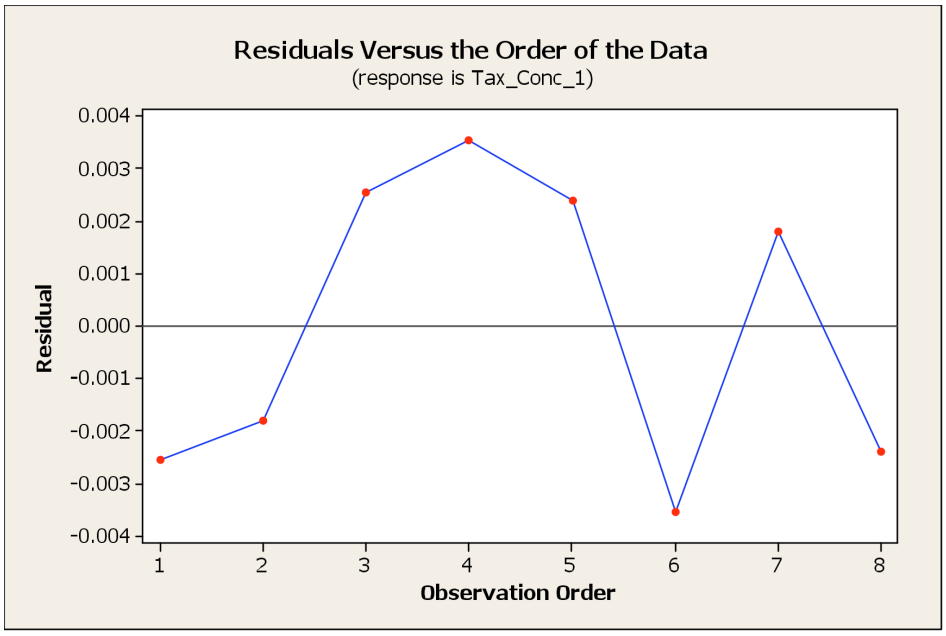

(b)

Figure 4.5 (a) Normality plot (b) randomness plot for taxol release data

A 2x2 factorial design was conducted to determine the main effects of the given factors on the total drug concentration released at the end of the sample collection period (i.e. 21 days). The findings showed that the variations in drug dosage and number of layers had strikingly significant effects ($p = 0.00$) on the total drug concentration released at $p < 0.05$. More specifically, the difference in data means for an increasing drug loading percentage was approximately 50 µg/ml and nearly 40 µg/ml for increasing the number of coating layers (Figure 4.6a). The interaction plot from the DOE analysis showed that the combined factors were also significant ($p = 0.00$) with regards to the drug release concentration at the end of the 21 days (Figure 4.6b). Details of the statistical output analysis can be found in Appendix A. The difference in data means for the samples having 5% w/w drug dosage showed a slight increase (approx. 10 µg/ml) as the number

of passes increased from 10 to 20 layers. Samples having 10% w/w drug dosage showed a more profound increase (approximately 60 µg/ml) among data means as the number of layers increased from 10 to 20 layers.

The percentage of drug released at the various time points was also obtained. It was evident that the burst period for each of the sample categories fell between t = 0 and t = 24 hours (i.e. after 24 hours the percentage of drug reached a steady state of release). Thus the percentage of the total drug released after 24 hours for the samples containing 5% and 10% w/w and 10 layers was 60.60% and 61.33%, respectively. For samples containing 5% and 10% w/w having 20 layers, the percentage of total drug release was 51.69% and 49.37%. It appeared that the samples, which contained the thinner coatings, had a more profound initial burst period. The samples having the thicker layer of coatings appeared to have a steadier rate of release during the initial burst period. However, a test of statistical significance was required to determine any real differences (Figures 4.7 a-d).

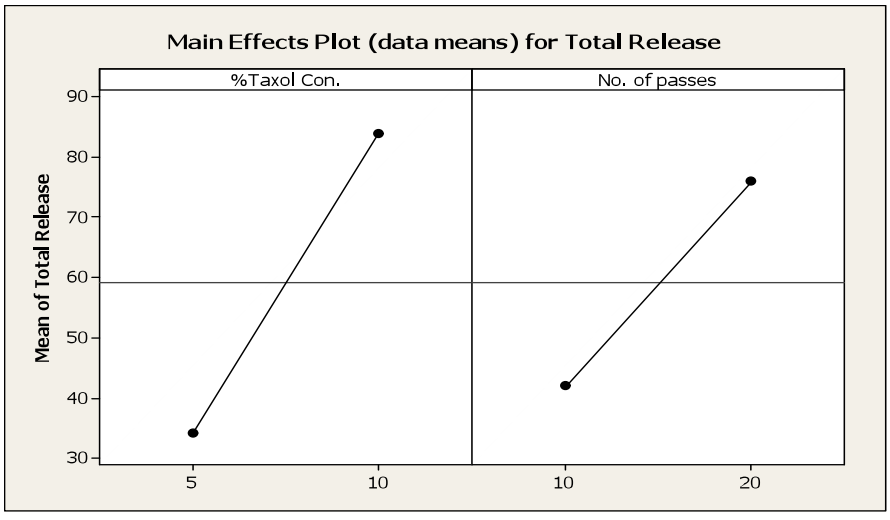

(a)

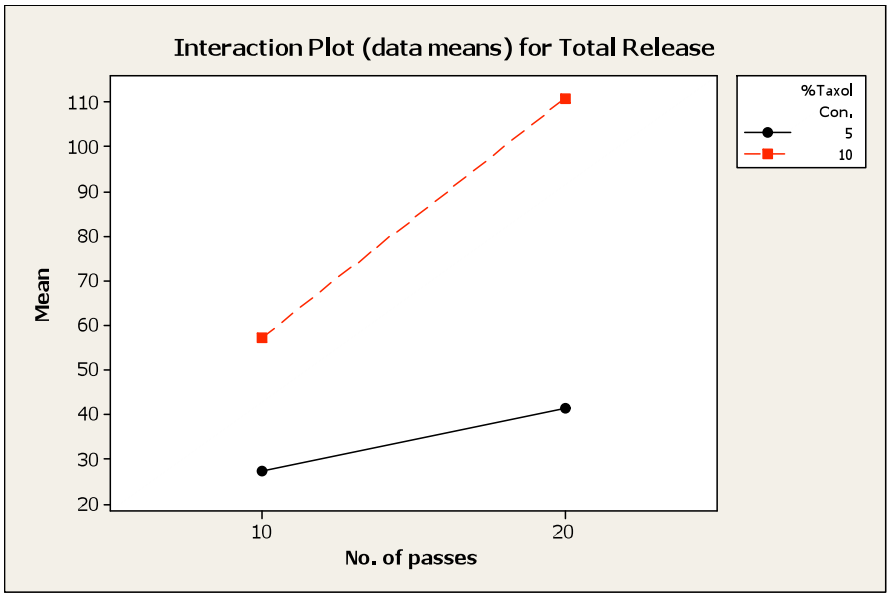

(b)

Figure 4.6 (a) Main affect and (b) interaction plot for total drug release after 21 days

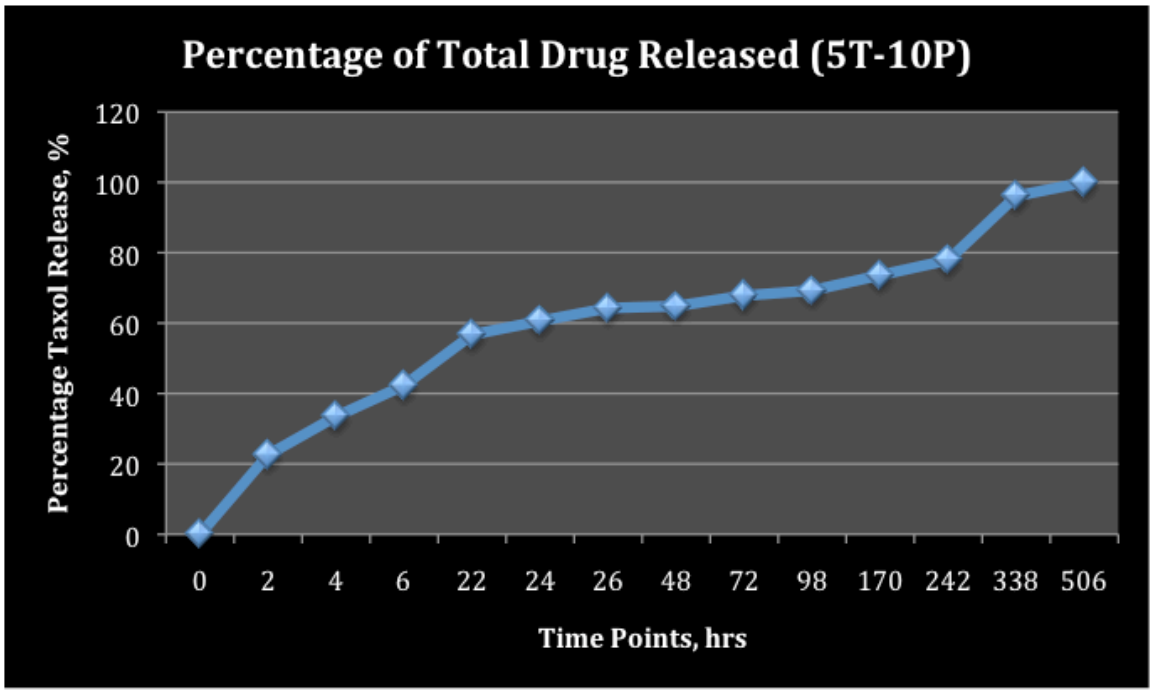

(a)

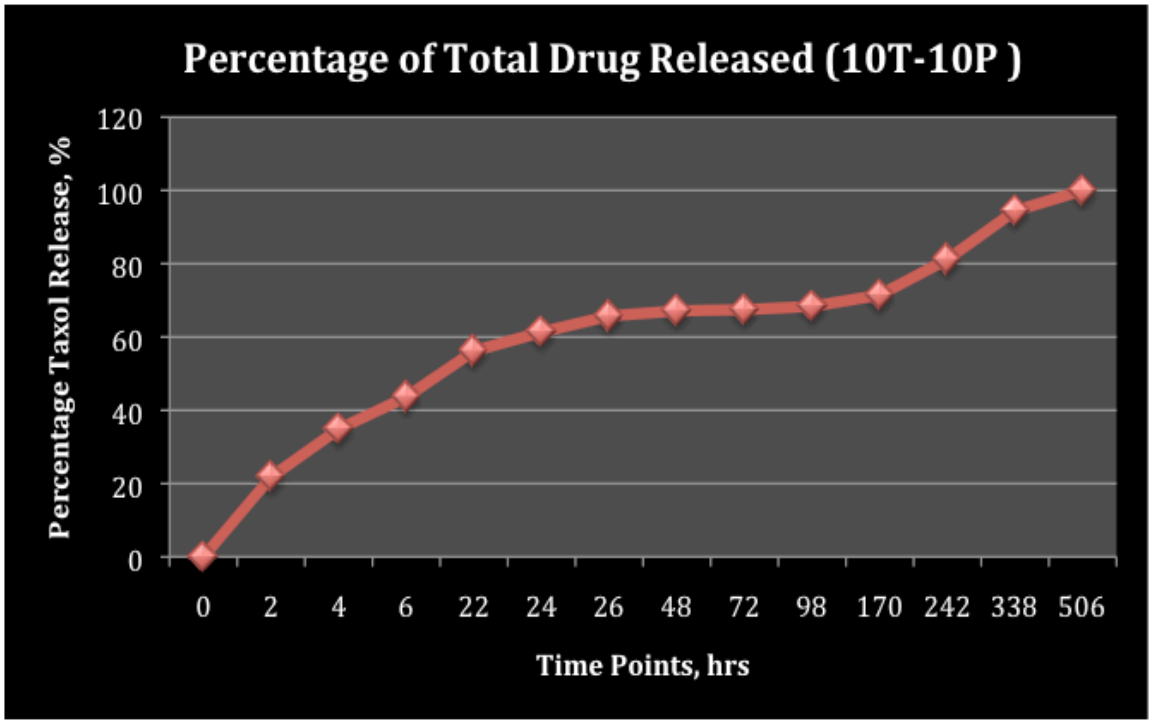
Percentage of Total Drug Released (10T-10P)
Percentage Taxol Release, %
120
100
80
60
40
20
0
0 2 4 6 22 24 26 48 72 98 170 242 338 506
Time Points, hrs

(b)

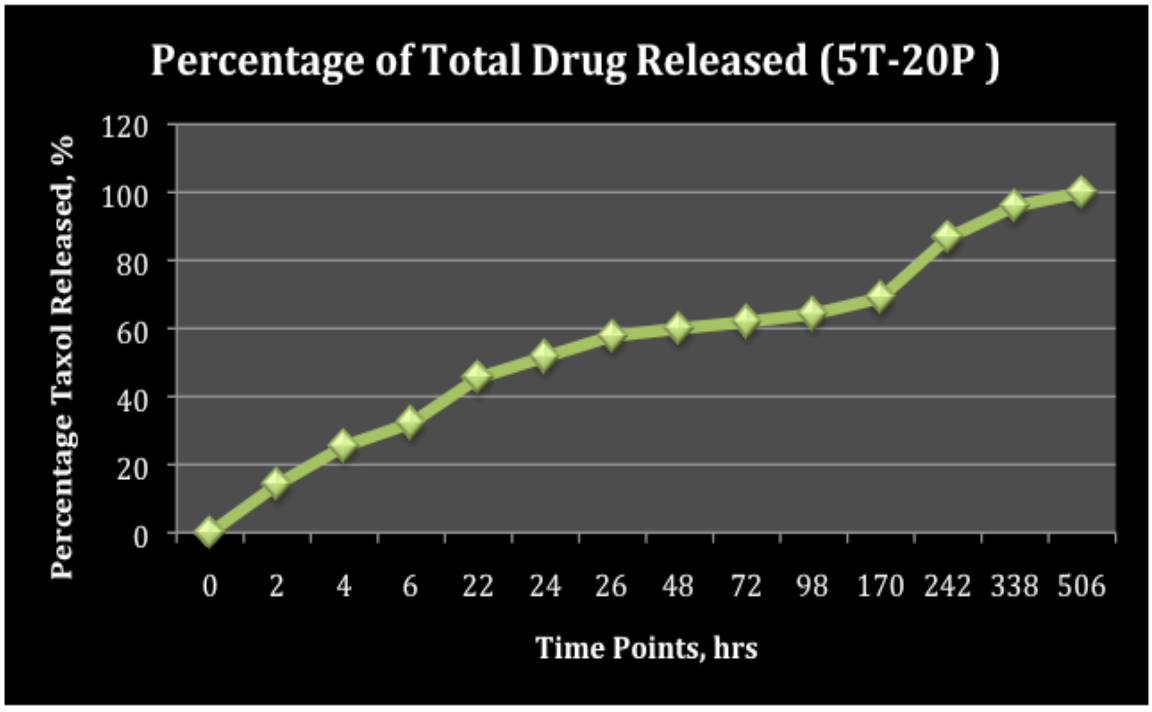
Percentage of Total Drug Released (5T-20P)
Percentage Taxol Released, %
120
100
80
60
40
20
0
0 2 4 6 22 24 26 48 72 98 170 242 338 506
Time Points, hrs

(c)

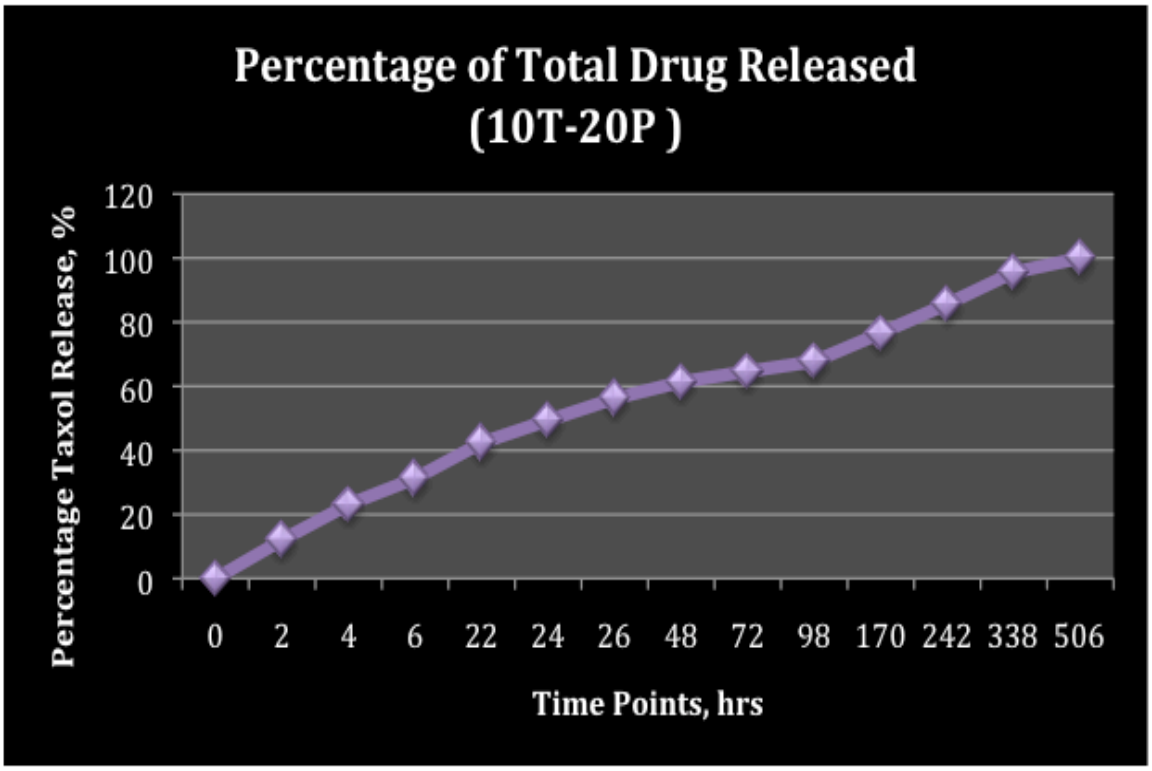

(d)

Figure 4.7 Percentage of total drug release over time for (a) 5 % taxol and 10 passes (b) 10 % taxol and 10 passes (c) 5 % taxol and 20 passes (d) 10 % taxol and 20 passes

The experimental data were assessed to ensure that the assumptions of normality and randomness were satisfied. It was determined that the data were normally distributed and did not exhibit any obvious trends or patterns. Therefore the data was random in nature. A depiction of the normality and randomness data is shown in figure 4.8 (a) and 4.8 (b), respectively. As a result, the statistical relevance of the independent variables on the percentage burst release was suitable for the application of analysis of Variance (i.e. ANOVA) statistical testing.

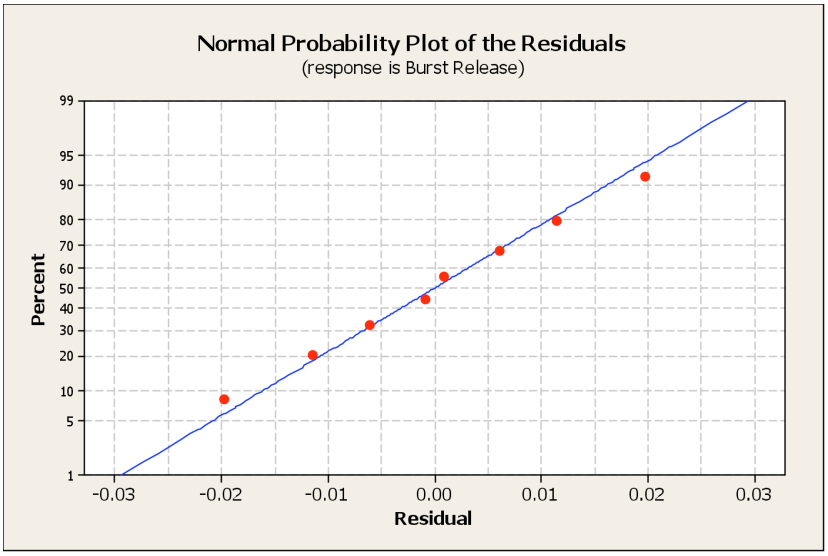

(b)

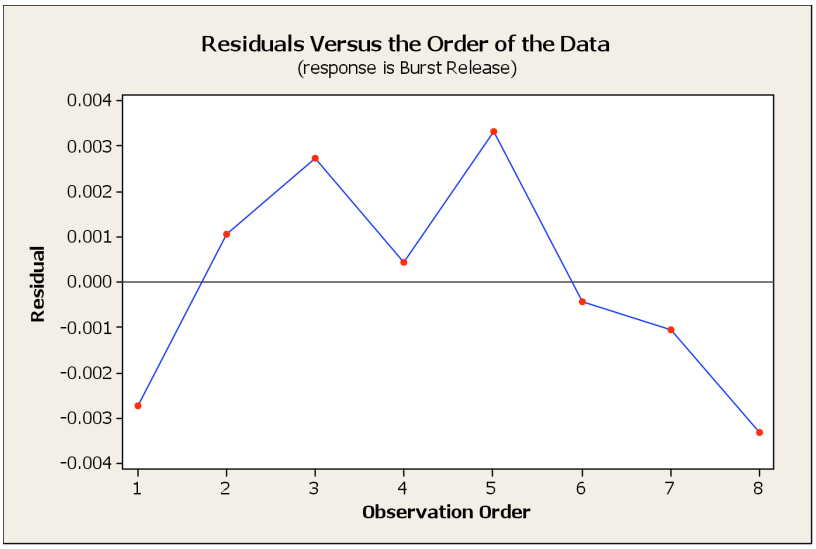

(b)

Figure 4.8 (a) Normality plot and (b) randomness plot for percentage burst release.

A 2x2 factorial design was conducted to determine the main effects of the given factors on the percentage of drug released during the burst period. The burst period identified for analysis was between 0 and 24 hours. The results showed that for both

factors (drug concentration and number of passes) there was a strikingly significant effect ($p = 0.00$) on the drug released during the burst phase at $p < 0.05$. Therefore, the null hypothesis was rejected. More specifically, by increasing the drug concentration from 5% w/w to 10% w/w a visibly higher difference in the data means was realized. Although increasing the number of layers from 10 to 20 showed a relatively lower difference in data means, the differences were still significant (Figure 4.9a). The statistical output pertaining to the main and interaction effects on burst release percentage can be found in Appendix A.

Interactions between the two factors also had significant effects ($p = 0.00$) on the burst release percentage. Thus any combination of the factors tested could be employed to achieve the desired drug release behaviors during the initial release period. Results showed that for the samples containing 5% w/w of drug loading, the data means showed a marginal decrease in the percentages the drug released during the burst period as the number of layers was increased from 10 to 20. For the samples with a 10% w/w drug loading, the samples showed a significant increase in the percentage drug release during the burst period as the number of layers was increased from 10 to 20 (Figure 4.9b).

4.3.2 Blood Collection and Compatibility Test

SEM micrographs taken at 500X and 2,000X show that evenly distributed clusters of platelets have attached to only the sample control surfaces containing PEUU only. Micrographs were also obtained for the samples containing 5% and 10% w/w of the taxol drug. One can visually see the decrease in adhering platelets as the taxol concentration is increased.

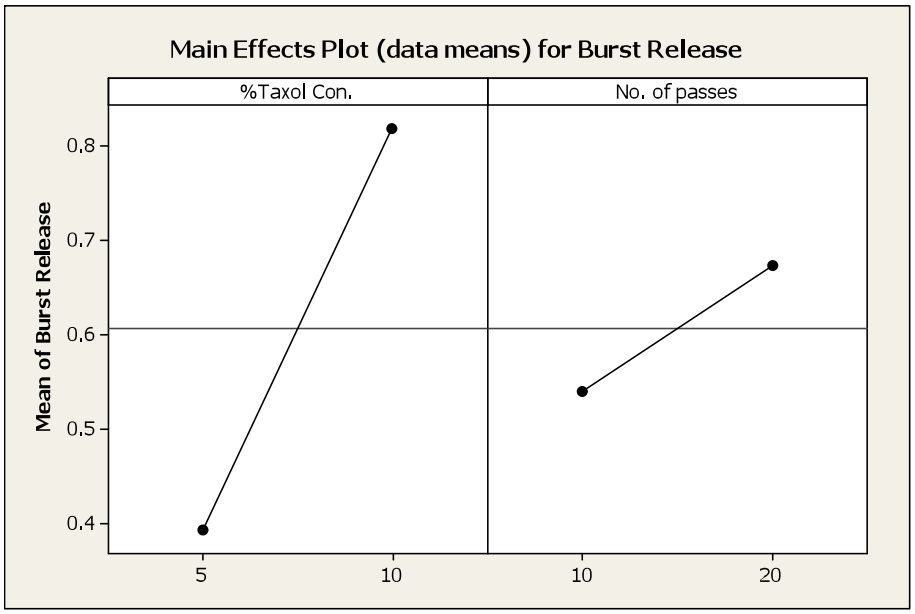

(a)

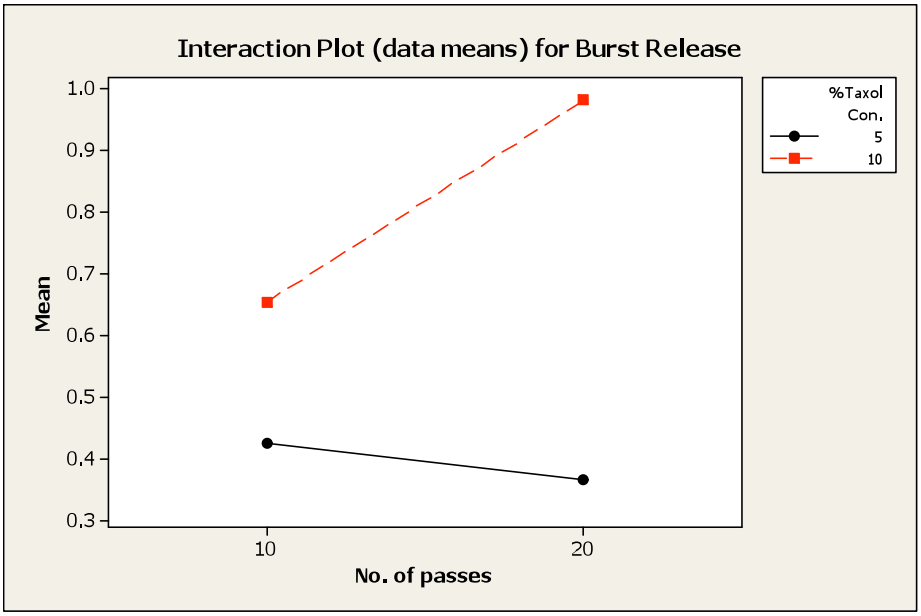

(b)

Figure 4.9 (a) Main and (b) interaction affects plot for percentage of total drug released during the burst release period

Platelet deposition onto the sample surfaces was determined by LDH assay. Samples containing PEUU with no taxol drug were fabricated as a control (Figures 4.11a and b). The data was presented as means with standard deviation. The average number of platelets was 10,191 cells/mm^2 with a standard deviation of 1,194. The sample with PEUU containing 5% taxol visually showed a decrease in platelet deposition compared to the control and the sample containing 10% taxol showed more sparse platelet deposition compared to the control (Figure 4.12-4.13a and b). The average platelet count with standard deviations for the 5% and 10% sample were 4,637 cells/mm^2 (1,339) and 3,933 cells/mm^2 (3,933), respectively.

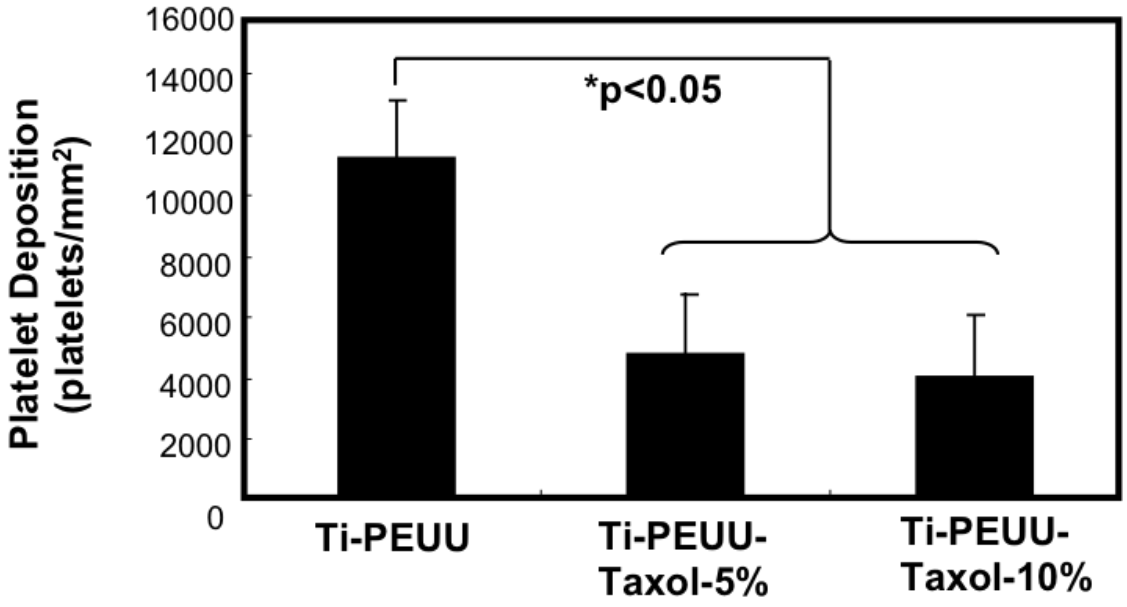

Figure 4.10 Statistical significance of drug concentration of blood platelet deposition

The statistical significance among sample groups was determined using One-way Analysis of Variance (ANOVA). Post-hoc Newman-Keuls testing was performed to determine specific differences. Statistical significance among the samples containing

only PEUU (control) and both sets of samples containing 5% and 10% taxol embedded in PEUU were found to exists at $p < 0.05$. Thus, the p- value to determine statistical significance between the control and the sample containing 5% taxol was 0.016376. This value is below 0.05. Therefore, the addition of a 5% w/w taxol drug loading had a statistically significant effect on platelet adhesion. The resulting p-value to determine statistical significance between the control and the sample containing 10% was 0.022789 (Figure 4.10). This value was also lower than the standard $p < 0.05$. Thus, the addition of a 10% w/v taxol concentration also had a significant effect on platelet adhesion (Table 4.2). The results also showed that the difference between the additions of 5% taxol versus the addition of 10% taxol was insignificant.

Table 4.2 Specific significance between groups for blood platelet deposition

	PEUU	TAXOL 5%	TAXOL10%
PEUU		0.016376	0.022798
TAXOL 5%	0.016376		0.689151
TAXOL 10%	0.022798	0.689151	

4.3.3 Inhibition of Rat Smooth Muscle Cells

The metabolic means of samples containing 10 and 20 layers with a 5% w/v drug loading were compared to the metabolic means of samples having 10 and 20 layers of PEUU with no drug, respectively. In addition, the metabolic means of samples containing 10 and 20 layers with a 10% w/v drug loading were compared to the metabolic means of samples having 10 and 20 layers of PEUU with no drug respectively. Lastly, the metabolic means of each of the experiment groups were compared with the mean metabolic index of cells cultured on Tissue Culture Polystyrene (TCPS).

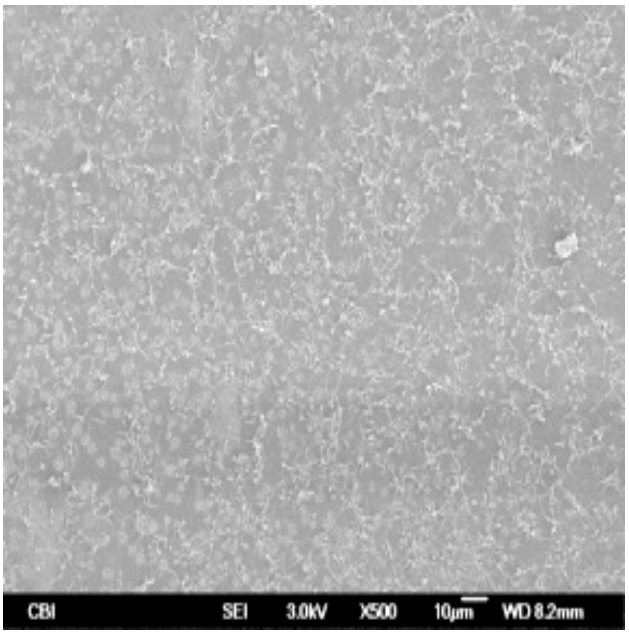

(a)

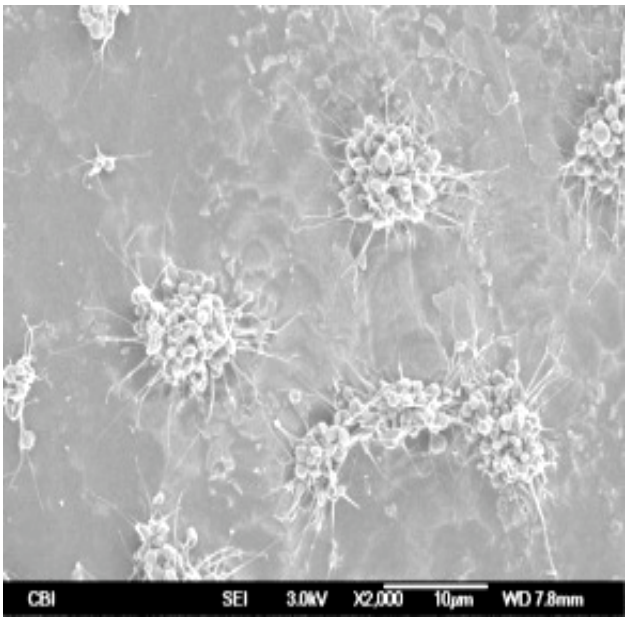

(b)

Figure 4.11 Platelet deposition for control, PEUU with no drug loading (a) 500x (b) 2,000x

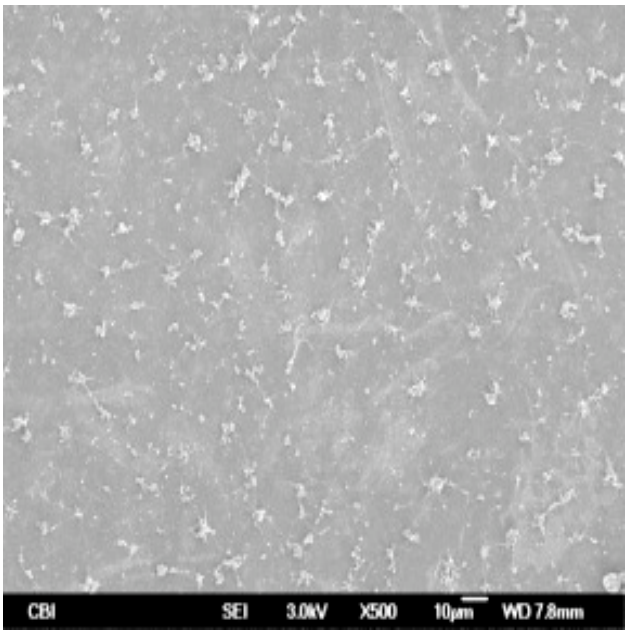

(a)

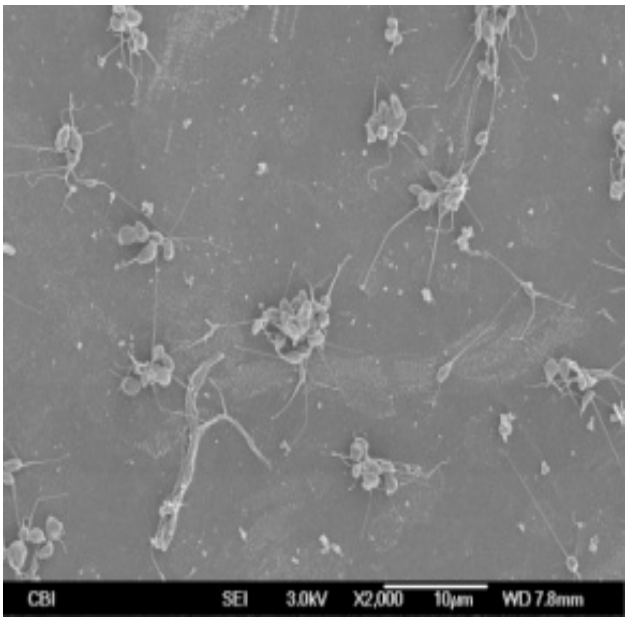

(b)

Figure 4.12 Platelet deposition on PEUU coating with 5% taxol concentration (a) 500x (b) 2,000x

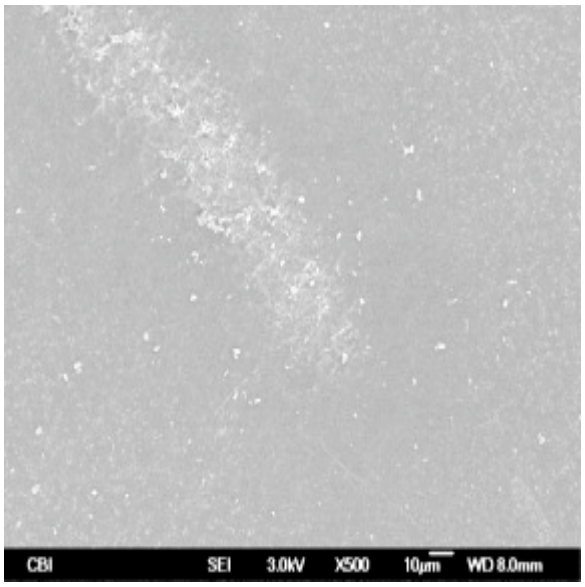

(a)

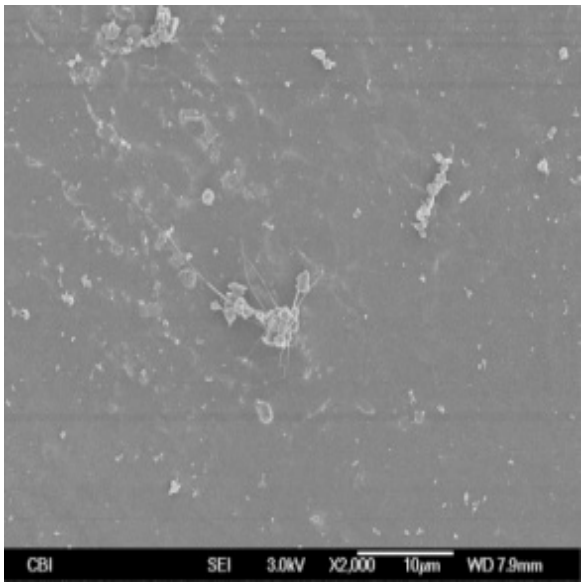

(b)

Figure 4.13 Platelet deposition on PEUU with 10% drug loading (a) 500x (b) 2,000x

The TCPS materials were used in the cell culture to encourage cell proliferation across the substrate. Thus, the metabolic index here is the natural metabolic index from cells as they were cultured over a 1, 4, and 7 day period. As compared to the cells

cultured on bare titanium substrate there was a slight increase in metabolic index. The TCPS samples were also compared to samples coated with 10 and 20 passes of PEUU without any drug loading and results showed an even further increase in metabolic activity for the 20 layer coatings. This fact indicates that there was an increase in cell count where a 20-layer coating was present, which means that the cells can adapt to the polymer coating itself. A description of this situation is shown in Figure 4.14.

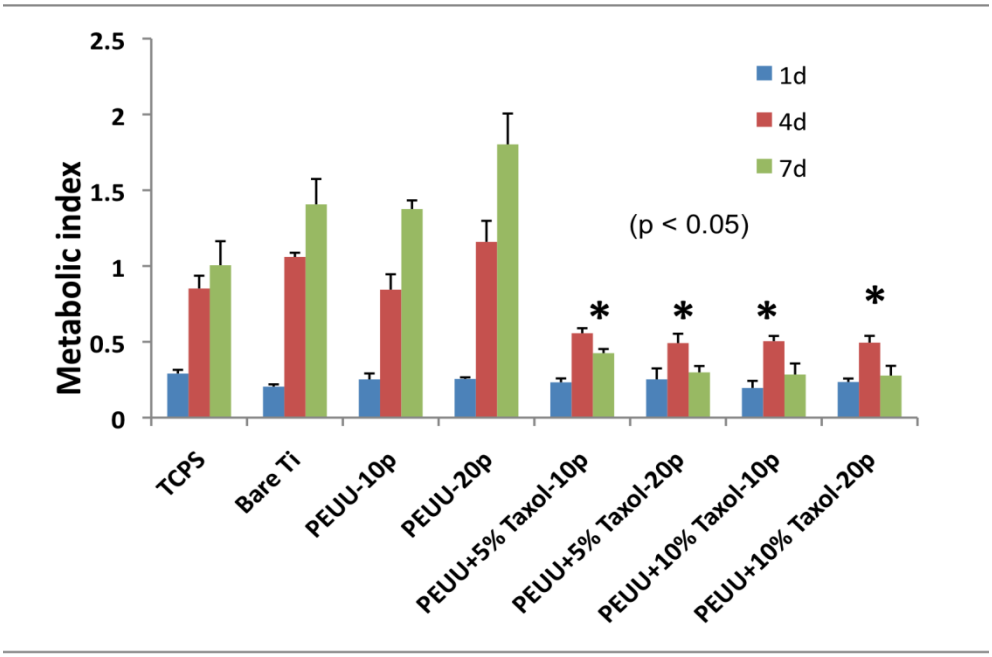

Figure 4.14 Statistical significance of controlled release experiment types on cell inhibition

In this research, it was hypothesized that taxol-loaded PEUU coatings would be used to inhibit cell proliferation of undesired cancer cells based on increased coating material and drug dosage. The results showed that there was a statistically significant difference between the control groups (i.e. TCPS, bare Ti, 10 layers of PEUU, and 20 layers of PEUU) when compared to each of the respective experiment groups. For

example, after 4 and 7 days there was a significant decrease in metabolic activity when 5% and 10% w/w of taxol were added to 10 layers of PEUU. The same finding is true when 5% and 10% w/w of taxol was added to 20 layers of PEUU. However, there does not appear to be a significant difference between the various experimental groups.

We proposed that the direct-write technique could be used to deposit a variety of other non-newtonian biopolymer fluids encompassing a variety of therapeutic agent for drug delivery. However, studies must be conducted to study the release profile of a given agent from a given polymer coating type.

CHAPTER 5

RESULTS AND DISCUSSION

5.1 Jetting Optimization

The direct-write inkjet technique was used to deposit non-newtonian biopolymer fluids for controlling the corrosion of magnesium alloys. The optimal jetting parameters were obtained by determining the appropriate frequency; the positive/negative jetting voltage, rise time, dwell time, fall time, and final rise time denoted by *f, +V/-V,* T_R*,* T_D*,* T_F*,* T_{FR}, respectively, and reservoir pressure. These obtained values are approximate values. This is because of the level of difficulty in obtaining the exact value for the reservoir pressure. Thus the remaining input values needed to be adjusted. The final jetting parameters obtained for PEUU at a reservoir pressure of approximately -16 psi were *f = 500Hz, +V/-V = 58 V/-58 V,* T_R *= 51 μs,* T_D = 50 *μs,* T_F *= 51 μs,* and T_{FR} *= 51 μs.* For PCL, the final jetting parameters obtained at a reservoir pressure between -8 psi and -12 psi were *f = 500Hz, +V/-V = 42 V/-42 V,* T_R *= 22 μs,* T_D = 25 *μs,* T_F *= 38 μs,* and T_{FR} *= 22 μs.* For PLGA, the final jetting parameters obtained at a reservoir pressure between -8 psi and -12 psi were *f = 500Hz, +V/-V = 32 V/-32 V,* T_R *= 22 μs,* T_D = 32 *μs,* T_F *= 24 μs,* and T_{FR} *= 22 μs.*

5.2 Polymer Coatings for Controlling the Corrosion of Mg Alloys (Phase 1)

Immersion testing was terminated at 21 hours, as the bare Mg alloy surface showed severe pitting and corrosion, thus was defunct for implantable conditions. It is important to note that the corrosion conditions for samples are at an accelerated pace as compared to the actual implant conditions. This situation occurs because implants are in

prominent contact with tissue and bone structures with relatively lower liquid interface from the site blood vessels. In contrast, the tests were conducted in complete liquid immersion to simulate longer durations in actual implant conditions.

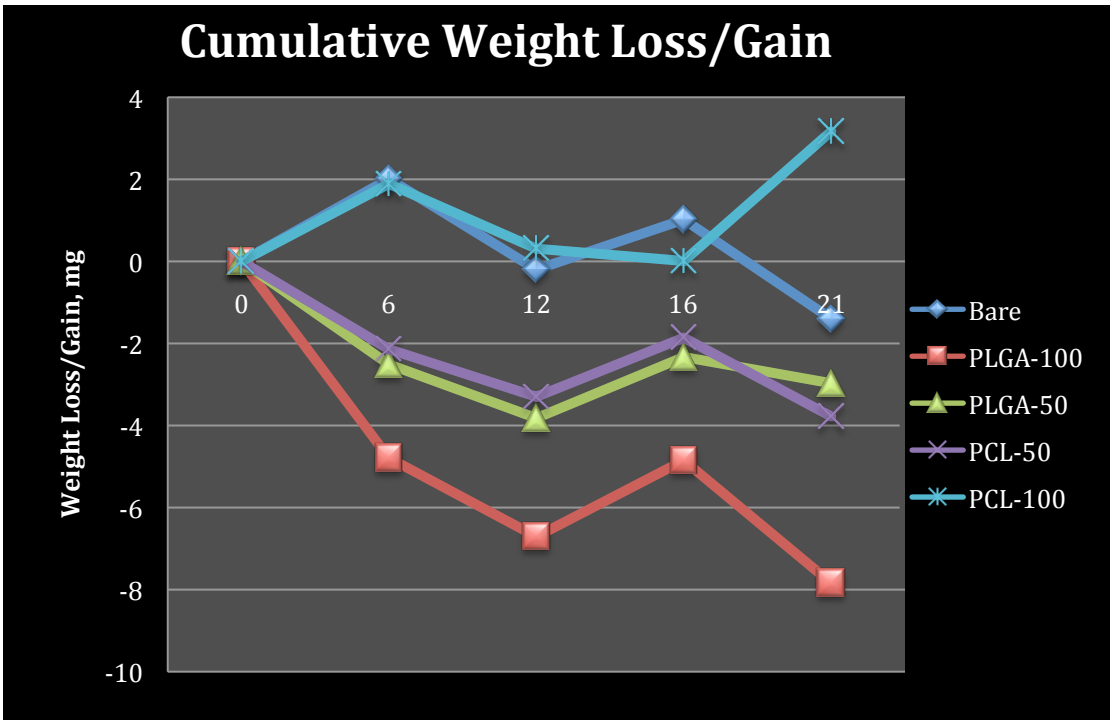

Figure 5.1 Cyclic corrosion mechanism in magnesium alloy samples

5.2.1 Cyclic Corrosion Mechanism in Mg Alloy Samples

In a typical corrosion reaction, the Mg alloy reacts with water leading to magnesium hydroxide and the release of hydrogen gas. This process is shown in Equation (3). The uncoated magnesium sample showed a cyclic corrosion mechanism as seen in figure 5.1. During the initial six hours exposed magnesium alloy surface underwent corrosion with the formation of magnesium hydroxide $Mg(OH)_2$ products on the surface.

$$Mg\,(s) + 2H_2O\,(g) \rightarrow Mg(OH)_2(aq) + H_2(g)$$

Equation 3 Chemical reaction for magnesium hydroxide

The corrosion products resulted in an increase in the weight of the sample. Further, at 12hrs duration the corrosion products detached from the underlying sample into the SBF resulting in weight loss of the sample. The freshly exposed surface of the sample underwent subsequent corrosion and formation of $Mg(OH)_2$ products at 16hrs. Finally, at 21hrs these corrosion products detached resulting in severe pitting and degradation of the underlying sample as seen in Figure 5.2 (right). Though, the bare sample has incremental weight gains during corrosion, it is evident from the Figure 5.1 that the overall trend is downward (weight loss) indicating cumulative weight loss of Mg alloy.

The PLGA based polymeric coating with 100-micron deposition spacing shows weight loss at 6 and 12 hours, respectively. This fact was attributed to the degradation of the PLGA coating during the initial period. The larger spacing of the deposited microdroplets formed a porous coating allowing media to infiltrate within the layers. At 16hrs the PLGA-100 coating shows weight gain due to the formation of corrosion products within the film when in contact with the entrapped media. Further, at 21hrs a particular region within the coating film detaches (Figure 5.3) allowing the corrosion products to escape. Thisprocess results in a weight loss from the PLGA-100 sample.

The PLGA-50 sample with tighter deposition pattern showed lower weight loss and corrosion behavior as compared to the PLGA-100 coating. This fact is due to PLGA-

50 coating is less porous and offers resistance to media infiltration. During the initial 12hr period, there was weight loss due to the degradation of the PLGA film. Further, at 16hrs corrosion products are formed within the PLGA-50 film at specific locations resulting in weight gain. This process is followed by a release of Mg alloy degradation product through the porous sections of the PLGA-50 film (Figure 5.4) at 21hrs and subsequent weight loss.

PCL (Polycaprolactone) is a tough biodegradable polymer with enhanced mechanical properties and chemical stability as compared to PLGA. Similar trends of initial weight loss (12hrs) due to polymer degradation were observed with the PCL-50 coating. This process was followed by Mg alloy degradation and weight gain as shown in Figure 5.1. Finally, at 21hrs duration, the degradation products were released to the media resulting in weight loss. It is important to note that the corrosion mechanism for PCL-50 is analogous to PLGA-50 the overall weight loss was lower in the former case. This is due to the enhanced film stability of PCL-50 as shown in Figure 5.5.

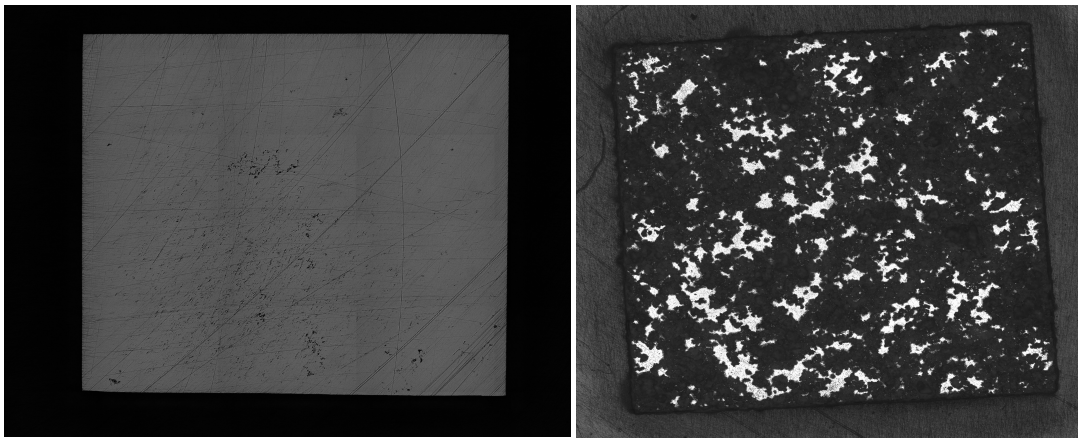

Figure 5.2 Uncoated magnesium alloy (left) before t=0 and (right) after t=21 hours

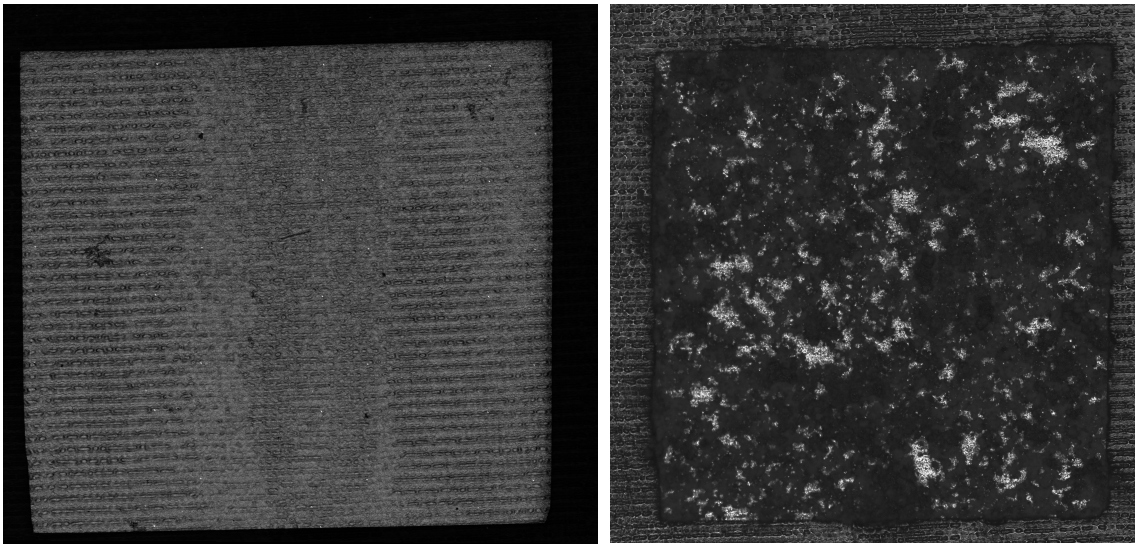

Figure 5.3 PLGA-100 Mg alloy (left) t=0 and (right) t=21 hours

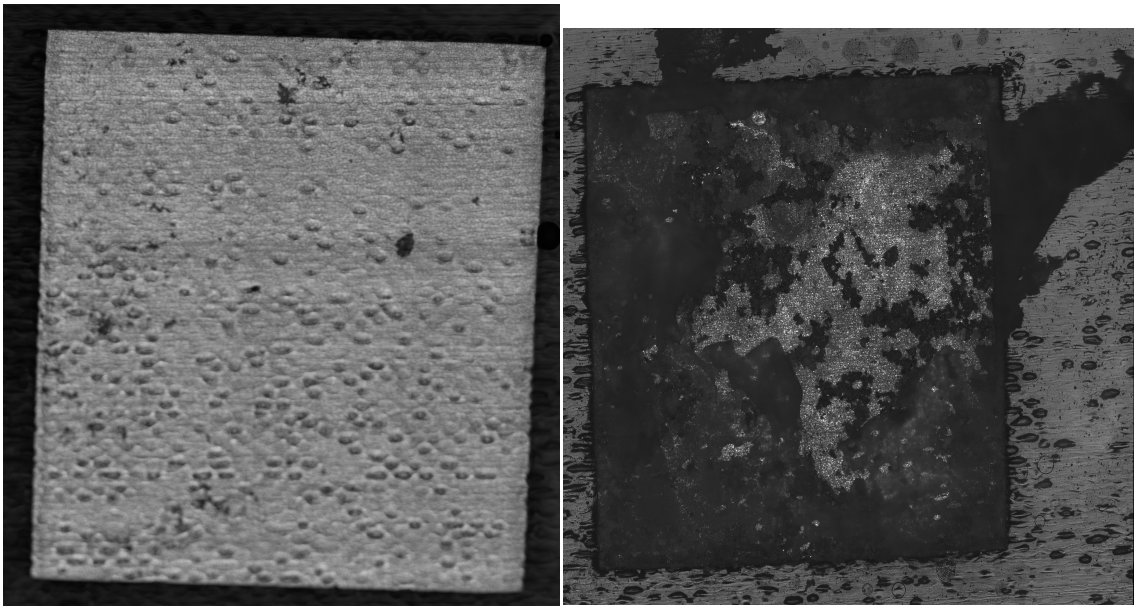

Figure 5.4 PLGA-50 Mg alloy (left) t=0 and (right) t=21 hours

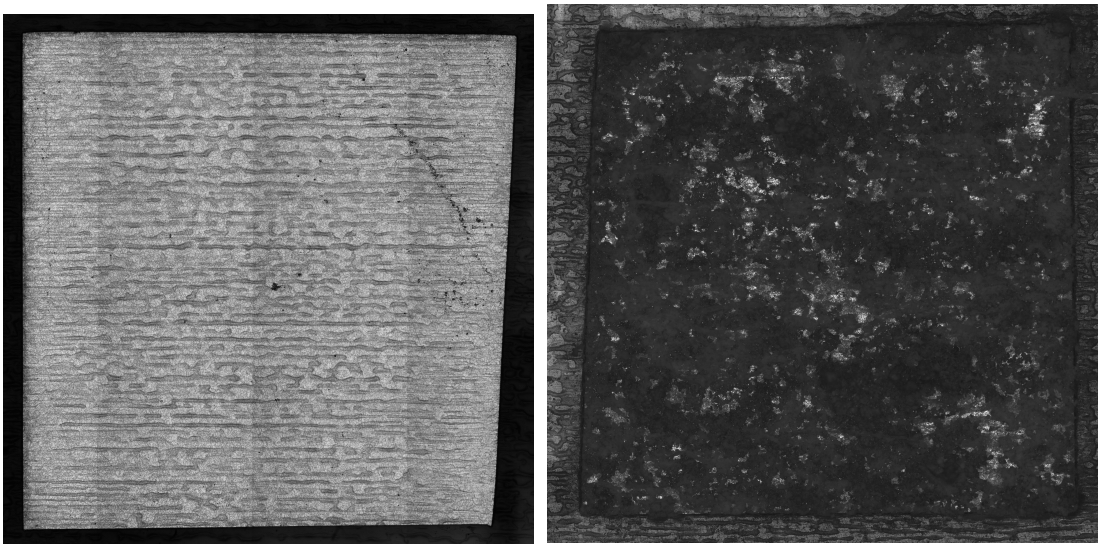

Figure 5.5 PCL-50 Mg alloy (left) t=0 and (right) t=21 hours

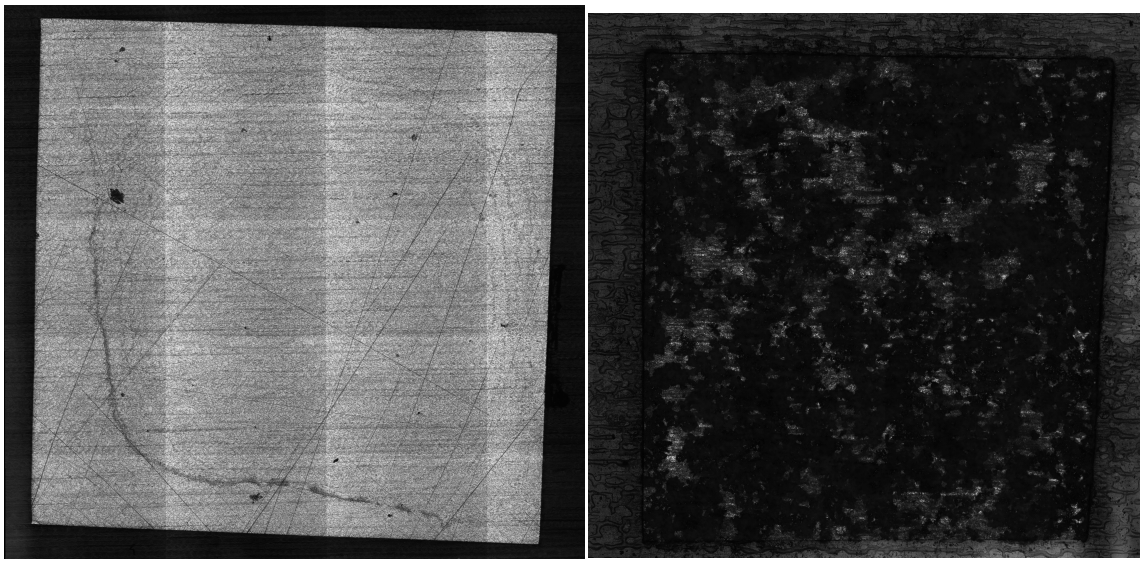

Figure 5.6 PCL-100 Mg alloy (left) t=0 and (right) t=21 hours

The PCL-100 coating had higher porosity and resulted in media infiltration during the initial 6hr period. However, because the PCL film has better adhesion properties to the Mg substrate, the corrosion products were retained within leading to a weight gain.

During the next 10hrs (6 to 16hrs) there was weight loss due to PCL degradation and the release of corrosion products through the porous film. This situation led to exposure of the underlying Mg alloy surface to fresh media resulting in corrosion products (Figure 5.6 right) and subsequent weight gain at 21hrs.

5.2.2 Total Weight Loss/Gain in Mg Alloy Samples

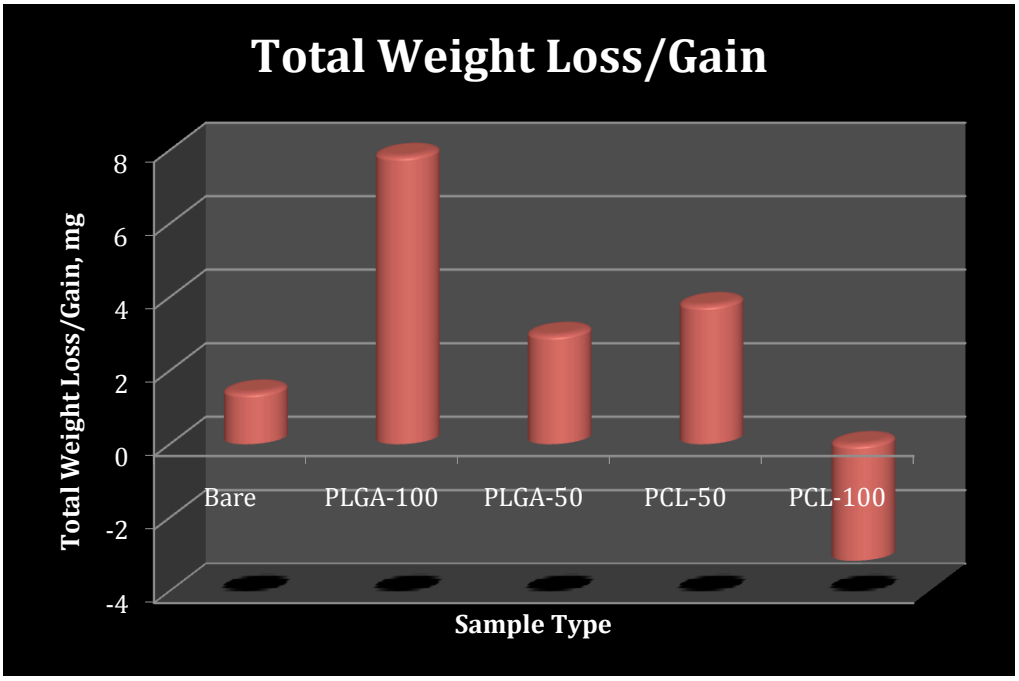

Figure 5.7 Weight loss/gain of various sample types

It is important to note the caveat that the polymeric coatings show higher weight loss as compared to bare Mg alloy. This situation is attributed to the combination of the weight loss of the polymer and Mg corrosion products, with the former being a significant proportion of the total weight loss. As can be seen from Figure 8 the sample PLGA-100 has the highest weight loss due to high corrosion rate and degradation of porous PLGA film. PLGA-50 and PCL-50 show comparable weight loss due to lower corrosion rates. PCL-100 shows weight gain at 21 hrs due to the retention of corrosion

products within the PCL film. It is important to note, that corrosion cycles for different samples may not coincide at the same time point. For example, PLGA is a fast degrading polymer and may gain and lose weight at frequent intervals as compared to PCL.

5.2.3 Corrosion Metrics Based on Polymer Type and Pitch Distance

Table 5.1 Corrosion impeding properties of polymer coatings

Polymer Type	Degradation Properties	Corrosion Rate of Mg alloy
PCL	Tough biodegradable polyester with slower dissolution characteristics	Low
PLGA	Tunable degradation rates based on the adjustable chemical composition of lactic and glycolic acids within polymer	High

Table 5.2 Relationship between pitch distance and corrosion rate

Pitch Distance	Porosity	Corrosion Rate of Mg alloy
50	Dense polymer microstructure with close overlap	Low
100	Lower overlap and presence of permeable polymer layers	High

Table 5.1 shows differences in the corrosion behavior of the Mg alloy surface based on the polymer type. PCL serves as a more robust polymer to protect the underlying Mg alloy surface from corrosion as compared to PLGA. However, the PLGA polymer may have tunable degradation rates, which are obtained by varying the ratio of lactic and glycolic acids within the polymer. Thus, depending on the application intent, one can employ either of these polymers to obtain controlled corrosion behavior. Table 5.2 shows the relationship between pitch distance (interspacing of deposited polymer microdroplets on substrate) and the corrosion rate of the Mg alloy surface. As shown in

Table 5.2, larger pitch distances (100μm) lead to porous polymer layers resulting in infiltration of the biological media to the Mg alloy surface. Thus, higher corrosion products are formed at this pitch distance for both the polymer types. On the contrary, tighter pitch distances (50μm) form dense and homogeneous polymer microstructures prolonging the life of the polymer coatings and lowering the corrosion of the underlying Mg alloy surface. These metrics play an important role in determining the choice of polymer type and pitch distance to control Mg alloy corrosion for specific implant applications.

5.3 Polymer Coatings for Controlling the Corrosion of Mg Alloys (Phase 2)

5.3.1 Immersion Testing (ICP)

The samples were immersed in simulated body fluid (SBF) to initiate the corrosion process. Sample aliquots taken at each of the specified time points were then tested for magnesium ion presence by inductively coupled plasma (ICP) elemental analysis. The immersion test was stopped after 8 days due to peeling of the polymeric coating. The effect that coating thickness (10 versus 20 layers) had on magnesium ion presence was compared among all polymer types. For example, a comparison between 10 layers of PEUU and 20 layers of PEUU was made to determine the effects of layer thickness for this polymer type on the magnesium presence.

For the PEUU sample coated with 10 and 20 layers, 0.0010 mol/L and 0.0028 mol/L of magnesium was present in the SBF solution, respectively (Figure 5.9). Samples coated with 10 and 20 layers of PLGA showed a 0.004 mol/L and 0.0016 mol/L magnesium presence in SBF, respectively (Figure 5.10). For the PCL sample coated with

10 and 20 layers, 0.0026 mol/L and 0.0059 mol/L of magnesium was present in the SBF solution, respectively (Figure 5.8). Therefore, it is shown that coating thickness does have some effect on magnesium presence. However statistical analysis was necessary to determine if the differences were significant.

It is apparent through the data analysis that for the PCL coating, an increase in the polymer material resulted in an adverse effect on the magnesium ion content that was ultimately released into the SBF solution after the 8-day immersion period (Figure 5.8). This phenomenon is explained because of the materials tendency to adhere to the surface of the magnesium alloy. Thus, maintaining any fluid and corrosion byproduct that may have seeped through the polymer coating. The fluid entrapped within the polymer coating causes increased corrosion of the magnesium alloy material.

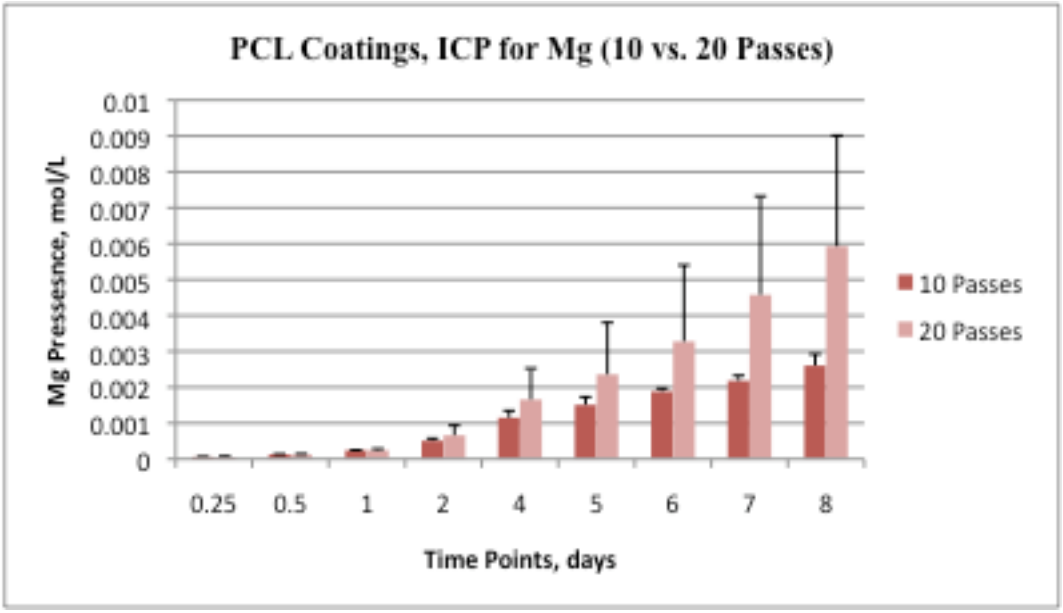

Figure 5.8 Magnesium content comparison of layer thickness for PCL coating

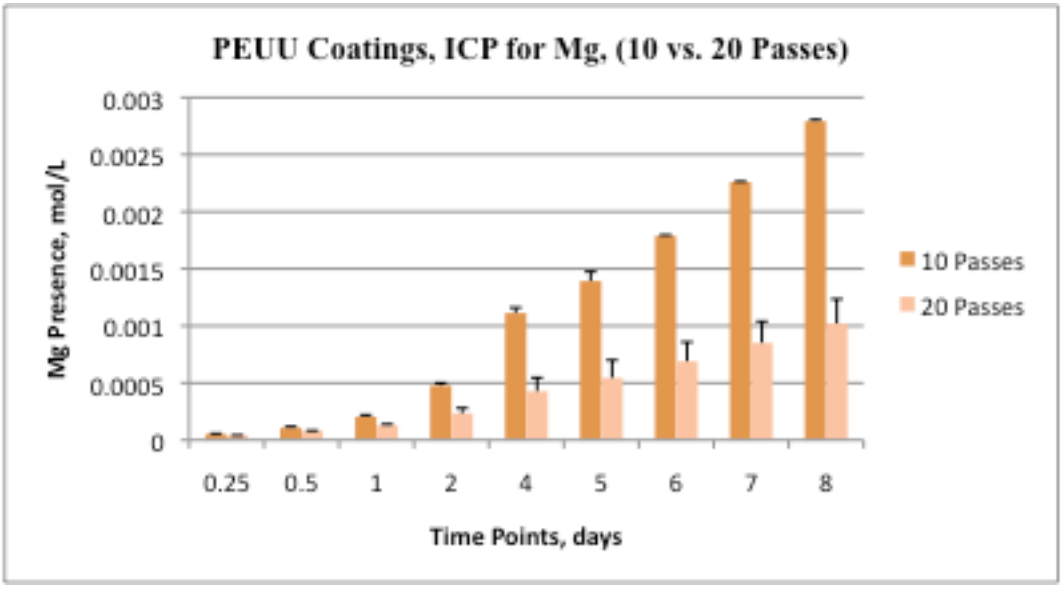

Figure 5.9 Magnesium content comparison of layer thickness for PEUU coating

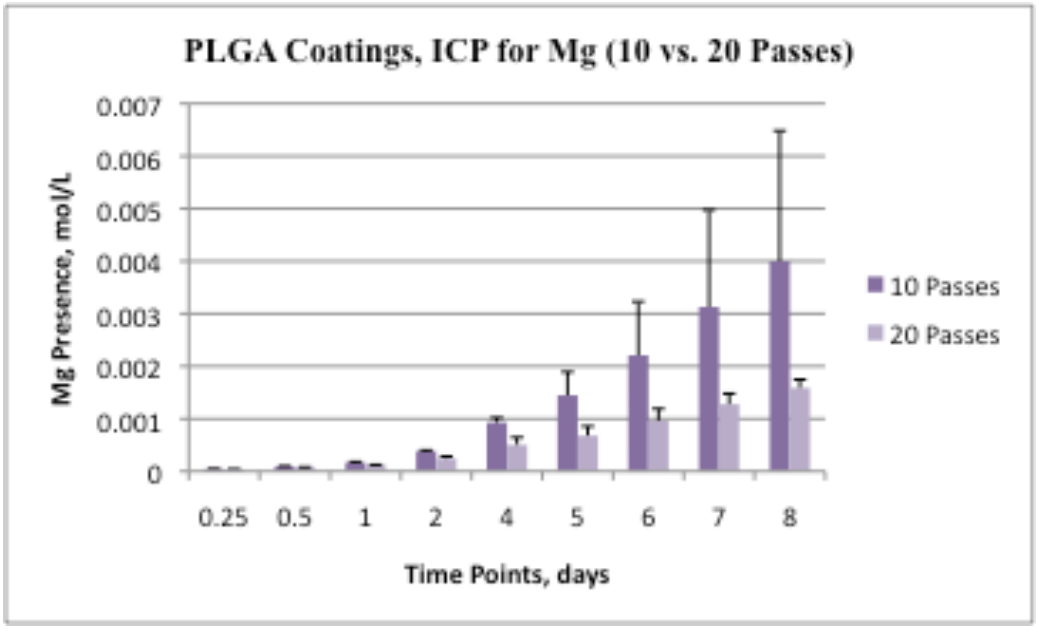

Figure 5.10 Magnesium content comparison of layer thickness for PLGA coating

A comparison between the uncoated magnesium sample and the samples coated with 10 layers of each polymer type was noted after an 8-day immersion period. For the uncoated sample, the amount of magnesium present in the SBF solution was 0.0078

mol/L. For the coated samples, both PCL and PEUU offered the best protective coatings having 0.0026 mol/L and 0.0028 mol/L magnesium presences respectively. The PLGA coating was shown to be the least protective coating with 0.0040 mol/L.

A comparison between the uncoated magnesium sample and the samples coated with 20 layers of each polymer type was also noted. This is shown in figure 5.11. For the uncoated sample the amount of magnesium present in the SBF solution was 0.0078 mol/L. For the coated samples, PEUU offered the best protective coating and a more consistent rate of corrosion having 0.0010 mol/L mg presences. The PLGA coating was also found to be a good protective coating with 0.0016 mol/L. The corrosion rate of the PCL coating was more comparable to that of the uncoated sample. It was evident that varying the levels of each of the identified factors did have some effect on the magnesium content present in the SBF solution, however statistical analysis was necessary to determine tany significant differences.

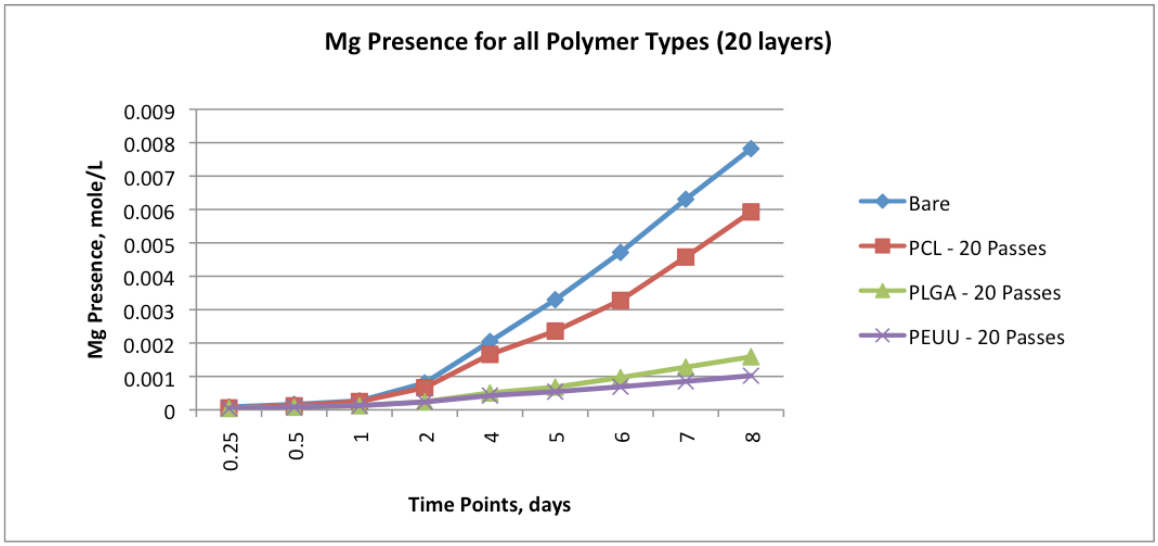

Figure 5.11 Magnesium content comparison between all treatment types

The experimental data were assessed to ensure that the assumptions of normality and randomness were satisfied. It was determined that the data were normally distributed and did not exhibit any obvious trends or patterns, thus the data was, in fact, random in nature. The normality and randomness plots for data comparing the polymer coating types amongst each other are depicted in figures 12a and 12b, respectively. As a result, the statistical relevance of the independent variables on magnesium ion content was suitable for the application of analysis of Variance (i.e. ANOVA) statistical testing.

A 3x2 factorial analysis was conducted to compare the effects of the polymer type and number of printed layers on the magnesium ion presence after the 8-day immersion period. Therefore, the uncoated samples were omitted from this analysis. The results of the analysis revealed that there is no actual significant effect amongst the polymer coating types. However, the main effects plot is consistent with the results, which shows that between the three coating types differences do exists although they may not be significant (Figure 5.13a). Here again, it is shown that PEUU offers the best protective coating followed by PLGA and PCL.

The interaction plot reveals also that increasing the number of layers of PLGA and PEUU offers better corrosion protection whereas increasing the number of PCL layers from 10 to 20 results in an increase in corrosion byproduct when fully immersed in the SBF solution (Figure 5.13b). For matching magnesium degradation to bone growth or repair, PCL should be eliminated as a possible surface coating material, as it does not significantly reduce the rate of corrosion. Details of the factorial design for magnesium ion content are shown in Appendix C.

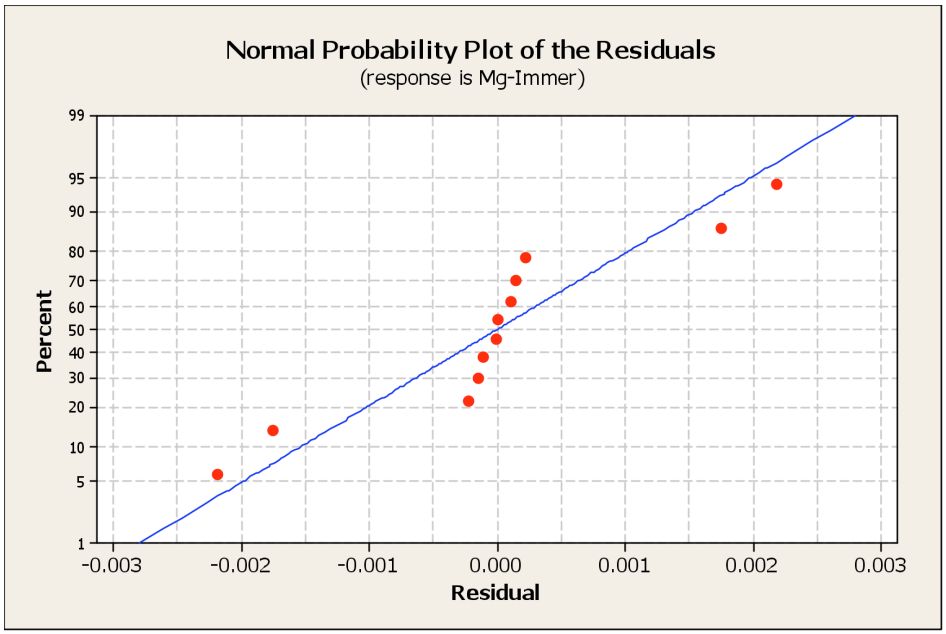

(a)

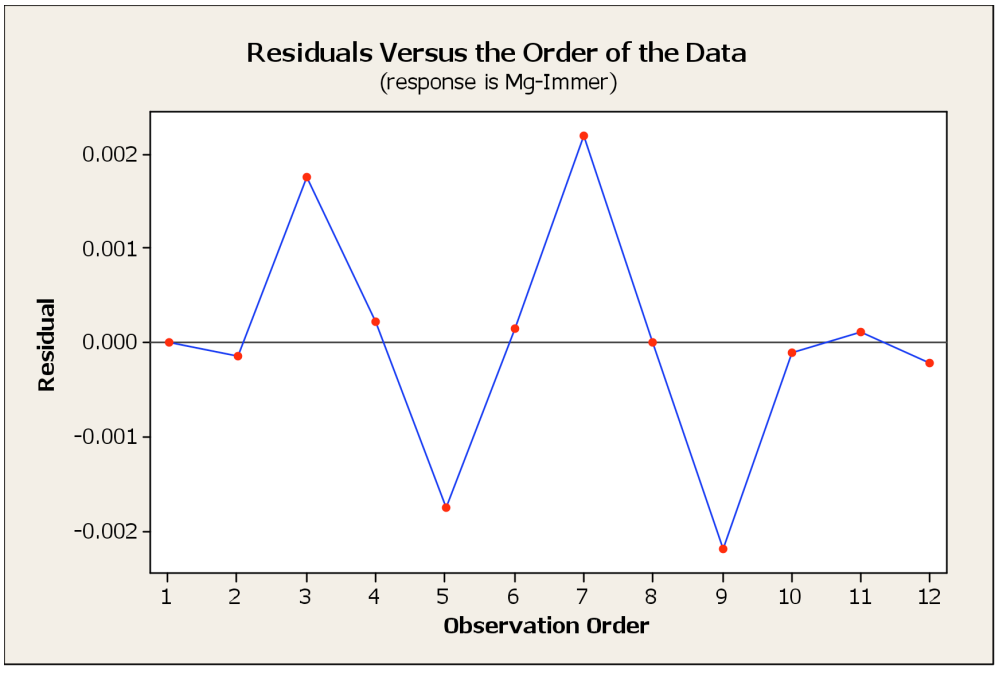

(b)

Figure 5.12 (a) Normality plot and (b) Randomness plot for data comparison amongst polymer coating types

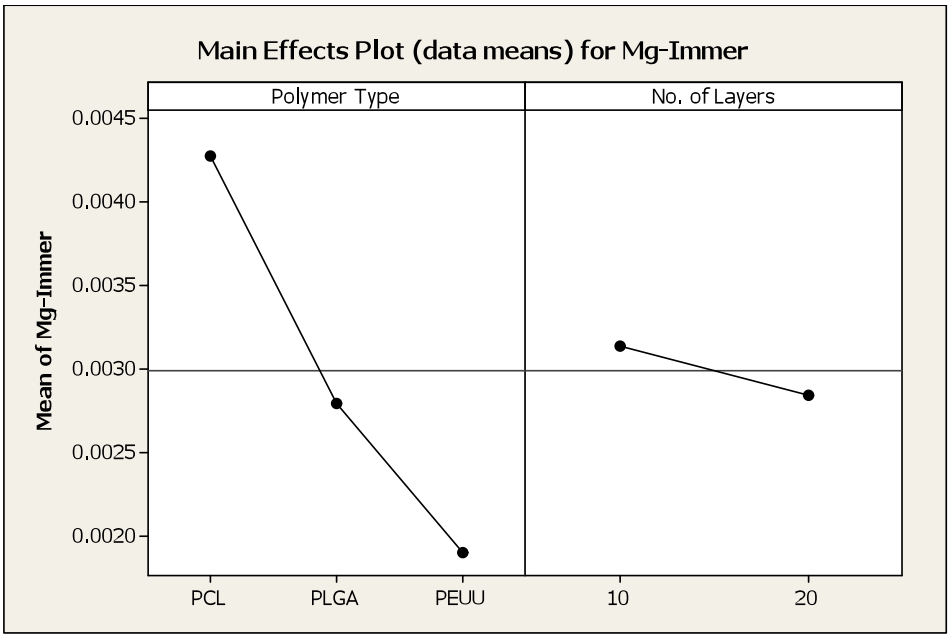

(a)

(b)

Figure 5.13 (a) Main and (b) interaction affect plots for polymer type and layer thickness amongst polymer coating types

The experimental data were assessed to ensure the assumptions of normality and randomness were satisfied. It was determined that the data were normally distributed and did not exhibit any obvious trends or patterns, thus the data was, in fact, random in nature. Normality and Randomness for data comparisons between all sample treatment types were validated and can be found in figures 5.14a and b, respectively. As a result, the statistical relevance of the independent variables on magnesium ion content was, again, suitable for the application of analysis of Variance (i.e. ANOVA) statistical testing.

A One-way ANOVA was conducted to compare each experiment type against the control (uncoated) for statistical significance. The results of this analysis showed that there was a statistical difference between at least two of the sample means given $p = 0.036$ which is less than the specified alpha level of 0.05 (Appendix C). A Tukey's post hoc analysis was conducted to determine exactly which of the data means were statistically different. A depiction of the differences between the data means is shown in figure 5.15. The result from the Tukey analysis showed that the difference in the data mean for the uncoated samples was statistically different from the mean samples coated with 20 passes of PEUU. This finding was consistent wit the hypothesis that the PEUU coating would provide the most corrosion protection for the magnesium alloy. This coating could be applied for controlled release of magnesium for cardiovascular and tracheal stent applications. There was no significant affect on the magnesium content for all other experiment categories.

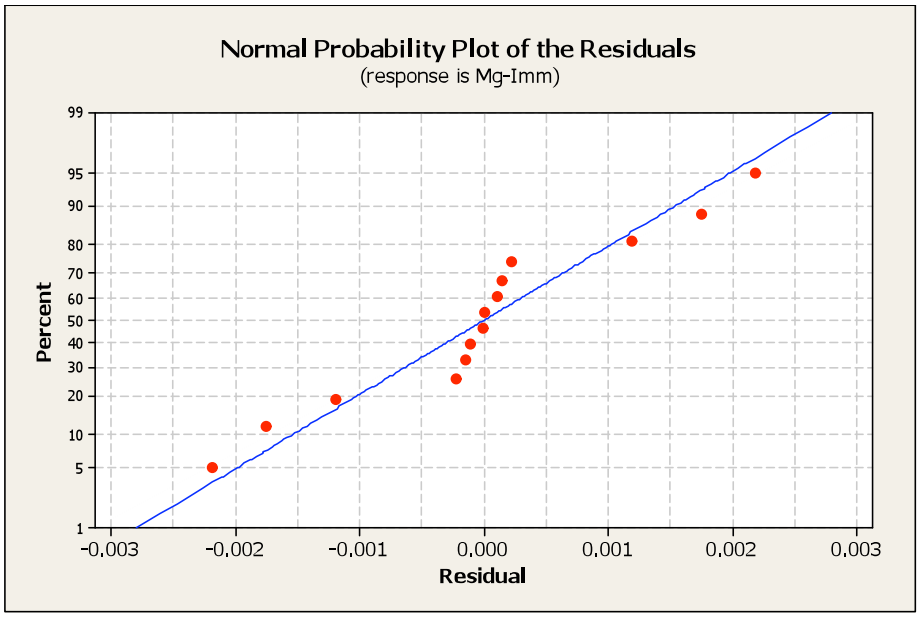

(a)

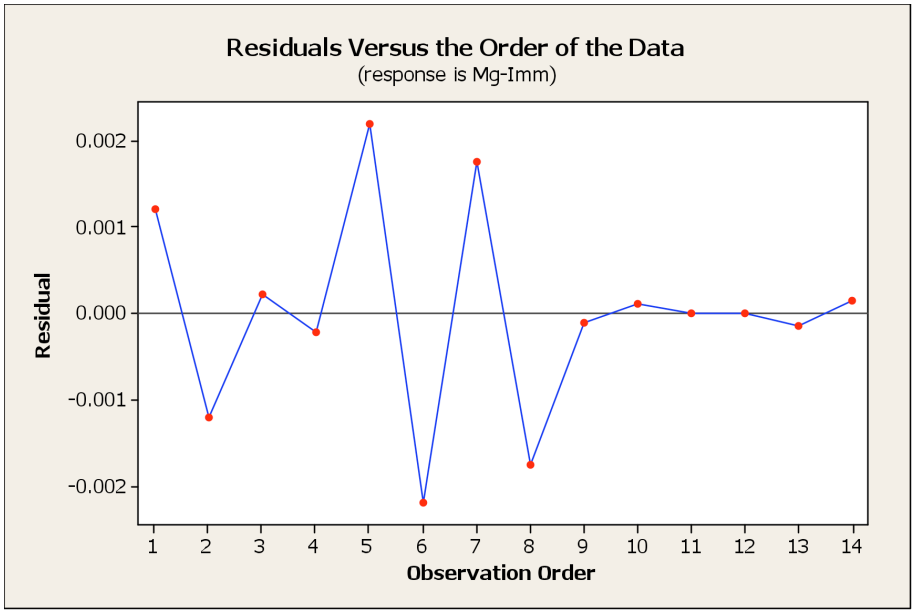

(b)

Figure 5.14 (a) Normality plot and (b) randomness plot for data comparison of all samples types

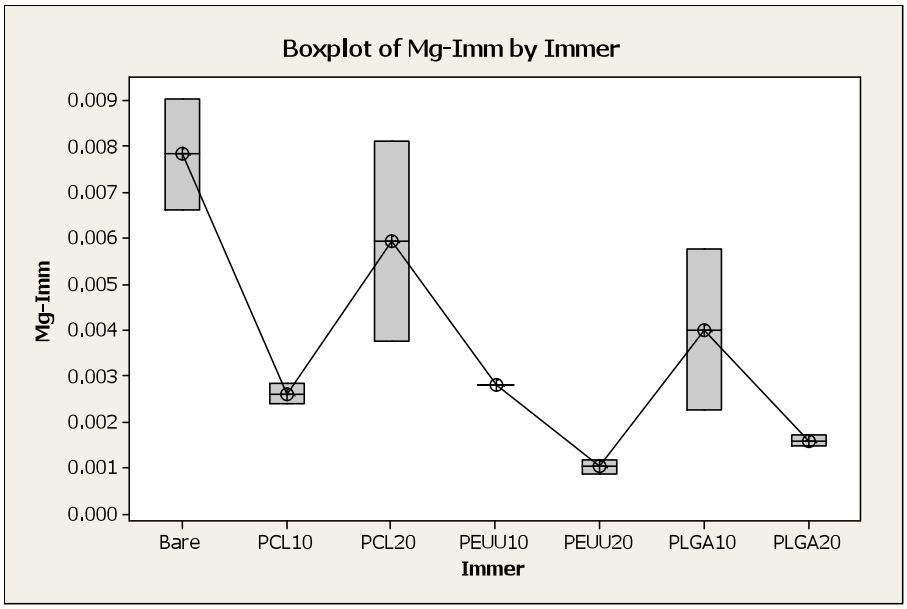

(b)

Figure 5.15 Box plot for ICP data depicting differences in data means

5.3.2 Biocompatibility of Polymer Coated Magnesium Alloys

LDH activity was assessed as previously described. Due to the variation between the cultured cells in each well, the cytotoxicity levels from the LDH assays were converted to percentage of the high control values. This was so that each of the samples could be compared to the total possible LDH activity. The treated samples were also compared to the percentage LDH activity of the low control samples, which saw no exposure to the magnesium alloy.

LDH activity was collected over the course of a 24 hour period at t = 0, 1, 4, 6, and 24 hours. The sample data collected at time zero represents two distinct events. The first was that this sample was collected at the end of a 24-hour period prior to initiation of the experiment. This was to gauge LDH release over a one-day period. This is apparent in the graph shown below which depicts a sample reading that shows significantly higher

LDH activity when compared to subsequent readings. Also, at time zero fresh media was added to each of the sample wells to initiate the new testing period. Thus, it is taken that each time point represents the end of a sample collection period.

First it is necessary to describe the pattern of LDH activity of the low control samples (i.e. samples unexposed to the magnesium alloy). From t = 0 to t = 1 hour, an apparent decrease in LDH activity was observed. During the one-hour period the cells seemed to be undisturbed thus not much LDH release had occurred. At t = 4 the media captured LDH activity for a slightly longer time period (i.e. three hours) and as a result slightly higher levels of LDH activity was recorded. After 24 hours, the cell media collected LDH activity for 18 hours thus there is a large spike in LDH activity. It is important to note that the cultured NHBE cells were cultured for 23 days, which included conversion into air liquid interface. Thus, the cells were expected to show some signs of stress irrespective of magnesium exposure around 24 hours after reaching confluency.

For the cultured wells containing the various treated sample types, results show that between t = 1 hour and t = 6 hours the cells seem to be responding in a similar manner irrespective of the treatment type. However, the cultures containing polymer coated samples showed decreasing LDH activity as compared to the samples containing no magnesium exposure (cells only), which showed increases in LDH release. This is an indication that the cells are responding positively to magnesium exposure. At the next sample collection, t = 24 hours, all of the well containing the various treated samples show an increase in LDH release. The data analysis was cut of at the 24-hour time period due to the naturally declining health of the cells in air-liquid interface. Also, the

difference of time between the 24-hour time point and the 29-hour time point was not enough time to collect relevant amounts of LDH activity. A depiction of LDH activity collected for each time point is shown in figure 5.16.

The cells, which were exposed to the uncoated magnesium surface, showed the least amount of LDH activity. To explain this phenomenon, one could say that more magnesium exposure contributed positively to the overall health of the cells. In addition, it could be said that a given polymer type is more compatible than others when placed in the physiological environment. However, further testing to study the cell activity at the various time points was required.

Although the results showed varying levels of LDH release, cytotoxicity levels had not reached a toxic range (i.e. > 30%) after 24 hours of exposure (Figure 5.17a). For LDH activity over a 24-hour period, cytotoxicity levels were expected to increase slightly over time due to the natural death process. However, at the end of the 24-hour period, the greatest difference existed between the cells only (i.e. low control) and the uncoated magnesium alloy cultures (Figure 5.17b). This indicates that any apparent toxicity that was present in the cultures was unlikely due to the polymer coating materials. These findings seem to be consistent with the results from the ICP tests in which it was concluded that there were no significant differences between polymer coating materials. However, an analysis of statistical significance for percentage LDH activity among the treatment types was necessary.

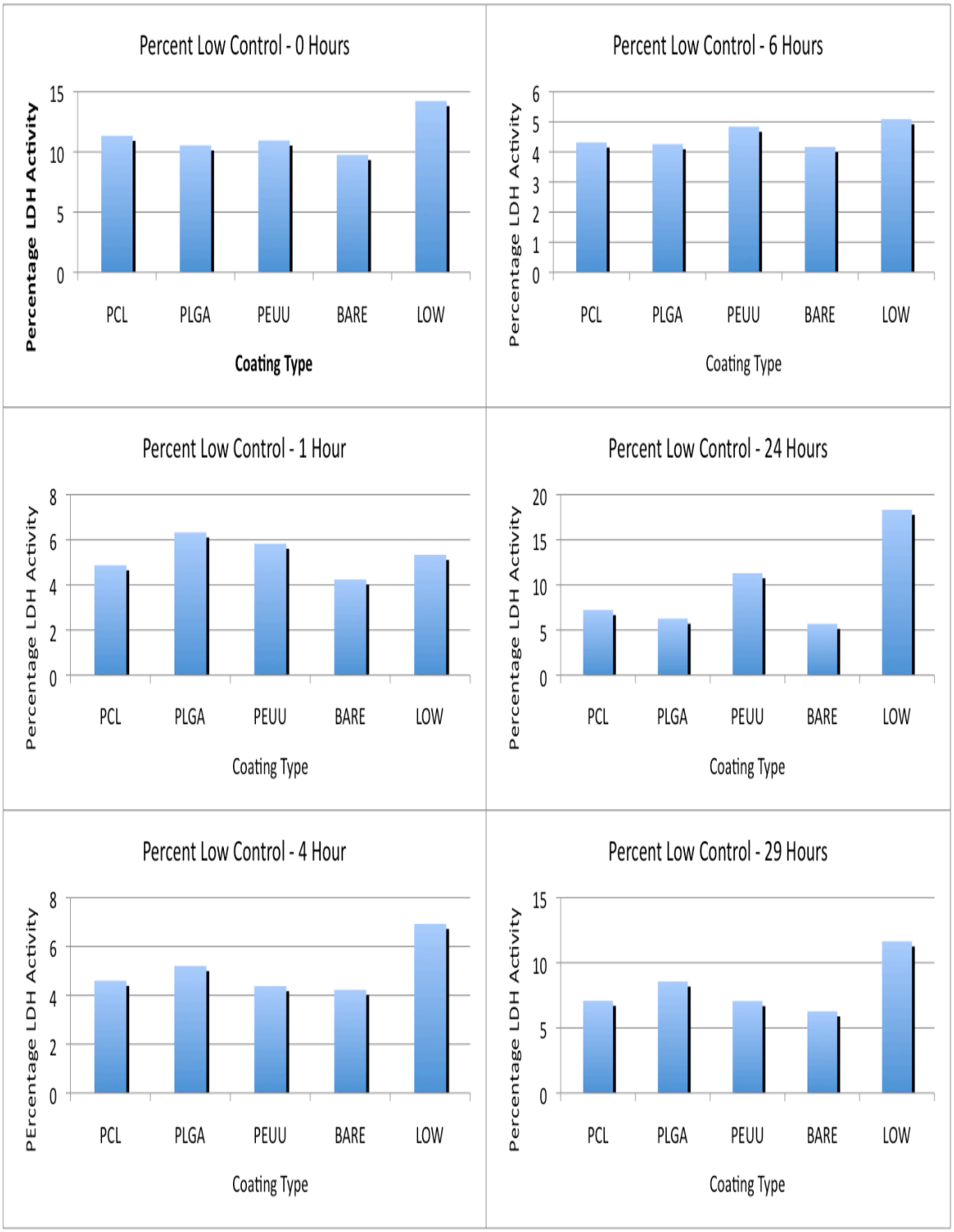

Figure 5.16 Depiction of fluctuating LDH activity for all time points

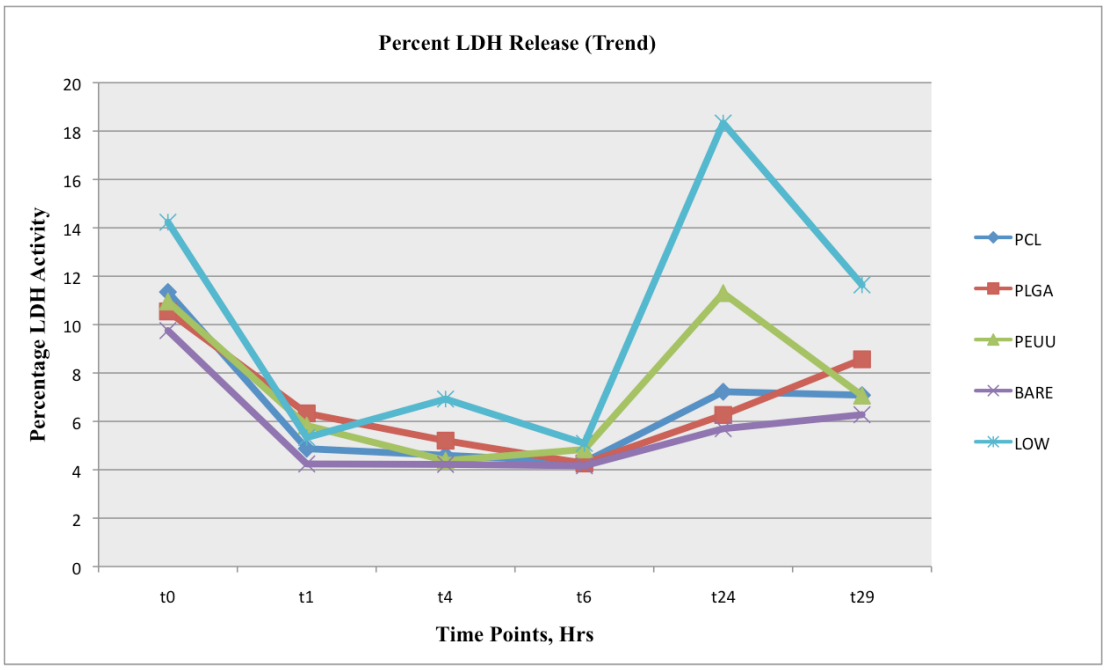

(a)

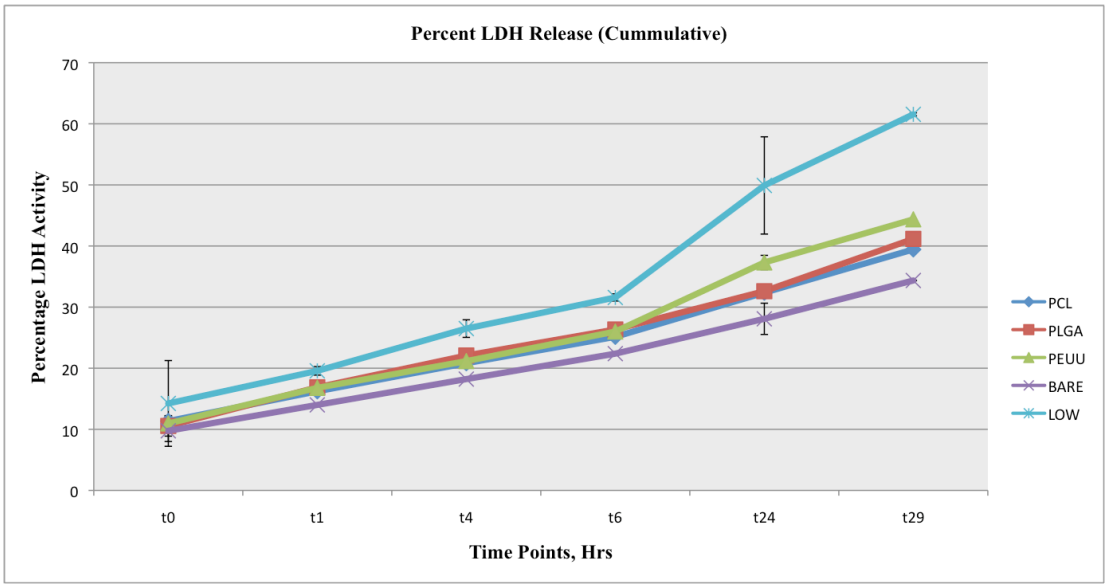

(b)

Figure 5.17 (a) Depiction of trends in LDH activity over 24 hours (b) increasing LDH activity over 24 hours

The experimental data were assessed to ensure the assumptions of normality and randomness were satisfied. It was determined that the data were normally distributed and did not exhibit any obvious trends or patterns, thus the data was, in fact, random in nature. A depiction of the normality and randomness plots for the LDH data set is shown in figure 5.18a and b, respectively. As a result, the statistical relevance of the independent variables on percentage LDH activity after 24 hours was suitable for the application of analysis of Variance (i.e. ANOVA) statistical tests.

A one-way analysis of variance was conducted on the percentages of LDH activity after a 24-hour period. The differences between the mean LDH release for each sample treatment type are depicted in figure 5.19. The results showed that significant differences between at least one of the means for LDH release were present given $p = 0.041$, amongst the experiment groups at $p < 0.05$ (Appendix D). Therefore it was necessary to reject the null hypothesis that there were no significant differences between the means of the identified experiment groups.

A follow-up post hoc analysis was performed to determine specific differences. Findings from the Tukey's post hoc analysis showed that there were significant differences between the low control (cells only) samples and the uncoated samples. It is important to note that the results of this analysis confirm also that the presence of magnesium does show that the LDH activity decreases significantly following magnesium exposure. Differences between all other experiment groups were found to be insignificant. Thus, these findings are consistent with the results from the immersion tests.

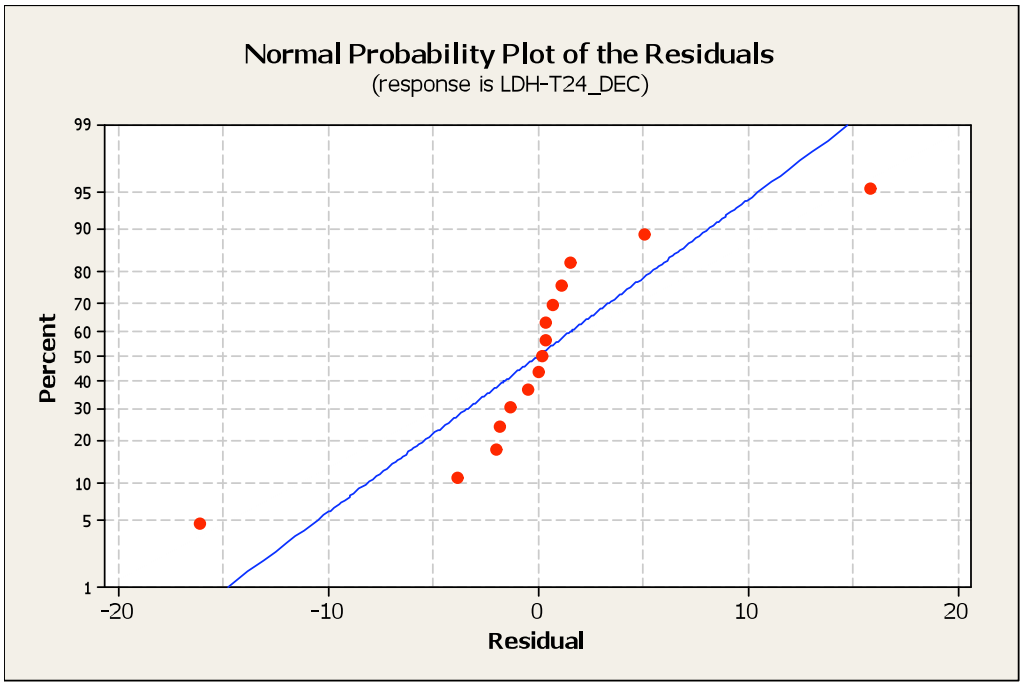

(a)

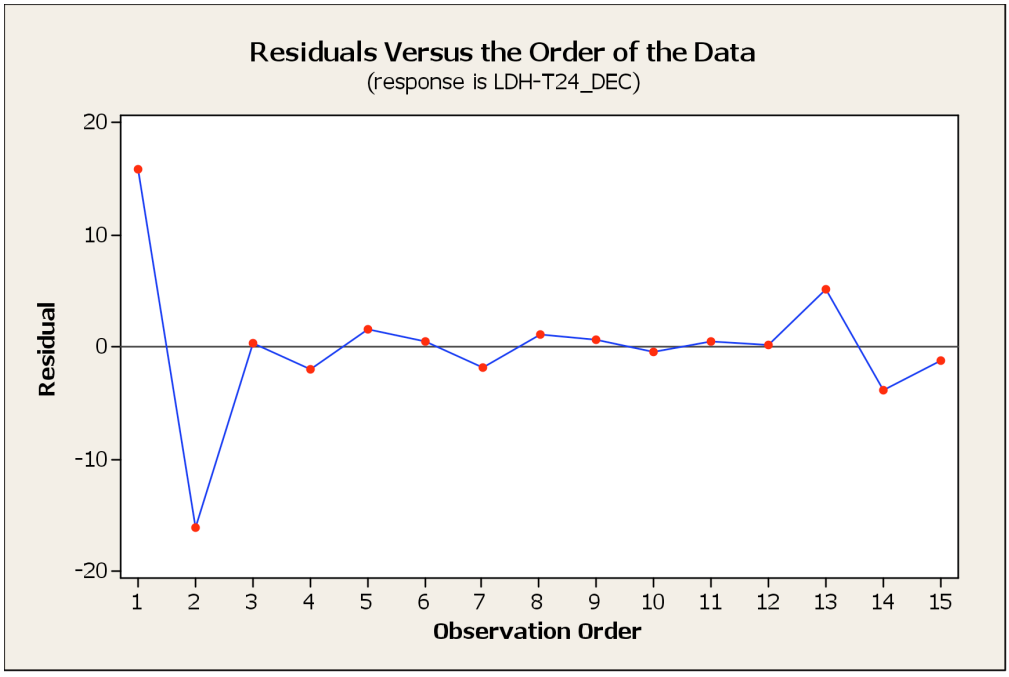

(b)

Figure 5.18 (a) Normality plot and (b) randomness plot for LDH data collection set

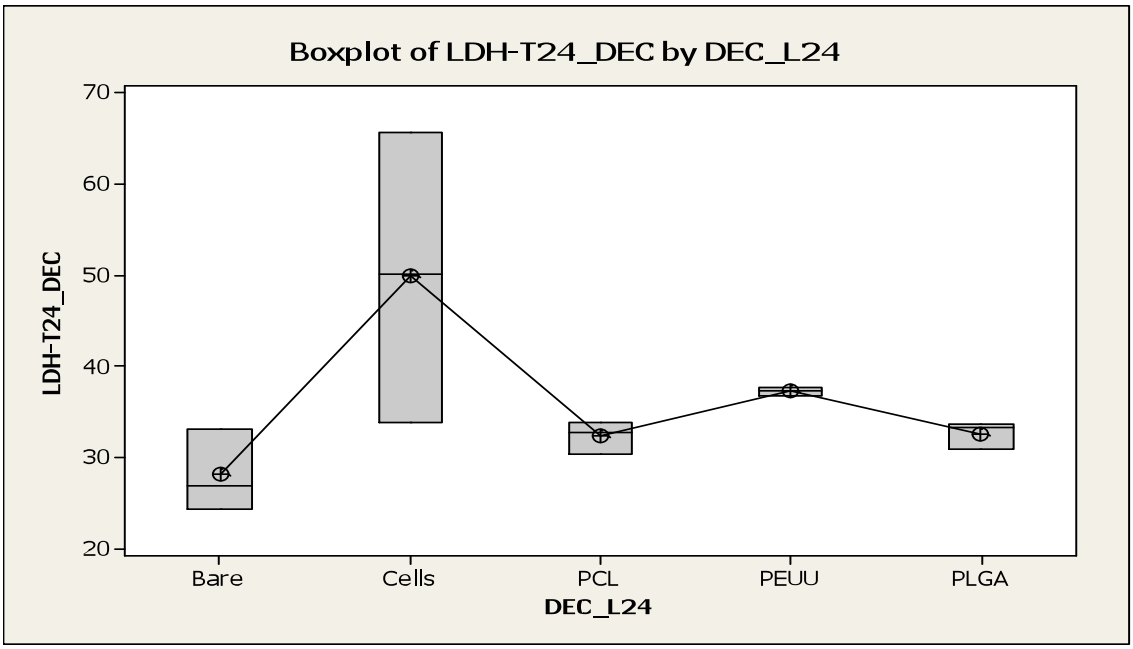

Figure 5.19 Box plot for LDH data depicting differences in data means

The samples from the LDH release experiment were preserved so that the magnesium ion content of the sample media collected could also be measured. The experimental data were assessed to ensure the assumptions of normality and randomness were satisfied. It was determined that the data were normally distributed and did not exhibit any obvious trends or patterns, thus the data was, in fact, random in nature. The normality and randomness data plot for magnesium content in the LDH samples are shown in figures 5.20a and b, respectively. As a result, the statistical relevance of the independent variables on magnesium ion content in the LDH samples was, again, suitable for the application of analysis of Variance (i.e. ANOVA) statistical testing.

A one-way ANOVA was also conducted on the magnesium content present within the samples cell wells to determine if there was a difference of means between at

least two of the experiment groups. The results of this analysis confirmed that there were highly significant differences given $p = 0.005$, between at least two of the groups at $p < 0.05$ (Appendix D). The differences between mean magnesium content for the LDH sample treatment types are depicted in figure 5.21. Here again, the null hypothesis was rejected and Tukey's post hoc analysis was conducted to determine specific differences.

The results showed that the difference in means between the low control (cell only) and the uncoated samples was significant. There was also a significant difference between the low control and the samples containing the PCL coating. Lastly, statistical differences were found between the samples containing the PEUU coating and both the uncoated and PCL coated samples. This is also consistent with the ICP results from the immersion test in which both the uncoated and PCL coated samples displayed similar corrosion behaviors. Also, from the immersion test, the PEUU coated samples released the lowest magnesium ion content, which is shown here to be comparable to the low control. Therefore, the statistical differences occur between the groups that were expected from the ICP results to have the highest and lowest magnesium content. In the following section we conduct a PCR analysis to determine if whether the LDH release is a result of the polymer coating type or increases in magnesium content.

Here again, these results confirm that although, PCL seems to offer the least protection from corrosion, the cells showed a positive reaction to the increased exposure to the magnesium. This again indicates that controlled magnesium exposure promotes good health in airway cells.

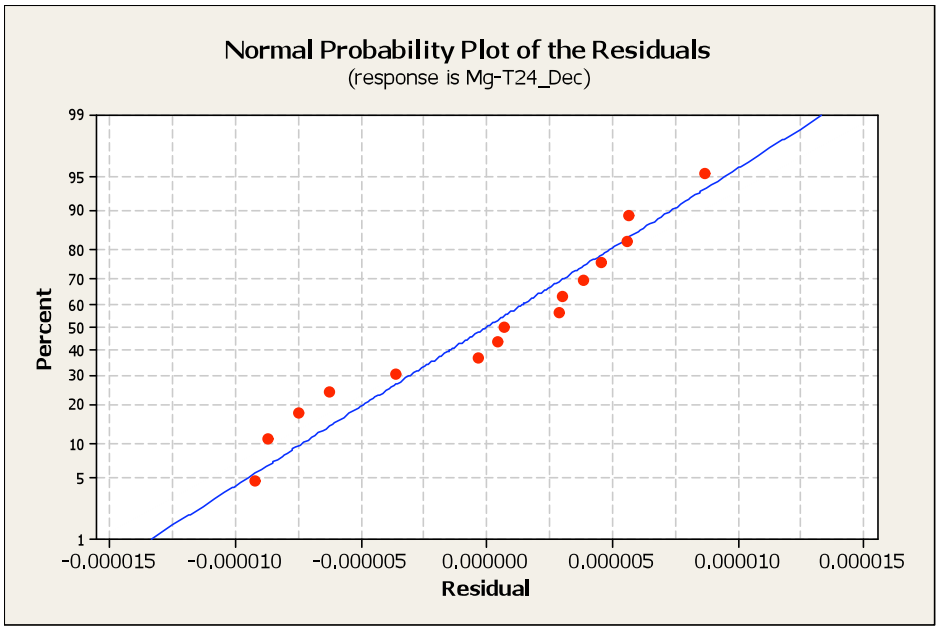

(a)

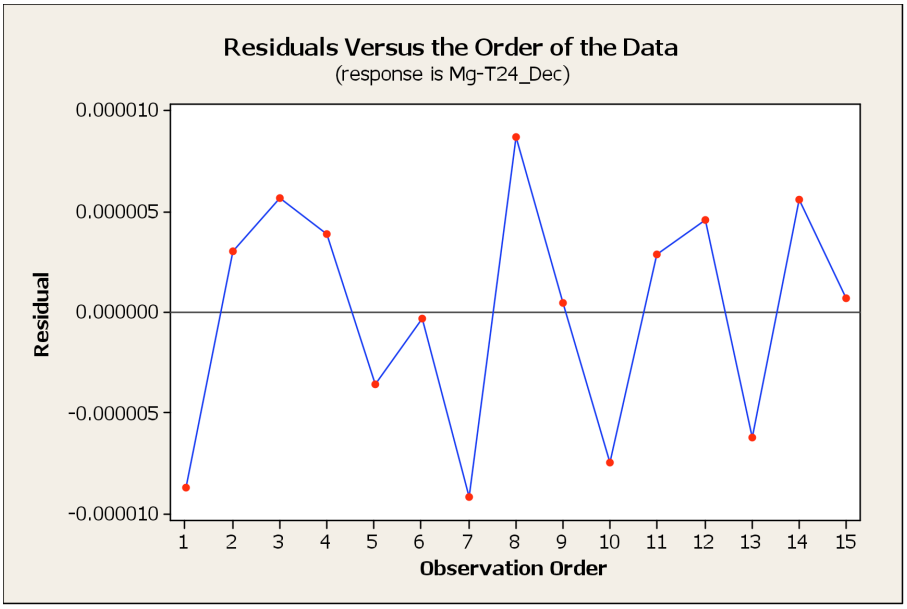

(b)

Figure 5.20 (a) Normality plot and (b) randomness plot for LDH data

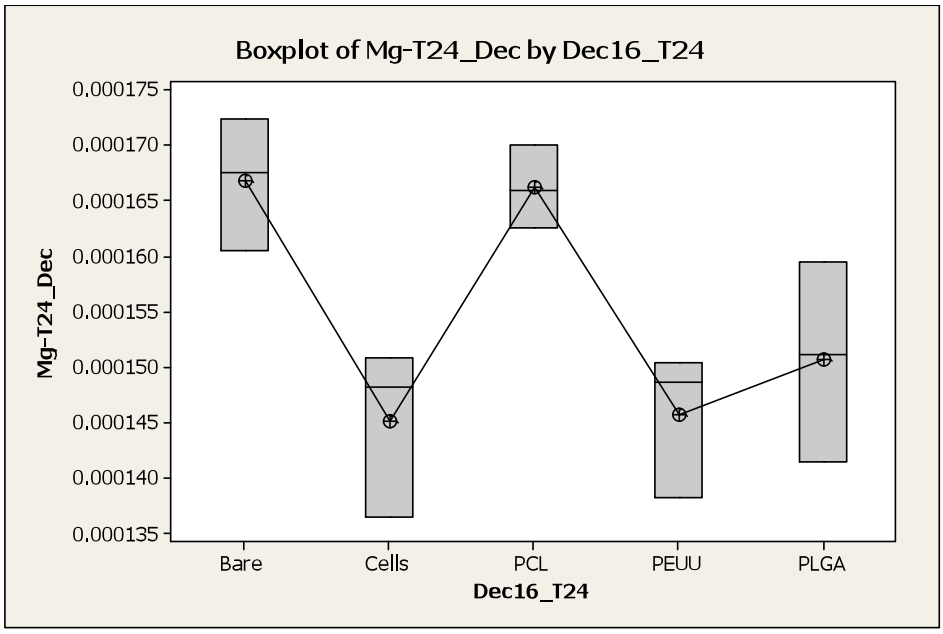

Figure 5.21 Box plot for LDH data depicting differences in data means

5.3.3 PCR Analysis

A polymerase chain reaction (PCR) analysis was performed to measure the Cox-2 gene expression in NHBE cells exposed to different sample conditions. The Cox-2 gene expression is indicative of the inflammatory response of the cells. This analysis was an end point analysis that allowed us to understand the health of the cells at the end of 29 hours. The corrosion of magnesium alloy samples resulted in release of magnesium ions within the media. The presence of magnesium ions within the media was measured using the ICP analysis. Thus, depending on their presence, it was hypothesized that higher magnesium ions resulted in higher Cox-2 gene expression based on the cell distress.

The PCR results for the different samples were labeled below as follows, 1-6 PCL, 7-12 PLGA, 13-18 PEUU, 19-21 Uncoated, 22-23 Cells only. The PCR for both Beta Actin and COX-2 were analyzed where Beta Actin was used as an internal control.

The average intensity of 6 bands was used to normalize the Cox-2 data sets. Base pair 150 was used to analyze intensity of Cox-2. The PCR image was inverted to measure darker intensities at base pair 150 for the different sample groups noted above. The darkness intensities were integrated to obtain volumetric intensities for further statistical analysis.

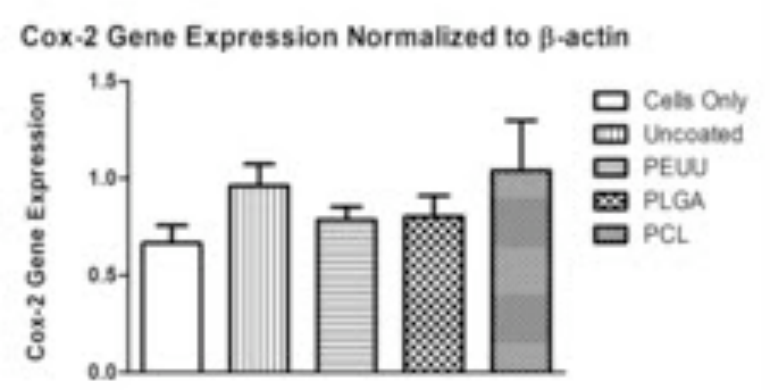

Figure 5.22 Normalized Cox-2 gene expression

The higher Cox-2 gene expression in both uncoated (bare) and PCL polymer coating, shown in Figure 5.22, is due to the corresponding higher presence of magnesium ions within the media. The PCL polymer coating resulted in the formation of pockets that entrap media leading to higher corrosion rates. The two polymers PLGA and PEUU offered higher protection to the underlying Mg alloy surface resulting in lower magnesium ion release and corresponding Cox-2 gene expression. The Cox-2 gene expression values for PEUU and PLGA are comparable to those of natural cells (low control). These results seemed to be consistent with the magnesium ion content within media for different sample types as explained previous sections. However, test for statistical differences was necessary.

The experimental data were assessed to ensure the assumptions of normality and randomness were satisfied. It was determined that the data were normally distributed and did not exhibit any obvious trends or patterns, thus the data was, in fact, random in nature. As a result, the statistical relevance of the independent variables on Cox-2 gene expression was suitable for the application of analysis of Variance (i.e. ANOVA) statistical testing.

A one-way ANOVA was conducted to test if significant differences existed among the different experiment types. Based on a p-value of 0.0266 from the results of the ANOVA it was concluded that significant differences exist for the Cox-2 gene expression. Thus, the null hypothesis was rejected. Further, a Tukey's post-hoc analysis was performed to identify significant differences between different sample types. As can be seen from Table 5.3, the uncoated (bare) sample and PCL polymer coating show statistically significant higher gene expression as compared the cells (low control). Also, PCL polymer exhibited statistically significant difference as compared to PEUU polymer.

Table 5.3 Tukey's post hoc analysis for Cox-2 gene expression

Tukey's Multiple Comparison Test	Mean Diff.	q	Significant? P < 0.05?	Summary	95% CI of diff
Cells Only vs PCL	-0.3737	6.344	Yes	**	-0.6185 to -0.1289
Cells Only vs PLGA	-0.1363	2.313	No	ns	-0.3810 to 0.1085
Cells Only vs PEUU	-0.1198	2.033	No	ns	-0.3645 to 0.1250
Cells Only vs Uncoated	-0.2957	5.019	Yes	*	-0.5404 to -0.05088
PCL vs PLGA	0.2374	4.03	No	ns	-0.007371 to 0.4822
PCL vs PEUU	0.2539	4.311	Yes	*	0.009142 to 0.4987
PCL vs Uncoated	0.07802	1.325	No	ns	-0.1668 to 0.3228
PLGA vs PEUU	0.01651	0.2803	No	ns	-0.2283 to 0.2613
PLGA vs Uncoated	-0.1594	2.706	No	ns	-0.4042 to 0.08539
PEUU vs Uncoated	-0.1759	2.986	No	ns	-0.4207 to 0.06888

From the results of the PCR analysis it was determined that the cell response exhibited through inflammation was due to the increase in magnesium ion content. It

was also determined that the differences between polymer materials when compared amongst each other were insignificant and showed no negative influences on cell health. Lastly, when the desire is to decrease the rate of corrosion for magnesium alloys, PCL was not the best candidate as its performance was similar to the uncoated samples. The PLGA and PEUU coatings offered better protective coatings.

CHAPTER 6

CONCLUSIONS

6.1 Overview

The objective of this research was to apply a novel surface modification technique namely Direct-Write Inkjet printing, to develop functional coatings for metallic biomaterials. Inkjet printing offers several advantages such as the capability to produce coatings on extremely complex structures, deposition onto the outer surfaces only, and flexibility to change coating design and materials. This technique also allows for the adjustment of coating thickness with the objective of obtaining desired release patterns.

6.2 Controlled Release Coatings

Controlled release coatings are fabricated to suit a variety of different applications. More specifically, the controlled release of various biological agents from biodegradable polymer coatings to treat a vast number of physiological ailments is of particular interest. The use of the Direct Write inkjet technique as a mechanism for developing controlled release coatings offers a variety of advantages for coating surfaces containing biological and pharmaceutical reagents [48]. For instance, this technique uses a data driven pressure source for deposition of material onto a given substrate, where other fabrication techniques use electricity, which may compromise the integrity of the biological substances [48]. Other techniques such as spin coating and dip coating are not able to accommodate the complex structures that are usually required by surgical implant devices. None of the deposition techniques discussed earlier offer the ability to deposit

target specific coatings, maintain the integrity of the deposition material, and eliminate cross-contamination of materials.

The need for a coating technique that encompasses all of the benefits mentioned above is necessary to develop controlled release coating where spatial requirements can be specified to develop coatings with specified porosity and degradation features. In this research, the intent was achieve a variety of drug release profiles that could be tailored to support the needs of a given drug delivery application. Here, the drug concentration and layers of coating material were varied to assess coating specifications resulting in a steady state release throughout its intended time of function. This result would be desirable for ailments requiring extended therapeutic sessions such as neointimal hyperplasia, using an anti proliferative such as Paclitaxel, following placement of a cardiovascular stent device [6]. Coatings having a more profound initial burst phase were also attempted. These coatings would be more suitable for applications such as antimicrobial and/or antifibrotic therapy were the majority of the reagent is required in the initial stages of treatment to treat infection at the implant site and promote healthy wound healing [83-84].

The coating process required that various concentrations of the synthesized biopolymer fluids were tested to determine their "jettability". In this research, the term jettability was defined as being able to maintain a steady jet for a time period of at least 2-3 hours. Thus, a steady jet was achieved for non-newtonian fluids. This process was known as the jetting optimization process. In a preliminary study jetting optimization was attempted for PEUU at 2% w/v, 1.5% w/v, 1% w/v, and 0.5% w/v. It was concluded

that the concentration for which a steady jet was obtained for PEUU was 0.5 % w/v. The specific jetting parameters for this material were provided in Chapter 4.

The non-contact, data-driven deposition process showed suitability for depositing drug-loaded polymer (Paclitaxel and PEUU) on to a titanium substrate simulating stent-coating applications. The coatings types were varied in polymer and drug concentration and thickness to determine how manipulating the three would affect the drug release profile. Preliminary studies revealed that drug release could be achieved for a period of 35 days, which was comparable to release periods of using other notable coating techniques found in literature. After 5 days, the samples with thicker coatings began to peel from the substrate and thus characterization release was not obtained after that time period. The thinner coatings with lower drug concentrations showed a steady release pattern.

Further studies were conducted in which the polymer concentration remained constant (0.5% w/v) and only the drug concentration and layer thickness were varied to determine their effect on the drug release profile as well as hemocompatibility and cell inhibition. The titanium substrates underwent standard cleaning procedures to improve polymer surface adhesion.

Drug release profiles were obtained for a 21-day period. A design of experiment (DOE) was used to determine the main and interaction affects of each factor on the total drug release as well as the percentage released during the burst release period. Higher percentages of drug release during the burst phases were observed for the samples with thinner coatings and vice versa. The overall drug concentrations observed at the end of

21 days where significantly lower for samples with lower drug loading. In terms of the coating thickness, an increased coating layer generally showed higher final concentrations then samples coated with fewer layers. The P-values obtained from the DOE were highly significant ($p < 0.01$). It was concluded that tunable drug release coatings could be fabricated to suit various therapeutic requirements.

The reagent chosen, Paclitaxel, has been proven to inhibit accelerated cell proliferation in cancerous environments, thus biological testing was conducted to relate the drug release profiles to cell inhibition. MTT assay was performed on rat smooth muscle cells after being cultured on the surfaces of taxol-loaded polymer coatings for 1, 4, and 7 days. Cells were also cultured on TCPS material, uncoated titanium, and 10 and 20 layers of PEUU with no drug as controls. A one-way ANOVA was performed to determine any significant differences within each of the experiment types and the controls. Significant differences were determined for each of the experiment types as compared to the controls.

Hemocompatibility test were also conducted to relate drug release to blood coagulation on the functionalized surfaces. Platelet deposition onto the sample surfaces was determined by LDH assay. The statistical significance between sample groups was determined using One-way Analysis of Variance (ANOVA) and post-hoc Newman-Keuls testing was performed to determine specific differences. Statistical significance between the samples containing only PEUU (control) and both sets of samples containing 5% and 10% taxol embedded in PEUU were observed. However, although differences were

observed when increasing drug concentration from 5% w/v to 10% w/v, the effect on blood platelet deposition was found to be insignificant.

6.3 Polymer Coatings for Controlling the Corrosion of Mg Alloys

Biofunctional coatings are necessary to suit a variety of different medical applications. The use of the Direct Write inkjet technique as a mechanism for enhancing the structural integrity of a given biomaterial via biofunctional coatings, namely magnesium and its alloys, is of growing interest. Uses for magnesium as a biomaterial offers several advantages and can spread across a number of applications. For instance, magnesium is essential to over 300 physiological functions within the body [85] and has also been identified as a potential biomaterial to facilitate bone growth and repair due to proven similarities of mechanical strength with the cortical bone [86].

Direct Write deposition can be used to fabricate coatings where spatial requirements can be specified to develop coatings with specified porosity and degradation features for inhibiting the corrosion of magnesium alloys. In this study, the intent was to investigate a variety of polymer coatings having various rates of degradation. Here, the polymer type and layers of coating material were varied to assess coating specifications for applications in corrosion protection and controlled release of magnesium alloys. Corrosion protection is essential to ensure that a polymer coating is applied, which can extend the life of the surgical device until its intended function is completed [86]. The controlled release of magnesium in the trachea can be beneficial in relaxing airway cells when exposed to an environment causing inflammation [87]. Magnesium deficiencies have also been linked to cardiovascular disease. Thus,

controlled release of magnesium via controlled release coatings can offer some benefit when applied to tracheal and cardiovascular stent devices [88].

The direct-write inkjet technique was used to develop polymer coatings that would aid in controlling corrosion of magnesium alloys for orthopedic and vascular applications. It was hypothesized that by manipulating droplet sizes and pitch distance as well as polymer type and thickness, desirable corrosion rates based on a given application could be obtained. The jetting optimization process was carried out to determine the highest printable concentration for both PCL and PLGA. It was determined that both polymers could be printed at 1% w/v concentration (provided in Chapter 4). The concentration for PEUU remained at 0.5% w/v.

In a preliminary study, the direct-write printing process was utilized to deposit precise layers of multilayer polymeric coatings on Mg alloy surface (Mg: 90%, Zn: 8.9%, Ca: 0.5%, rest impurities). PLGA and PCL polymers coatings displayed distinct corrosion characteristics based on their varying degradation properties. The uncoated (bare) Mg alloy sample showed incremental weight gain and loss due to formation and release of $Mg(OH)_2$ corrosion products, respectively. The coating types were classified based on polymer type (PCL and PLGA) and pitch distance (50 μm, 100 μm). Coatings with larger deposition pitch (100μm) had higher porosity in both polymer types. This resulted in media infiltration and corrosion of local regions on the substrate. The corrosion behavior of PCL-50 and PLGA-50 was analogous, though PCL-50 showed slower corrosion rate. The PCL-100 film retained corrosion products due to better adhesion properties with the Mg substrate. The results showed that by varying polymer

type and printing conditions one could adjust the corrosion rate of magnesium alloys for its intended uses. Manipulation of the step and pitch sizes allowed for added control of coating degradation based on one of the given applications provided above.

In a further study, the pitch distance remained constant (50 μm) to achieve more protective coatings with a third polymer type (PEUU). Immersion testing was conducted to determine the affect of polymer type and coating thickness on the presence of magnesium released in simulated body fluid (SBF). Uncoated samples were also tested as a control and sample aliquots were collected over an 8-day period. Magnesium ion content was measured using inductively coupled plasma (ICP) spectroscopy technique.

Statistical analysis was conducted to determine the main and interaction effects amongst the treated samples. Though there were visible trends from the data, the differences of means amongst the coating types were not significant. A analysis was conducted to compare each experiment type against the control (uncoated). The results from this analysis showed that the difference in the data mean for the uncoated samples was statistically different from the mean samples coated with 20 passes of PEUU. This suggests that PEUU with increased coated materials would be ideal for applications such as bone growth and repair where slower corrosion rates is required to match the rate of bone growth.

The controlled release of magnesium in the trachea can be beneficial in relaxing airway cells when exposed to an environment causing inflammation [87]. Cell viability and surface interaction between NHBE (airway) cells and the magnesium alloy with various coating types were also investigated in culture. LDH activity was assessed to

determine the effect of magnesium exposure from different samples on cytotoxicity. Although the results showed varying levels of LDH release for the coated samples, cytotoxicity levels were within permissible physiological limits (i.e. < 30%) after 24 hours of exposure. ANOVA results concluded that there was a significant difference between the mean LDH release from cells containing uncoated magnesium samples and the cells having no magnesium exposure. The analysis also revealed that, compared to the cells with no magnesium exposure, the cells exposed to magnesium showed increased health during the testing period. This confirms that airway cells would benefit from the controlled release of magnesium to promote good health within the trachea.

ICP analysis was conducted to evaluate the magnesium content present within samples. The low control (cell only) had statistically significant lower Mg ion presence as compared to the uncoated samples. There was also a significant difference between the low control and the samples containing the PCL coating. Statistical differences were found between the samples containing the PEUU coating and both the PCL and uncoated samples.

From the results, it was determined that the PCL-coated samples produced equivalent magnesium content in SBF when compared to uncoated. Thus, the PCL polymer is not an ideal polymer material if the intent is to retard the corrosion process. The magnesium content observed in the sample media from the PEUU-coated magnesium was similar to the amount observed from the low control (cells only). PLGA offered slightly lower protection than the PEUU. Because the PCL coating was similar to that of the uncoated sample and PEUU was similar to the low control, significant

differences were found between PEUU and PCL. These findings were also consistent with the results from the immersion and LDH tests thus, validating the relationship between magnesium exposure and cell health.

A polymerase chain reaction (PCR) analysis was performed to measure the Cox-2 gene expression in NHBE cells exposed to different sample conditions. The Cox-2 gene expression is indicative of the inflammatory response of the cells exposed to the various polymer-coating types. Higher Cox-2 gene expression was found in both the uncoated and PCL polymer coated which was consistent with the findings from the previous experiments. This suggests that after 29 hours of continuous exposure to high levels of magnesium, percentage of LDH began to approach the level of acceptability (i.e. 30%). The results also revealed that the PEUU and PLGA polymer coating material seemed to be the most biocompatible, as the Cox-2 gene expression for those samples were most similar to that of the cells alone.

In conclusion, there is sufficient evidence to state that the inflammatory response of the cells is proportional to the increasing magnesium exposure. If the intent is to control the corrosion rate of magnesium alloys for a given application, PCL can be excluded as a potential candidate for coating as it corrodes at similar rates as the magnesium alloy with no coating. PEUU and PLGA polymers may be considered for further testing as the showed good biocompatibility and corrosion control. Therefore, this research establishes a foundation for determining the best candidate polymer material for controlling the corrosion of magnesium alloys as they apply to numerous applications for controlled degradation of biomaterials for surgical implant devices.

6.4 Future Work

6.4.1 Controlled Release Coating

- New polymeric materials should be incorporated as possible candidate to achieve desired drug release profiles.
- Biphasic and bio-triphasic drug delivery coatings should be developed to achieve a desired therapeutic effect.

6.4.2 Polymer Coatings for Corrosion Retardation

- Further biological testing should be conducted regarding cell response to polymer-coated magnesium.
- Chemical properties of a given polymer type should be adjusted to inhibit the corrosion process, namely PLGA.
- Biphasic and bio-triphasic drug delivery coatings should be incorporated to enhance the surface of the magnesium substrate.

REFERENCES

1. Anderson, J.M. (1982) Chapter 7: In Vivo Studies on Drug-Polymer Sustained-Release Systems. *Biological Activities of Polymers, ACS Symposium Series Volume 186. American Chemical Society*.

2. Pan C., Tang J., Weng Y., Wang J., and Huang N. (2009) Preparation and In Vitro Release Profiles of Drug-Eluting Controlled Biodegradable Polymer Coating Stents. *Colloids and Surfaces B: Biointerface,s* 73, 199-206.

3. Okuda T., Tominaga K., and Kidoaki S.(2010) Time-Programmed Dual Release Formulation by Multilayered Drug-Loaded Nanofiber Meshes. *Journal of Controlled Release,* 143, 258-264.

4. Sanders S.W. (1996) Transition from Temporal to Biological Control in the Clinical Development of Controlled Drug Delivery Systems. *Journal of Controlled Release,* 39 389-397.

5. Lincoff, A.M., Tool, E.J., Ellis, S.G. (1994) Local Drug Delivery for the Prevention of Restenosis: fact, Fantasy, and Future. *Circulation*, 90, 2070-2084.

6. Axel, D.I., Kunert, W., Gogglemann, C. (1997) Paclitaxel Inhibits arterial Smooth Muscle Cell Proliferation and Migration In Vitro and In Vivo Using Local Drug Delivery. *Circulation,* 96, 636-645.

7. Nakayama, Y., Nishi, S., and Ueda, H. (2003) Fabrication of Drug-Eluting Covered Stents With Micropores and Differential Coating of Heparin and FK506. *Cardiovascular Radiation Medicine,* 4, 77-82.

8. Raval, A. (2007) Novel Biodegradable Polymeric matrix Coated Cardiovascular Stent for Controlled Drug Delivery. *Trends in Biomaterials and Artificial Organs*, 20, 101-110.

9. Pan Ch. J. (2006) Preparation, Characterization and anticoagulation of Curcumin-Eluting Controlled Biodegradable Coating Stents. *Journal of Controlled Release,* 116, 42-49.

10. Niinomi, M. (2002) Recent Metallic Materials for Biomedical Applications. *Metallurgical and Materials Transactions A*, 33A, 477-486.

11. Niinomi, M. (2007) Fatigue Characteristics of Metallic Biomaterials. *International Journal of Fatigue*, 29, 992-1000.

12. Purnama, A., Hermawan, H. (2009) Assessing the Biocompatability of Degradable Metallic Materials: State-of-the-art and Focus on the Potential of Genetic Regulation. *Acta Biomaterialia*, 6, 1800-1807.

13. Okazaki, Y., and Gotoh, E. (2005) Comparison of Metal Release from Various Metallic Biomaterials In Vitro. *Biomaterials*, 26, 11-21.

14. Koster R. (2000) Nickel ad Molybdenum Contact Allergies in Patients with Coronary In-Stent Restenosis. *The Lancet,* 356, 1895-1897.

15. Lim, I.A. (2004) Biocompatability of Stent Materials. *Massachusetts Institute of Technology Undergraduate Research Journa*l, 11, 33-37.

16. Hench, L., Best, S. (1996) Ceramics, Glasses, and Glass-Ceramics. *Biomaterials Science*, 2, 153-170.

17. Elias, C.N., Lima, J.H.C., Valiev, R., and Meyers, M.A. (2008) Biomedical Applications of Titanium and its Alloys. *Biological Materials Science*, 60 (2008) 46-49.

18. Monnier, P. Mudry, A. Stanzel, F., Haeussinger, K., Heitz, M., Probst, R., and Bolliger, C.T. (1996) The Use of the Covered Wallstent for the Palliative Treatment of Inoperable Treacheobronchial Cancers. *Chest Journal* 110, 1161-1168.

19. Grillo, H. C. (2004) *Surgery of the Trachea and Bronchi*. Hamilton, Ontario, BC Decker Inc.

20. Yeung, S. J., Escalante, C. P., and Gagel, R. F. *Medical Care of the Cancer Patient,* Shelton, Connecticut, People's Medical Publishing House.

21. Levine, G. N., Chodos, A. P., Lascalzo, J. (1995) Restenosis Following Coronary Angioplasty: Clinical Representations and Therapeutic Options. *Clinical Cardiology,*18, 693-703.

22. Rude RK. (1998) Magnesium deficiency: A cause of heterogeneous disease in humans. *Journal of Bone and Mineral Research*, 13, 749-58.

23. Song G, Song S. (2007) A possible biodegradable magnesium implant material. *Advanced Engineering Materials*, 9(4), 298–302.

24. Peacock JM, Folsom AR, Arnett DK, Eckfeldt JH, Szklo M (1999) Relationship of serum and dietary magnesium to incident hypertension: the Atherosclerosis Risk in Communities (ARIC) Study. *Annals of Epidemiology* 9, 159 – 165.

25. Ma, X., Wu, T., Robich, M., Wang, X., Wu, H., Buchholz, B., McCarthy, S. (2010) Drug-eluting Stents. *International Journal of Clinical and Experimental Medicine,* 3, 192-201.

26. Bhargave, B., Reddy, N.K., Karthikeyan, G., Raju, R., Mishra, M., Singh, S., Waksman, R., Virmani, R., and Somaraju, B. (2006) A Novel Paclitaxel-Eluting Carbon-Carbon Nanoparticle Coated, Nonpolymeric Cobalt-Chronium: Evaluation in a Porcine Model. *Catheterization and Cardiovascular Interventions,* 67, 698-702.

27. Lansky, A.J. (2004) Non-Polymer-Based Paclitaxel-Coated Coronary Stents for the Treatment of Patients With De Novo Coronary Lesions: Angiographic Follow-Up of the DELIVER Clinical Trial. *Circulation,* 109, 1948-1954.

28. Moreno, R. (2005) Drug-Euting Stent Thrombosis. *Journal of the American College of Cardiology,* 45, 954-959.

29. Whelan, D. M., Van Der Giessen, W. J., Krabbendam, S. C., Van Vliet, E. A., Verdouw, P. D., Serruys, P. W., Van Beusekom, H. M. M. (2000) Biocompatability of Phosphorylcholine Coated Stents in Normal Porcine Cornary Arteries. *Heart*, 83, 338-345.

30. Zilberman, M,. Eberhart, R. C. (2006) Drug-Eluting Bioresorbable Stents for Various Applications. *The Annual Review of Biomedical Engineering*, 8, 153-180.

31. Wu, P., Grainger, D. W. (2006) Drug/Device Combinations for local drug therapies and infection prophylasix. *Biomaterials*, 27, 2450-2467.

32. Stone GW, Moses JW, Ellis SG, Schofer, J., Dawkins, K., Morice, M., Colombo, A., Schampaert, E., Grube, E., Kirtane, A., Cultip, D., Fahy, M., Pocock, S., Mehran, R., and Leon, M. (2007) Safety and efficacy of sirolimus- and paclitaxel-eluting coronary stents. *The New England Journal of Medicine,* 356, 998-1008.

33. Chew, S. Y., Wen, J., Yim, E. F. Y., and Leong, K. W. (2005) Sustained Release of Protiens from Electrospun Biodegradable Fibers. *Biomacromolecules*, 6, 2017-2024.

34. Oh, S. H., Ward, C. L., Atala, A., Yoo, J. J., Harrison, B. S. (2008) Oxygen Generating Scaffolds for Enhancing Engineered Tissue Survival. *Biomaterials*, 30, 757-762.

35. Ektessabi, A.M. (1997) Surface Modification of Biomedical Implants Using Ion-Beam-Assisted Sputter Deposition. *Nuclear Instruments and Methods in Physics Research B*, 127/128, 1008-1014.

36. Xie, J., Tan, J., Wand, C. (2007) Biodegradable Films Developed by Electrospray Deposition for Sustained Drug Delivery. *American Pharmacists Association Journal Pharmaceutical Science*, 97, 3109-3122.

37. Jaworek, A. (2007) Electrospray Droplet Sources for Thin Film Deposition. *Journal of Material Science*, 42, 266-297.

38. Rietveld, I.B., Kobayashi, K. (2009) Process Parameters for Fast Production of Ultra-thin Polymer Film with Electrospray Deposition Under Ambient Conditions. *Journal of Colloid and Interface Science*, 339, 481-488.

39. Lu, P., and Ding, B. (2008) Applications of Electrospun Fibers. *Recent Patents on Nanotechnology*, 2, 169-182.

40. Fang H. (2008) Dip Coating assisted Polylactic Acid Deposition on Steel Surface: Film Thickness Affected by Drag Force and Gravity. *Materials Letters,* 62, 3739-3741.

41. Norman, K., Siahkali, A., and Larsen, B. (2005) 6 Studies of Spin-Coated Polymer Films. *Annual Reports Section "C" (Physical Chemistry)*, 101, 174-201.

42. Decher, G., Ecklem M., Scmitt, J., Struth, B. (1998) Layer-byLayer Assembled Multicomposite Films. *Current Opinion in Colloid & Interface Science*, 3, 32-39.

43. Crespilho, F. (2006) Electrochemistry of Layer-by-Layer Films: A Review. *International Journal of Electrochemical Science*, 1 (2006) 194-214.

44. Kotov, N.A. (2006) Biomedical Applications of Layer-by-Layer Assembly: From Biomimetics to Tissue Engineering. *Advanced Materials*, 18, 3203-3224.

45. Wang, X. (2009) Piezoelectric Inkjet Technology – From Graphic Printing to Material Deposition. *Nanotech Conference & Expo*, Houston, Texas.

46. Calvert, P. (2001) Inkjet Printing for Materials and Devices. *Chemical Materials,* 13, 3299-3305.

47. Schubert, U. (2004) Inkjet Printing of Polymer: State of the Art and Future Developments. *Advanced Materials*, 16, 203-213.

48. *MicroFab Technology: Biomedical Applications*. Retrieved August 14, 2011 from http ://www.microfab.com/technology/biomedical/Stents.html.

49. Hendry, J.A., Pilliar, R.M. (2001) The Fretting Corrosion Resistance of PVD Surface-Modified Orthopedic Implant alloys. *The Journal of Biomedical Material*

Research, 58, 156–166.

50. Goa, J. C., Qiao, L. Y., Xin, R. L. (2010) Corrosion of Bone Response of Magnesium Implants After Surface Modification by Heat-Self-Assembled Monolayer. *Frontiers of Materials Science*, 4(2), 120–125.

51. Tsai, W. B., Wei, T. C., Lin, M. C., Wang, J. Y., and Chen, C. H. (2005) The Effect of Radio-Frequency Glow Discharge Treatment of Polystyrene on the Behavior of Porcine Chondrocytes In Vitro. *Journal of Biomaterials Science and Polymer Education*, 16(6), 699–714.

52. Ferretti, S., Paynter, S., Russell, D., Sapsford, K. (2000) Self-Assembled Monolayers: A Versatile Tool for the Formulation of Bio-Surfaces. *Trends in Analytical Chemistry*, 19 (9), 530-540.

53. Ye, S. H., Johnson, C., Woolley, J., Snyder, T., Gamble, L., Wagner, W. (2008) Covalent Surface Modification of a Titanium Alloy with a Phosphorycholine-Containing Copolymer for Reduced Thrombogenicity in Cardiovascular Devices. *Journal of Biomedical Materials Research Part A*, 91(1), 18-28.

54. Staiger, M. P., Peitak, A. M., Huadmai, J., Dias, G. (2006) Magnesium and its Alloys as Orthopedic Biomaterials: A Review. *Biomaterials*, 27, 1728-1734.

55. Gu, X., Zheng, Y., Cheng, Y., Zhong, S., Xi, T. (2009) In Vitro Corrosion and Biocompatibility of Binary Magnesium Alloys. *Biomaterials*, 30, 484-498.

56. Hanzi, A., Gerber, I., Schinhammer, M., Loffler, J. F., Uggowitzer, P. J. (2010) On the In Vitro and In Vivo Degradation Performance and Biological Response of New Biodegradable Mg-Y-Zn Alloys. *Acta Biomaterialia*, 6, 1824-1833.

57. Li, Z., Gu, X., Lou, S., Zheng, Y. (2008) The Development of Binary Mg-Ca Alloys for use as Biodegradable Materials Within Bone. *Biomaterials*, 29, 1329-1344

58. Yang, J., Cui, F., and Lee, S. (2011) Surface Modifications of Magnesium Alloys for Biomedical Applications. *Annals of Biomedical Engineering*, 39 (7), 1857-1871.

59. Torchilin, V. (2001) Structure and Design of Polymeric Surfactant-Based Drug Delivery Systems. *Journal of Controlled Release*, 73 (2-3), 137-172.

60. Guzman, L., Labhasetwar, V., Song, C., Jang, Y., Lincoff, M., Levy, R., Topol, E. (1996) Local Intraluminal Infusion of Biodegradable Polymeric Nanoparticles: A Novel Approach for Prolonged Drug Delivery After Balloon Angioplasty. *Circulation*, 94, 1441-1448.

61. Humphry, W., Erickson, L., Simmons, C., Northrup, J., Wishka, D., Morris, J., Labhasetwar, V., Song, C., Levy, R., Shebuski, R. (1997) The Effect of Intramural Delivery of Polymeric Nanoparticles Loaded with the Antiproliferative 2-aminochromone U-86983 on Neointimal Hyperplasia Development in Balloon-injured Porcine Coronary Arteries. *Advanced Drug Delivery Reviews*, 24 (1), 87-108.

62. Labhasetwar, V., Song, C., Levy, R. (1997) Nanoparticle Drug Delivery System for Restinosis. *Advanced Drug Delivery Reviews*, 24 (1), 63-85.

63. Wildemann, B., Bamdad, P., Holmer, Ch., Haas, N. P., Raschke, M., Schmidmaier, G. (2004) Local Delivery of Growth Factors from Coated Titanium Plates Increases Osteotomy Healing in Rats. *Bone*, 34, 862-868.

64. Okuda, T., Tominaga, K., Kidoaki, S. (2010) Time-Programmed Dual Release Formulation by Multilayered Drug-Loaded Nanofiber Meshes. *Journal of Controlled Release*, 143, 258-264.

65. Li, Y., Shawgo, R., Tyler, B., Henderson, P., Vogel, J., Rosenberg, A., Storm, P., Langer, R., Brem, H., Cima, M. (2004) In Vivo Release from a Drug Delivery MEMS Device. *Journal of Controlled Release*, 100, 211-219.

66. Yu, R., Chen, H., Chen, T., Zhou, X. (2008) Modeling and Simulation of drug release from Multi-layered Biodegradable Polymer Microstructure in Three Dimensions. *Simulation Modeling Practice and Theory*, 16 (1), 15-25.

67. Nakayama, Y., Nishi, S., Ueda-Ishibashi, H., Matsuda, T. (2003) Fabrication of Micropored Elastomeric Film-Covered Stents and Acute-Phase Performances. *Journal of Biomedical Materials Research*, 64A (1), 52-61.

68. Raval, A., Chubey, A., Engineer, C., Kotadia, H., Kothwala, D. (2007) Novel Biodegradable Polymeric Matrix Coated Cardiovascular Stent for Controlled Drug Delivery. *Trends in Biomaterials and Artificial Organs*, 20 (2), 101-110.

69. Wessly, R., Hausleiter, J., Michaelis, C., Jaschke, B., Vogeser, M., Milz, S., Behisch, B., Schratzenstaller, T., Gluszko, M., Stover, M., Wintermantel, E., Kastrati, A., Schomig, A. (2005) Inhibition of Neointima Formation by a Novel Drug-Eluting Stent System That Allows for Dose-Adjustable, Multiple, and On-Site Stent Coating. *Journal of the American Heart Association*, 25, 748-753.

70. Steigerwald, K., Merl, S., Kastrati, A., Wieczoreck, A., Vorpahl, M., Mannhold, R., Vogeser, M., Hausleiter, J., Schomig, A., Wessley, R. (2009) The Pre-Clinical Assessment of Rapamycin-Eluting, Durable Polymer-Free Stent Coating Concepts. *Biomaterials*, 30 (4), 632-637.

71. De Gans, B., Duineveld, P., Schubert, U. (2004) Inkjet Printing of Polymers: State of the Art and Future Developments. *Advanced Materials*, 16 (3) 203-213.

72. Cooley, P., Wallace, D., Antohe, B., MicroFab Technologies Inc, (2001) Application of Ink-Jet Printing Technology to BioMEMS and Microfluidic Systems. *Proceedings, SPIE Conference on Microfluidics and BioMEMS.*

73. Antohe, B., Wallace, D. (2008) Ink-Jet as a Manufacturing Method for Drug Delivery Applications. *Proceedings of the 2008 International Manufacturing Science and Engineering Conference*, October 7-10, 2008, Evanston, Illinois, USA.

74. Khan, M., Fon, D., Li, X., Tian, J., Forsythe, J., Garnier, G., Shen, W. (2010) Biosurface Engineering Through Ink-Jet Printing. *Colloids and Surfaces B: Biointerfaces*, 75 (2), 441-447.

75. Suh, H. (1998) Recent Advances in Biomaterials. *Yonsei Medical Journal*, 39 (2), 87-96.

76. Makadia, H., Siegel, S. (2011) Poly Lactic-co-Glycolic Acid (PLGA) as Biodegradable Controlled Drug Delivery Carrier. *Polymers*, 3, 1377-1397.

77. Sinha, V. R., Bansal, K., Kaushik, R., Trehan, A. (2004) Poly-e-Caprolactone Microspheres and Nanospheres: An Overview. *International Journal of Pharmaceutics*, 278, 1-23.

78. Martina, M., Hutmacher, D. (2007) Biodegradable Polymers Applied in Tissue Engineering Research: A Review. *Polymer International*, 56 (2), 145-157.

79. Ma, X., Wu, T., Robich, M., Wang, X., Wu, H., Buchholz, B., McCarthy, S. (2010) Drug-Eluting Stents. *International Journal of Clinical and Experimental Medicine*, 3 (3), 192-201.

80. Singla, A., Garg, A., Aggarwal, D. (2002) Paclitaxel and its Formulations. *International Journal of Pharmaceutics*, 235, 179-192.

81. *MicroFab. JetLab User's Manual*. (2003) Retrieved July 5, 2006 from www.microfab.com.

82. Calvert, P. (2001) Inkjet Printing for Materials and Devices. *Chemistry of Materials*, 13, 3299-3305.

83. Kraft CN, Hansis M, Arens S (1996) Controlled release of antibiotics from coated orthopedic implants. *Journal of Biomedical Materials Research,* 30, 281–286.

84. Jarvinen TA, Ruoslahti E (2010). "Target-seeking antifibrotic compound enhances wound healing and suppressed scar formation in mice". *Proceedings of the National Academy of Sciences of the United States of America., 1-6*

85. Jahnen-Dechent W, Ketteler M. (2012) Magnesium basics. *Clinical Kidney Journal*, 5, 3-14.

86. Xu LP, Yu GN, Zhang E, Pan F, Yang K. (2007) In vivo corrosion behavior of Mg–Mn Zn alloy for bone implant: application. *Journal of Biomedical Materials Research A,* 83A, 703–711.

87. K.I Gourgoulianis, G Chatziparasidis, A Chatziefthimiou, P.A Molyvdas (2001) Magnesium as a relaxing factor of airway smooth muscles. *Journal of Aerosol Medicine*, 14, 301–307.

88. Vitale J (1992) Magnesium deficiency and cardiovascular disease. *Lancet*, 340, 1224.

APPENDIX A

CONTROLLED RELEASE COATINGS

Full Factorial Design for Burst Release

Factors: 2 Base Design: 2, 4
Runs: 8 Replicates: 2
Blocks: 1 Center pts (total): 0

All terms are free from aliasing.

Design Table (randomized)

Run	A	B
1	-	+
2	+	-
3	+	+
4	+	-
5	-	+
6	-	-
7	-	-
8	+	+

Factorial Fit: Burst Release versus %Taxol Con., No. of passes

Estimated Effects and Coefficients for Burst Release (coded units)

Term	Effect	Coef	SE Coef	T	P
Constant		0.60569	0.005898	102.69	0.000
%Taxol Con.	0.42379	0.21190	0.005898	35.93	0.000
No. of passes	0.13340	0.06670	0.005898	11.31	0.000
%Taxol Con.*No. of passes	0.19379	0.09690	0.005898	16.43	0.000

S = 0.0166827 R-Sq = 99.76% R-Sq(adj) = 99.59%

Analysis of Variance for Burst Release (coded units)

Source	DF	Seq SS	Adj SS	Adj MS	F	P
Main Effects	2	0.394790	0.394790	0.197395	709.26	0.000
2-Way Interactions	1	0.075111	0.075111	0.075111	269.88	0.000
Residual Error	4	0.001113	0.001113	0.000278		
Pure Error	4	0.001113	0.001113	0.000278		
Total	7	0.471014				

Estimated Coefficients for Burst Release using data in uncoded units

Term	Coef

Constant 0.641970
%Taxol Con. -0.0315170
No. of passes -0.0447980
%Taxol Con.*No. of passes 0.00775170

Least Squares Means for Burst Release

	Mean	SE Mean
%Taxol Con.		
5	0.3938	0.008341
10	0.8176	0.008341
No. of passes		
10	0.5390	0.008341
20	0.6724	0.008341
%Taxol Con.*No. of passes		
5 10	0.4240	0.011796
10 10	0.6540	0.011796
5 20	0.3636	0.011796
10 20	0.9812	0.011796

Alias Structure
I
%Taxol Con.
No. of passes
%Taxol Con.*No. of passes

Total Release DOE

Factorial Fit: Total Release versus %Taxol Con., No. of passes

Estimated Effects and Coefficients for Total Release (coded units)

Term	Effect	Coef	SE Coef	T	P
Constant		59.14	0.3650	162.04	0.000
%Taxol Con.	49.72	24.86	0.3650	68.11	0.000
No. of passes	33.81	16.91	0.3650	46.32	0.000
%Taxol Con.*No. of passes	20.01	10.00	0.3650	27.41	0.000

S = 1.03233 R-Sq = 99.95% R-Sq(adj) = 99.91%

Analysis of Variance for Total Release (coded units)

Source	DF	Seq SS	Adj SS	Adj MS	F	P
Main Effects	2	7230.07	7230.07	3615.04	3392.17	0.000
2-Way Interactions	1	800.40	800.40	800.40	751.06	0.000
Residual Error	4	4.26	4.26	1.07		
Pure Error	4	4.26	4.26	1.07		
Total	7	8034.73				

Estimated Coefficients for Total Release using data in uncoded units

Term	Coef

Constant	23.8700
%Taxol Con.	-2.06000
No. of passes	-2.62000
%Taxol Con.*No. of passes	0.800200

Least Squares Means for Total Release

	Mean	SE Mean
%Taxol Con.		
5	34.29	0.5162
10	84.00	0.5162
No. of passes		
10	42.24	0.5162
20	76.05	0.5162
%Taxol Con.*No. of passes		
5 10	27.38	0.7300
10 10	57.09	0.7300
5 20	41.19	0.7300
10 20	110.91	0.7300

Alias Structure
I
%Taxol Con.
No. of passes
%Taxol Con.*No. of passes

APPENDIX B

POLYMER COATINGS FOR COROSION RETARDATION: A PILOT STUDY

Overview

Appendix B details the preliminary experiment procedure for cell culture and surface-cell interactions experiments. The experimental results and statistical analysis from this preliminary test are also presented here.

Cell Culture Procedure

Normal Human Bronchial Epithelial (NHBE) cells were cultured in complete media, which consisted of a 50:50 mixture of BEBM/DMEM supplemented with antibiotics and growth factors. The cells were rapidly thawed from liquid nitrogen in a 37^{o}C water bath and seeded in 6-well culture dishes fitted with rat tail collagen-coated polycarbonate membrane Transwell® inserts (0.4 μm pore). Complete media (500 mL) was prepared by combining 250 mL of BEBM and 250 mL of DMEM into a flask with SingleQuot® components. The cells were fed apically and basolaterally every other day until they reached 100% confluency (at approximately 7 days). At that point, an air liquid interphase (ALI) was established by removing medium from the apical chamber and cells were fed basolaterally everyday for 14 days to allow full differentiation of the airway epithelial phenotype. . The cells were cultured at 37°Celcius in humidified air and 5% CO_2.

Cell – Surface Interface Testing Procedure

The 10X10 mm Mg samples (n=3 per coating) were coated with 20 layers of polymer and sterilized under a laminar flow hood with a UV sterilization bulb for 15

minutes on each side. Due to apparent differences in cells across the wells, the wells, which looked the healthiest, were chosen for the experiment. Each of the samples were assigned a well number were they were placed face down such that the coated magnesium surface was in direct contact with the epithelial cell layer. The wells were labeled as the low control, thus they were cells, which were untreated. Initial media samples were collected from each well at time zero and stored at -20oC until need for lactate dehydrogenase (LDH) and or elemental analysis via inductively coupled plasma mass spectrometry (ICP-MS). Fresh medium was placed in the lower chamber of each well and the plates were placed in incubation at 37°C and 5% CO_2.

Balolateral medium samples were collected again at 1 hour, 4, hours, 6 hours, 24 hours, and 48 hours. During the sample collection period, 1.5 mL of the sample media was collected from each of the wells and placed into a small tube. The tubes were labeled and frozen at -20°C. Any remaining media was aspirated from the cell well and two mL of fresh media was reapplied to the lower chamber. During this period, selected wells were imaged by phase contrast microscopy using an Evos xl inverted microscope (AMG). After the final sample collection, the wells containing the untreated cells were lysed such that all LDH activity would be released. These samples were then labeled as the high control and used for LDH analysis.

LDH Assay

Following exposure to coated Mg samples, reactions were terminated by removing materials from the apical surface, collection of basolateral culture medium and plates were wrapped in foil and stored at -80^{o} C until needed for gene expression analysis.

The Roche cytotoxicity detection kit was used to determine LDH release by the cells at the indicated time points. The low control consisted of the untreated cells (n=3) and the high control consisted of the lysed cells, which provided information about the maximum amount of released LDH activity in the cells. The assay was performed according to manufacture's recommendation and samples (in triplicate) were transferred into a 96-well plate according to the template found below.

Table A.1 96-well template for preliminary LDH data collection

	96-WELL PLATE								
	SAMPLE 1			SAMPLE 2			SAMPLE 3		
LOW	N1	N2	N3	N1	N2	N3	N1	N2	N3
PCL	N1	N2	N3	N1	N2	N3	N1	N2	N3
PLGA	N1	N2	N3	N1	N2	N3	N1	N2	N3
PEUU	N1	N2	N3	N1	N2	N3	N1	N2	N3
BARE	N1	N2	N3	N1	N2	N3	N1	N2	N3
HIGH	N1	N2	N3	N1	N2	N3	N1	N2	N3

Absorbance measurements were taken for each time point at 492 nm on a VersaMAX microplate reader (Molecular Devices). To determine the percentage cytotoxicity, the average of the triplicates were obtained and the cytotoxicity percentage was calculated using equation. Where, exp. is the experimental value obtained from the absorbance readings, low control is the absorbance value obtained from cells with no magnesium exposure, and high control is the absorbance value obtained from samples containing the maximum LDH activity.

Experimental Design

The purpose of this experiment was to gauge the effects of polymer coating material on the percentage of LDH activity from the cultured cells. The various

conditions identified for comparison were untreated magnesium alloys, samples coated with PCL, PLGA, and PEUU. A low control that consisted of cultured cells with no magnesium exposure. Having this low control would allow us to compare the magnesium containing samples to the natural cell death process. A one-way analysis of variance was chosen to determine the statistical differences between the means of the various experiment groups.

The question was posed, *"Can direct-write inkjet printing be used as a mechanism for depositing uniformly distributed protective thin films?"* Furthermore, *"Can these thin films aid in retardation of the corrodible AZ31 magnesium alloy in physiological solutions?"* More specifically, we seek to answer the following questions:

1. *Does polymer type and coating thickness have a significant effect on the rate of metal ion release? (Phase 1)*
2. *Does polymer coating type have a significant effect on the percentage of LDH activity from Human Bronchial Epithelial Cells? (Phase 2)*

Results

Preliminary cell culture testing was conducted to determine the effects of polymer coating type on the percentage of LDH activity and magnesium presence in sample media at various time points. LDH activity was collected over a course of a 48 hour period at t = 0, 1, 4, 6, 24 and 48 hours. The sample data collected at time zero represents two distinct events. The first is that this sample was collected at the end of a 24-hour feeding during which some LDH activity had already occurred. This is apparent in the graph shown below which depicts a sample reading that shows significantly higher LDH activity when

compared to subsequent readings. Also, at time zero fresh media was added to each of the sample wells to initiate the new testing period. Thus, it is taken that each time point represents the end of a sample collection period.

The samples collected at each time period were evaluated as percentages of the high control, that is, the total amount of LDH that could be released from the cells. Given that the samples collected at time zero contained 24 hours worth of LDH activity before magnesium exposure, this provided some indication of the cell health before the experiment was started. The sample data collected at time zero indicates that the cell health of the wells that were chosen as the low control was significantly lower than the wells assigned to the other experiment groups due to a high percentage of LDH release.

Sample media collected between t = 1 and t = 6 hours showed very little LDH release occurred and that activity was fairly consistent between the experiment groups. Between t = 6 and t = 24 hours a slight jump in percentage LDH activity is realized with PEUU coated samples having the highest activity and uncoated samples showing the least. Finally, at t = 48 hours the data shows a great increase in all of the experiment groups, however it remains that the PEUU show the highest release percentage where the uncoated samples continue to show the least. The results indicated that the cells are able to maintain good health as they are exposed to the magnesium. However the cells seem to react more to the polymer coatings, specifically, PEUU.

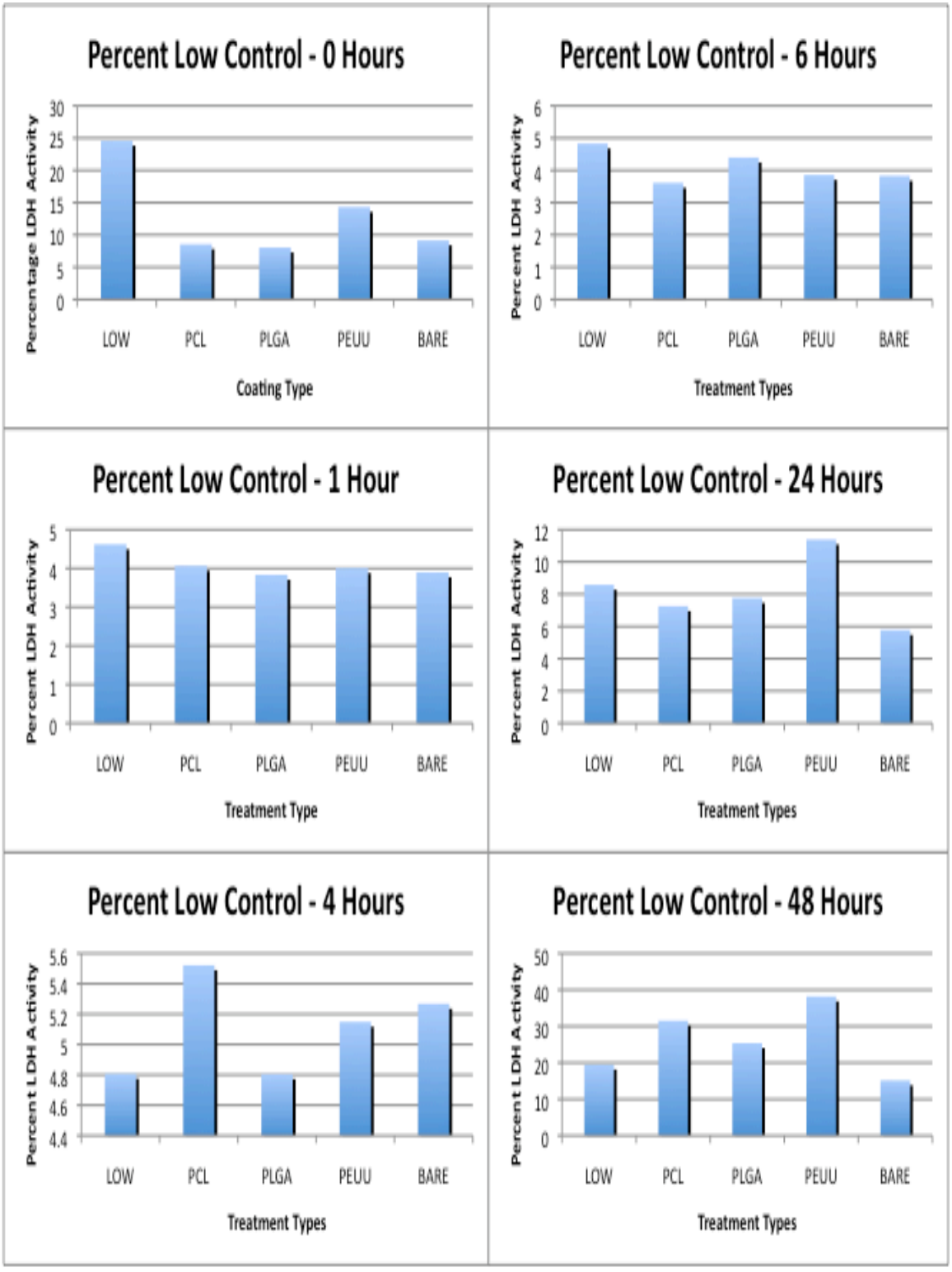

Figure A.1 Depiction of fluctuating LDH for all time points of preliminary study

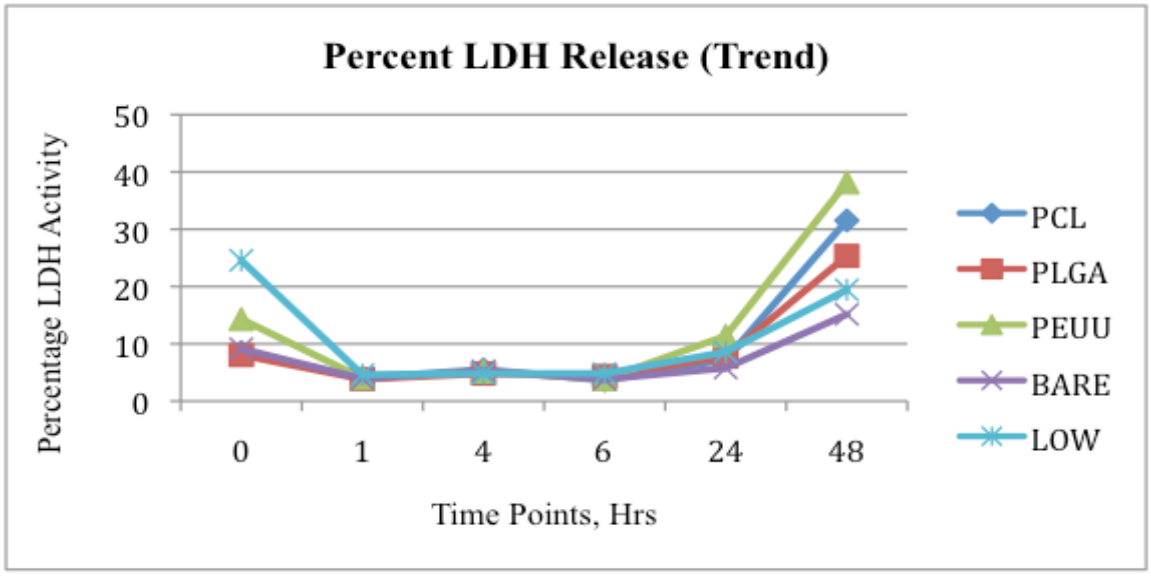

(a)

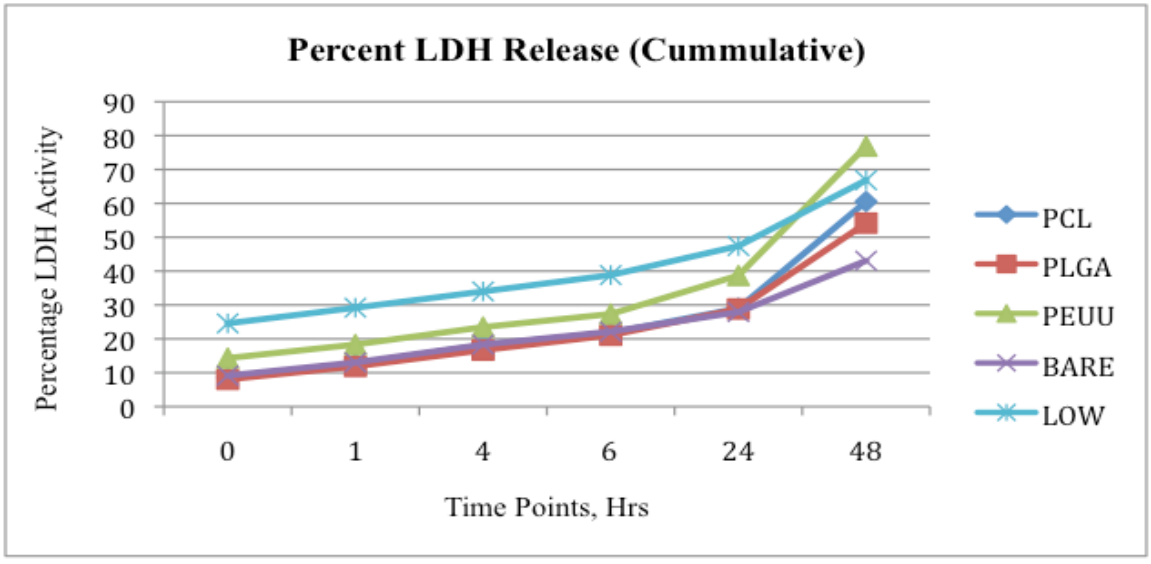

(b)

Figure A.2 (a) Depiction of trends in LDH activity over 24 hours (b) increasing LDH activity over 24 hours for preliminary data set

A one-way analysis of variance (ANOVA) was conducted to determine if there are significant differences between the means of the experiment groups. The results showed that significant differences do exist between at least two of the sample types ($p < 0.05$). Therefore, the null hypothesis stating that there are no differences between the means was rejected and further analysis was required. Tukey's analysis was conducted to determine specific differences between groups. Here results showed that statistical differences occurred between the low control (cells only) and the uncoated samples. The differences amongst all other sample types were shown to be insignificant.

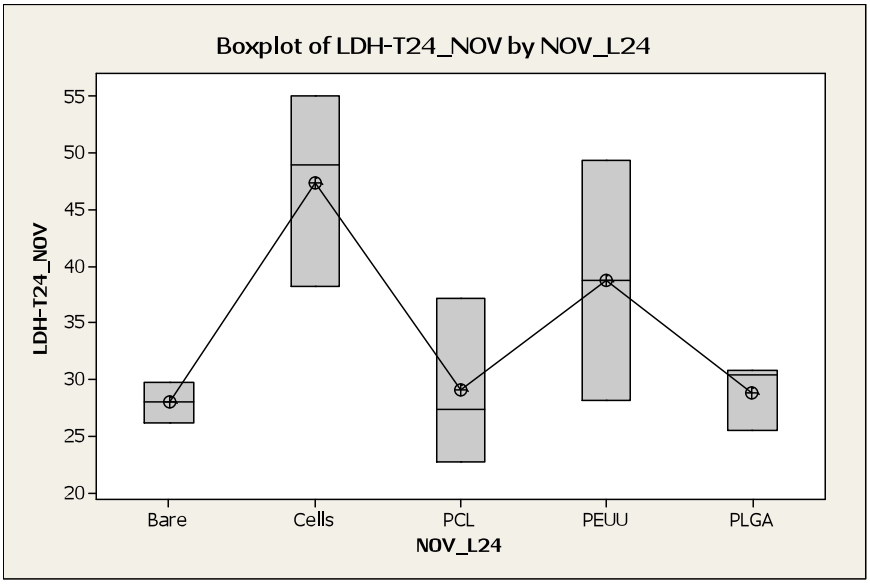

Figure A.3 Depiction of differences in LDH for preliminary data set

Samples from each experiment group were also collected for inductively coupled plasma (ICP) analysis. The ICP analysis was to determine whether or not the various treatment types affected magnesium presences within the collected samples. The data shows higher magnesium presences from PCL-coated samples and lower magnesium presence for PEUU-coated samples. A one-way ANOVA was performed on the data,

which revealed that the differences in means for magnesium presences were not significant thus; the results here were likely due to chance and possibly variations in the sample types. Overall, it seemed that cells may be reacting to the polymer type as oppose to magnesium exposure.

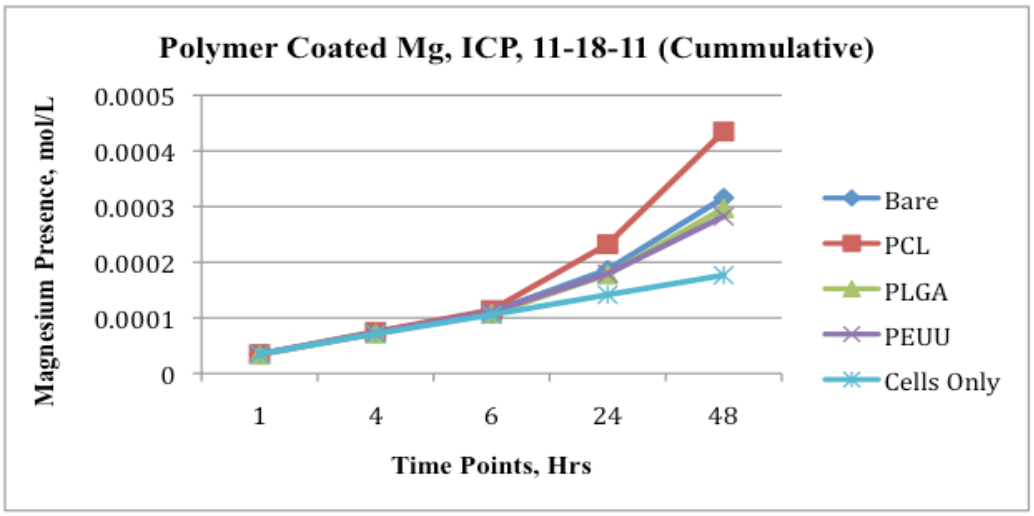

Figure A.4 Magnesium presence in LDH samples for preliminary data set

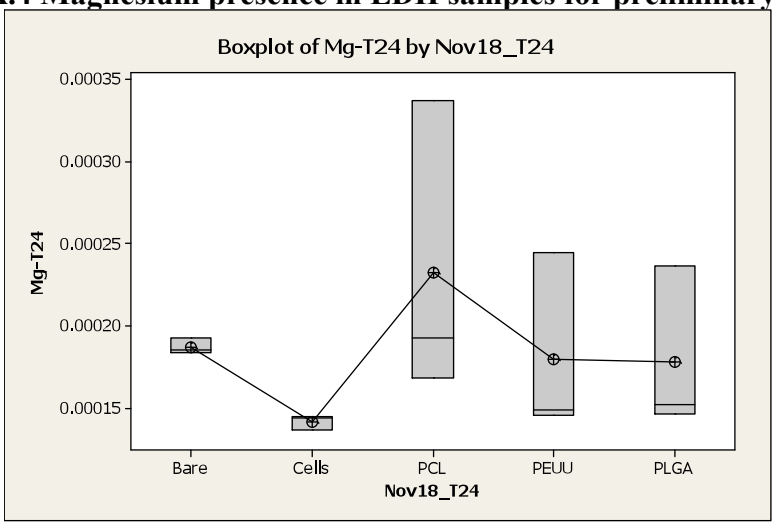

Figure A.5 Depiction of mean differences in mg content for preliminary data Conclusions

Normal Human Bronchial Epithelial cells were culture in Air-Liquid Interface. Magnesium samples set in epoxy resin material were coated using direct-write techniques. Cell wells were selected bases on apparent cell health at the start of the experiment and randomly assigned to an experiment group. The samples were placed for surface interaction between the cells and polymer coated magnesium surfaces in which the samples were tested for percentage of LDH activity and magnesium presence in the sample fluid.

Statistical analysis (ANOVA) was conducted on the results for a 48-hour period, which determined that there were no significant differences in the polymer coating types on the percentage of LDH activity. However the difference in means between the cells and the uncoated samples was significant indication a positive reaction to the magnesium from the uncoated samples. It is also evident from the results of the test that declining cell health could be a response to the biocompatibility of the polymer types rather than increased magnesium exposure.

In conclusion, this test should be conducted again with cells having similar health at the start of the experiment. Also smaller samples sizes should be used to eliminate the possibility of weight contributing to accelerated cell stress.

Statistical Analysis for Preliminary Experiments

LDH shows statistical significance for NOV

One-way ANOVA: Nov LDH

Source	DF	SS	MS	F	P
NOV_L24	4	869.7	217.4	4.31	0.028
Error	10	504.9	50.5		
Total	14	1374.6			

S = 7.106   R-Sq = 63.27%   R-Sq(adj) = 48.58%

Individual 95% CIs For Mean Based on Pooled StDev

```
Level  N   Mean  StDev  -+---------+---------+---------+--------
Bare   3  27.916  1.765  (--------*--------)
Cells  3  47.403  8.556                  (--------*---------)
PCL    3  29.004  7.374  (--------*--------)
PEUU   3  38.709 10.630           (--------*--------)
PLGA   3  28.822  2.958  (--------*--------)
                  -+---------+---------+---------+--------
                  20        30        40        50
```

Pooled StDev = 7.106

Tukey 95% Simultaneous Confidence Intervals
All Pairwise Comparisons among Levels of NOV_L24

Individual confidence level = 99.18%

NOV_L24 = Bare subtracted from:

```
NOV_L24   Lower  Center  Upper  ---------+---------+---------+---------+
Cells     0.411  19.487  38.563                 (---------*--------)
PCL      -17.988  1.088  20.164          (---------*--------)
PEUU      -8.283 10.793  29.870                (--------*---------)
PLGA     -18.169  0.907  19.983          (--------*---------)
                        ---------+---------+---------+---------+
                             -20        0        20        40
```

NOV_L24 = Cells subtracted from:

```
NOV_L24   Lower  Center  Upper  ---------+---------+---------+---------+
PCL      -37.475 -18.399  0.677  (---------*--------)
PEUU     -27.770  -8.694 10.382       (---------*--------)
PLGA     -37.657 -18.581  0.495  (---------*--------)
                        ---------+---------+---------+---------+
                             -20        0        20        40
```

NOV_L24 = PCL subtracted from:

```
NOV_L24   Lower  Center  Upper  ---------+---------+---------+---------+
PEUU      -9.371  9.705  28.781               (---------*--------)
PLGA     -19.258 -0.182  18.894          (---------*--------)
                        ---------+---------+---------+---------+
                             -20        0        20        40
```

NOV_L24 = PEUU subtracted from:

```
NOV_L24   Lower  Center  Upper  ---------+---------+---------+---------+
PLGA     -28.963 -9.887  9.189       (--------*---------)
                        ---------+---------+---------+---------+
                             -20        0        20        40
```

NOV ICP Data does not show statistical significance

One-way ANOVA: Nov ICP NHBE

```
Source     DF        SS        MS     F      P
Nov18_T24   4  0.0000000  0.0000000  1.12  0.400
Error      10  0.0000000  0.0000000
Total      14  0.0000000

S = 0.00005312   R-Sq = 30.93%   R-Sq(adj) = 3.30%



Level  N       Mean       StDev
Bare   3  0.00018672  0.00000492
Cells  3  0.00014152  0.00000460
PCL    3  0.00023239  0.00009136
PEUU   3  0.00017941  0.00005646
PLGA   3  0.00017791  0.00005027

      Individual 95% CIs For Mean Based on Pooled StDev
Level  --------+---------+---------+---------+-
Bare          (----------*----------)
Cells  (----------*----------)
PCL                 (----------*----------)
PEUU         (----------*----------)
PLGA         (----------*----------)
       --------+---------+---------+---------+-
           0.000120  0.000180  0.000240  0.000300

Pooled StDev = 0.00005312


Tukey 95% Simultaneous Confidence Intervals
All Pairwise Comparisons among Levels of Nov18_T24

Individual confidence level = 99.18%


Nov18_T24 = Bare subtracted from:

Nov18_T24       Lower       Center       Upper
Cells     -0.00018780  -0.00004520  0.00009741
PCL       -0.00009693   0.00004567  0.00018828
PEUU      -0.00014991  -0.00000730  0.00013530
PLGA      -0.00015141  -0.00000880  0.00013380

Nov18_T24  ---------+---------+---------+---------+
Cells         (----------*----------)
PCL                 (----------*----------)
PEUU              (----------*----------)
PLGA              (----------*----------)
          ---------+---------+---------+---------+
              -0.00012   0.00000   0.00012   0.00024
```

Nov18_T24 = Cells subtracted from:

Nov18_T24	Lower	Center	Upper
PCL	-0.00005173	0.00009087	0.00023348
PEUU	-0.00010471	0.00003789	0.00018050
PLGA	-0.00010621	0.00003640	0.00017900

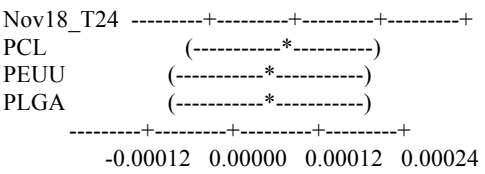

Nov18_T24 = PCL subtracted from:

Nov18_T24	Lower	Center	Upper
PEUU	-0.00019558	-0.00005298	0.00008963
PLGA	-0.00019708	-0.00005448	0.00008813

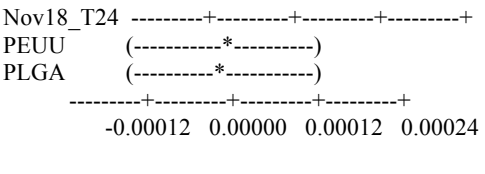

Nov18_T24 = PEUU subtracted from:

Nov18_T24	Lower	Center	Upper
PLGA	-0.00014410	-0.00000150	0.00014111

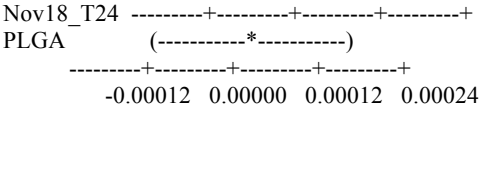

APPENDIX C

Statistical Output for Magnesium Ion Content from Immersion Testing

DOE ICP Mg –Immersion Test

Multilevel Factorial Design

Factors: 2 Replicates: 2
Base runs: 6 Total runs: 12
Base blocks: 1 Total blocks: 1

Number of levels: 3, 2

Design Table (randomized)

Run	Blk	A	B
1	1	3	1
2	1	3	2
3	1	2	1
4	1	1	1
5	1	2	1
6	1	3	2
7	1	1	2
8	1	3	1
9	1	1	2
10	1	2	2
11	1	2	2
12	1	1	1

General Linear Model: Mg-Immer versus Polymer Type, No. of Layers

Factor	Type	Levels	Values
Polymer Type	fixed	3	PCL, PLGA, PEUU
No. of Layers	fixed	2	10, 20

Analysis of Variance for Mg-Immer, using Adjusted SS for Tests

Source	DF	Seq SS	Adj SS	Adj MS	F	P
Polymer Type	2	0.0000114	0.0000114	0.0000057	2.15	0.198
No. of Layers	1	0.0000002	0.0000002	0.0000002	0.09	0.770
Polymer Type*No. of Layers	2	0.0000197	0.0000197	0.0000099	3.74	0.088
Error	6	0.0000159	0.0000159	0.0000026		
Total	11	0.0000472				

S = 0.00162534 R-Sq = 66.41% R-Sq(adj) = 38.43%

Term	Coef	SE Coef	T	P
Constant	0.002990	0.000469	6.37	0.001

Polymer Type
PCL 0.001277 0.000664 1.92 0.103
PLGA -0.000195 0.000664 -0.29 0.778
No. of Layer
10 0.000144 0.000469 0.31 0.770
Polymer Type*No. of Layer
PCL 10 -0.001804 0.000664 -2.72 0.035
PLGA 10 0.001062 0.000664 1.60 0.161

Least Squares Means for Mg-Immer

Polymer Type		Mean	SE Mean
PCL		0.004267	0.000813
PLGA		0.002794	0.000813
PEUU		0.001908	0.000813
No. of Layer			
10		0.003133	0.000664
20		0.002846	0.000664
Polymer Type*No. of Layer			
PCL	10	0.002606	0.001149
PCL	20	0.005927	0.001149
PLGA	10	0.003999	0.001149
PLGA	20	0.001589	0.001149
PEUU	10	0.002794	0.001149
PEUU	20	0.001021	0.001149

ANOVA ICP Mg – Immersion Test

One-way ANOVA: Mg-Imm versus Immer

Source	DF	SS	MS	F	P
Immer	6	0.0000714	0.0000119	4.45	0.036
Error	7	0.0000187	0.0000027		
Total	13	0.0000901			

S = 0.001635 R-Sq = 79.23% R-Sq(adj) = 61.42%

Individual 95% CIs For Mean Based on Pooled StDev

Level	N	Mean	StDev	-----+---------+---------+---------+----
Bare	2	0.007821	0.001690	(------*-------)
PCL10	2	0.002606	0.000318	(------*-------)
PCL20	2	0.005927	0.003085	(-------*-------)
PEUU10	2	0.002794	0.000011	(-------*-------)
PEUU20	2	0.001021	0.000213	(-------*-------)
PLGA10	2	0.003999	0.002483	(------*-------)
PLGA20	2	0.001589	0.000157	(-------*------)

```
                  -----+---------+---------+---------+----
                     0.0000    0.0035    0.0070    0.0105
```

Pooled StDev = 0.001635

Tukey 95% Simultaneous Confidence Intervals
All Pairwise Comparisons among Levels of Immer

Individual confidence level = 99.46%

Immer = Bare subtracted from:

Immer	Lower	Center	Upper
PCL10	-0.011699	-0.005214	0.001271
PCL20	-0.008378	-0.001893	0.004592
PEUU10	-0.011511	-0.005026	0.001459
PEUU20	-0.013284	-0.006799	-0.000314
PLGA10	-0.010306	-0.003821	0.002664
PLGA20	-0.012717	-0.006232	0.000253

```
Immer   ---------+---------+---------+---------+
PCL10     (---------*--------)
PCL20          (--------*---------)
PEUU10     (--------*--------)
PEUU20  (--------*---------)
PLGA10      (---------*--------)
PLGA20   (--------*--------)
       ---------+---------+---------+---------+
           -0.0070    0.0000    0.0070    0.0140
```

Immer = PCL10 subtracted from:

Immer	Lower	Center	Upper
PCL20	-0.003164	0.003321	0.009806
PEUU10	-0.006297	0.000188	0.006673
PEUU20	-0.008070	-0.001585	0.004900
PLGA10	-0.005092	0.001393	0.007878
PLGA20	-0.007503	-0.001017	0.005468

```
Immer   ---------+---------+---------+---------+
PCL20               (---------*--------)
```

```
PEUU10          (--------*---------)
PEUU20        (---------*--------)
PLGA10          (--------*--------)
PLGA20        (---------*--------)
      ---------+---------+---------+---------+
           -0.0070    0.0000    0.0070    0.0140
```

Immer = PCL20 subtracted from:

Immer	Lower	Center	Upper
PEUU10	-0.009618	-0.003133	0.003352
PEUU20	-0.011391	-0.004906	0.001579
PLGA10	-0.008413	-0.001928	0.004557
PLGA20	-0.010824	-0.004339	0.002146

```
Immer   ---------+---------+---------+---------+
PEUU10      (---------*--------)
PEUU20    (--------*--------)
PLGA10      (--------*---------)
PLGA20    (--------*--------)
      ---------+---------+---------+---------+
           -0.0070    0.0000    0.0070    0.0140
```

Immer = PEUU10 subtracted from:

Immer	Lower	Center	Upper
PEUU20	-0.008258	-0.001773	0.004712
PLGA10	-0.005280	0.001205	0.007690
PLGA20	-0.007690	-0.001205	0.005280

```
Immer   ---------+---------+---------+---------+
PEUU20        (--------*---------)
PLGA10          (---------*--------)
PLGA20        (--------*---------)
      ---------+---------+---------+---------+
           -0.0070    0.0000    0.0070    0.0140
```

Immer = PEUU20 subtracted from:

Immer	Lower	Center	Upper
PLGA10	-0.003507	0.002978	0.009463

PLGA20 -0.005917 0.000568 0.007053

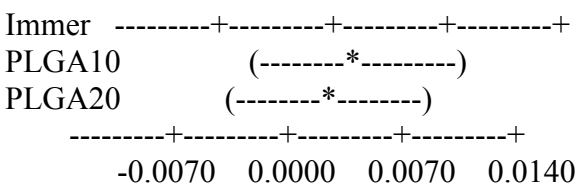

Immer = PLGA10 subtracted from:

Immer	Lower	Center	Upper
PLGA20	-0.008896	-0.002411	0.004074

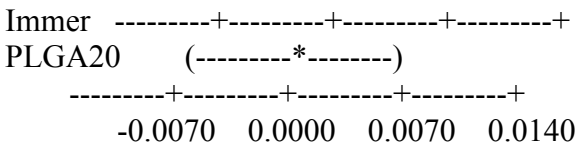

APPENDIX D

STATISTICAL OUTPUT FOR FINAL LDH ACTIVITY AND MG CONTENT IN CULTURE MEDIA

LDH shows statistical significance for DEC

One-way ANOVA: LDH-T24_DEC

```
Source   DF     SS     MS     F      P
DEC_L24   4   848.0  212.0  3.75  0.041
Error    10   564.7   56.5
Total    14  1412.6

S = 7.514   R-Sq = 60.03%   R-Sq(adj) = 44.04%


                    Individual 95% CIs For Mean Based on
                    Pooled StDev
Level  N    Mean   StDev  -----+---------+---------+---------+----
Bare   3  28.080   4.594  (-------*-------)
Cells  3  49.908  15.981                  (-------*-------)
PCL    3  32.357   1.779     (-------*-------)
PEUU   3  37.302   0.449         (-------*-------)
PLGA   3  32.604   1.575     (-------*-------)
                  -----+---------+---------+---------+----
                     24        36        48        60

Pooled StDev = 7.514


Tukey 95% Simultaneous Confidence Intervals
All Pairwise Comparisons among Levels of DEC_L24

Individual confidence level = 99.18%


DEC_L24 = Bare subtracted from:

DEC_L24    Lower  Center   Upper  ---------+---------+---------+---------+
Cells      1.655  21.829  42.002                  (---------*---------)
PCL      -15.896   4.277  24.451           (---------*---------)
PEUU     -10.951   9.222  29.396              (---------*---------)
PLGA     -15.650   4.524  24.698           (---------*---------)
                          ---------+---------+---------+---------+
                              -20        0        20        40


DEC_L24 = Cells subtracted from:

DEC_L24    Lower   Center  Upper  ---------+---------+---------+---------+
PCL      -37.725  -17.551  2.622  (---------*---------)
PEUU     -32.780  -12.606  7.568     (---------*---------)
PLGA     -37.478  -17.305  2.869  (---------*---------)
```

```
                    ---------+---------+---------+---------+
                        -20        0       20       40


DEC_L24 = PCL subtracted from:

DEC_L24   Lower  Center  Upper  ---------+---------+---------+---------+
PEUU    -15.229  4.945  25.119           (---------*----------)
PLGA    -19.927  0.247  20.420         (---------*---------)
                    ---------+---------+---------+---------+
                        -20        0       20       40


DEC_L24 = PEUU subtracted from:

DEC_L24   Lower  Center  Upper  ---------+---------+---------+---------+
PLGA    -24.872 -4.698  15.475        (---------*---------)
                    ---------+---------+---------+---------+
                        -20        0       20       40
```

DEC ICP Data shows statistical significance

One-way ANOVA: Dec Mg ICP for NHBE

```
Source    DF        SS        MS     F      P
Dec16_T24   4  0.0000000  0.0000000  7.56  0.005
Error      10  0.0000000  0.0000000
Total      14  0.0000000

S = 0.000006802   R-Sq = 75.16%   R-Sq(adj) = 65.22%


                        Individual 95% CIs For Mean Based on
                        Pooled StDev
Level  N       Mean      StDev  ----+---------+---------+---------+-----
Bare   3  0.00016682  0.00000595                    (--------*--------)
Cells  3  0.00014512  0.00000765  (--------*--------)
PCL    3  0.00016616  0.00000375                    (--------*--------)
PEUU   3  0.00014572  0.00000655   (--------*-------)
PLGA   3  0.00015067  0.00000897       (--------*-------)
                        ----+---------+---------+---------+-----
                          0.000140  0.000150  0.000160  0.000170

Pooled StDev = 0.00000680


Tukey 95% Simultaneous Confidence Intervals
All Pairwise Comparisons among Levels of Dec16_T24

Individual confidence level = 99.18%


Dec16_T24 = Bare subtracted from:

Dec16_T24        Lower       Center        Upper
Cells     -3.99556E-05  -2.16933E-05  -3.43106E-06
PCL       -1.89136E-05  -6.51333E-07   0.000017611
```

```
PEUU      -3.93596E-05  -2.10973E-05  -2.83506E-06
PLGA      -3.44056E-05  -1.61433E-05   0.000002119

Dec16_T24   +---------+---------+---------+---------
Cells       (--------*--------)
PCL                 (--------*--------)
PEUU        (--------*---------)
PLGA          (--------*--------)
          +---------+---------+---------+---------
        -4.0E-05  -2.0E-05  0.000000  0.000020


Dec16_T24 = Cells subtracted from:

Dec16_T24        Lower       Center        Upper
PCL        0.000002780  0.000021042  0.000039304
PEUU      -1.76663E-05  0.000000596  0.000018858
PLGA      -1.27123E-05  0.000005550  0.000023812

Dec16_T24   +---------+---------+---------+---------
PCL                         (---------*--------)
PEUU                (--------*--------)
PLGA                  (--------*--------)
          +---------+---------+---------+---------
        -4.0E-05  -2.0E-05  0.000000  0.000020


Dec16_T24 = PCL subtracted from:

Dec16_T24        Lower       Center        Upper
PEUU      -3.87083E-05  -2.04460E-05  -2.18373E-06
PLGA      -3.37543E-05  -1.54920E-05   0.000002770

Dec16_T24   +---------+---------+---------+---------
PEUU        (--------*--------)
PLGA          (--------*--------)
          +---------+---------+---------+---------
        -4.0E-05  -2.0E-05  0.000000  0.000020


Dec16_T24 = PEUU subtracted from:

Dec16_T24        Lower       Center        Upper
PLGA      -1.33083E-05  0.000004954  0.000023216

Dec16_T24   +---------+---------+---------+---------
PLGA                (--------*---------)
          +---------+---------+---------+---------
                    -4.0E-05  -2.0E-05  0.000000  0.000020
```